Aus dem Zentrum für Kinder- und Jugendmedizin der Universität zu Köln
Klinik und Poliklinik für Kinder- und Jugendmedizin
Direktor: Universitätsprofessor Dr. med. J. Dötsch

Apoptoseinduktion neuartiger organischer zum Teil metallhaltiger Wirkstoffe in Leukämie- und soliden Tumorzellen mit Überwindung der Resistenz gegenüber herkömmlichen Zytostatika

Inaugural-Dissertation zur Erlangung der Doktorwürde
der Medizinischen Fakultät
der Universität zu Köln

vorgelegt von
Sina Marie Hopff
aus Wermelskirchen

promoviert am 24. Januar 2023

Gedruckt mit Genehmigung der Medizinischen Fakultät der Universität zu Köln
Druckjahr 2021

Dekan: Universitätsprofessor Dr. med. G. R. Fink
1. Gutachter: Universitätsprofessor Dr. med. M. Fischer
2. Gutachter: Universitätsprofessor Dr. rer. nat. H. Kashkar

Erklärung

Ich erkläre hiermit, dass ich die vorliegende Dissertationsschrift ohne unzulässige Hilfe Dritter und ohne Benutzung anderer als der angegebenen Hilfsmittel angefertigt habe; die aus fremden Quellen direkt oder indirekt übernommenen Gedanken sind als solche kenntlich gemacht.[1]

Bei der Auswahl und Auswertung des Materials sowie bei der Herstellung des Manuskriptes habe ich keine Unterstützungsleistungen erhalten.

Weitere Personen waren an der Erstellung der vorliegenden Arbeit nicht beteiligt. Insbesondere habe ich nicht die Hilfe einer Promotionsberaterin/eines Promotionsberaters in Anspruch genommen. Dritte haben von mir weder unmittelbar noch mittelbar geldwerte Leistungen für Arbeiten erhalten, die im Zusammenhang mit dem Inhalt der vorgelegten Dissertationsschrift stehen.

Die Dissertationsschrift wurde von mir bisher weder im Inland noch im Ausland in gleicher oder ähnlicher Form einer anderen Prüfungsbehörde vorgelegt.

Die dieser Arbeit zugrunde liegenden Messergebnisse wurden von mir im Labor der AG Experimentelle Onkologie, Abteilung für Kinderonkologie-/hämatologie, Kinderkrankenhaus Amsterdamer Straße, Köln ermittelt.

Die in dieser Arbeit angegebenen Experimente sind nach entsprechender Anleitung durch Herrn Prof. Dr. med. Dr. rer. nat. Aram Prokop von mir selbst ausgeführt worden.

Erklärung zur guten wissenschaftlichen Praxis:

Ich erkläre hiermit, dass ich die Ordnung zur Sicherung guter wissenschaftlicher Praxis und zum Umgang mit wissenschaftlichem Fehlverhalten (Amtliche Mitteilung der Universität zu Köln AM 132/2020) der Universität zu Köln gelesen habe und verpflichte mich hiermit, die dort genannten Vorgaben bei allen wissenschaftlichen Tätigkeiten zu beachten und umzusetzen.

Köln, den 15.11.2021

Unterschrift: S. M. Hapff

[1]Bei kumulativen Promotionen stellt nur die eigenständig verfasste Einleitung und Diskussion die Dissertationsschrift im Sinne der Erklärung gemäß dieser Erklärung dar.

Danksagung

Mein Dank gilt an erster Stelle meinem Arbeitsgruppenleiter Herrn Prof. Dr. med. Dr. rer. nat. Aram Prokop, der mir diese spannende Promotionsarbeit ermöglicht hat. Die enge Betreuung meiner Forschungsprojekte und die zahlreichen wissenschaftlichen und medizinischen Diskussionen haben diese Arbeit erst möglich gemacht. Ich bin sehr dankbar über die mit der Arbeit einhergegangenen Herausforderungen, die wir gemeinsam bewältigt haben und die mir geholfen haben als Wissenschaftlerin zu wachsen. Durch die zusätzlichen Einblicke in den ärztlichen Alltag auf der Station für Kinderhämatologie und -onkologie im Kinderkrankenhaus Amsterdamer Straße, die mir zahlreich ermöglicht wurden, wuchs meine Motivation diesem wichtigen Forschungsthema nachzugehen.

Meinem Doktorvater Herrn Prof. Dr. med. Matthias Fischer danke ich sehr für die angenehme und unkomplizierte Betreuung meiner Promotionsarbeit, die mir sehr zum Gelingen der Arbeit verholfen hat.

Herrn Prof. Dr. rer. nat. Albrecht Berkessel und seiner Arbeitsgruppe möchte ich danken für die Bereitstellung der spannenden Substanzen, sowie die angenehmen Austausche und zahlreichen Unterstützungen, insbesondere bei chemischen Fragen.

Darüber hinaus bedanke ich mich bei unserer Laborfee Corazon Frias, die mir den Einstieg in die experimentelle Forschung so leicht gemacht hat und mit der ich sehr viele aufregende Stunden im Labor verbracht habe. Auf deine Unterstützung war jederzeit Verlass, egal wie herausfordernd die Zellkulturen oder wie kompliziert die Versuchsanleitungen waren. Auch allen anderen Mitarbeitern der Arbeitsgruppe danke ich für die schöne und unvergessliche Zeit im Labor und die spannenden Diskussionen in unseren Lab-Meetings.

Den größten Dank richte ich an meinen Freund, meine Eltern und meine beiden Geschwister, die immer an mich glauben und mir den nötigen Halt gegeben haben, um diese Arbeit zu absolvieren. Danke für euer Verständnis für die vielen Stunden, die ich im Labor verbracht habe. Meiner Schwester danke ich dafür, dass sie mir ebenfalls für spannende wissenschaftliche Diskussionen zur Seite stand und immer ein offenes Ohr hatte, wenn ich vor neuen Herausforderungen während meiner Forschungsarbeit stand.

Als letztes gilt mein Dank meinen lieben Freunden in Köln, die immer für mich da sind und mir den nötigen Ausgleich neben meinem Studium und meiner Forschungsarbeit gegeben haben.

Inhaltsverzeichnis

Abkürzungsverzeichnis

ABC-Transporter	ATP-bindende Kassetten Transporter
ALL	akute lymphoblastische Leukämie
AML	akute myeloische Leukämie
APAF-1	apoptotic protease activating-factor 1
ATP	Adenosintriphosphat
Bad	Bcl-2 antagonist of cell death
Bak	Bcl-2 antagonist killer
BAX	Bcl-2 associated X gene
Bax	Bcl-2 associated X protein
Bcl-2	B-cell lymphoma-2 gene
BCP-ALL	B-Vorläuferzellen-Akute lymphatische Leukämie
BCR-ABL1	Breakpoint Cluster Region – Abelson-Tyrosinkinase 1
BH3	Bcl-2 homology domain 3
Bid	BH3 interacting domain death antagonist
Bim	Bcl-2 interacting mediator of cell death
Bik	Bcl-2 interacting killer
Bmf	Bcl-2-modifying factor
CD95	cluster of differentiation 95, Fas
DISC	death-inducing signaling complex
DMSO	Dimethylsulfoxid
DNA	Desoxyribonukleinsäure
FACS	Fluorescence-Activated Cell Sorting
FADD	Fas associated death domain
Fas-L	Fas ligand
JC-1	5,5',6,6'-tetrachloro1,1',3,3'-tetramethylbenzimidazolylcarbocyanine iodide
LDH	Laktatdehydrogenase
MEK-Inhibitor	Mikrotubuli-assoziierter Proteinkinase-Inhibitor
MMP	Matrix-Metalloprotease
Noxa	Phorbol-12-myristate-13-acetate-induced protein 1, PMAIP1
PCR	Polymerase-Kettenreaktion
P-gp	P-Glykoprotein
PUMA	p53 upregulated modulator of apoptosis
RAS	rat sarcoma
SMAC	second mitochondria-derived activator of caspase, DIABLO
TNF	tumor necrosis factor

TNFR1	tumor necrosis factor receptor 1
TRAIL	tumor necrosis factor related apoptosis-inducing ligand

1. Zusammenfassung

In der vorliegenden Arbeit wurde die Wirksamkeit eines Salalen-Liganden und zwei Metall-Salen-Komplexen in verschiedenen Tumorzellen *in vitro* getestet. Dabei stellte sich heraus, dass der Salalen Ligand WQF 044 im Vergleich zu den beiden Metall-Komplexen im niedrigsten mikromolaren Bereich wirksam war. Er leitete die Apoptose in Leukämie- (Nalm-6), Lymphom- (BJAB), Ewing Sarkom (RM82), Mammakarzinom- (MCF-7) und Melanomzellen (MelHO) ein. Als Wirkmechanismus wurde der mitochondriale Apoptosesignalweg detektiert. WQF 044 überwand die Multiresistenz in Leukämie-, Lymphom- und Ewing Sarkom Zellen. Dabei ließ sich eine Unabhängigkeit von P-Glykoprotein (P-gp) und dem extrinsischen Apoptosesignalweg erkennen. Darüber hinaus zeigte der Ligand eine Synergie mit Vincristin in BJAB Zellen und eine Selektivität gegenüber Tumorzellen.

Die zweitbeste Wirksamkeit in BJAB, Nalm-6 und MCF-7 Zellen hatte der Aluminium-Salen-Komplex MBR-8. Dabei wiesen die Reduktion des mitochondrialen Membranpotentials, die Abhängigkeit von Caspase-3 in MCF-7 Zellen und die Aktivierung dieser Caspase in der Western Blot Analyse auf eine Apoptoseinduktion über den intrinsischen Weg hin. Besonders beeindruckend waren die hohen synergistischen Effekte von MBR-8 mit anderen herkömmlichen Zytostatika, die sich neben Nalm-6 Zellen auch in den multiresistenten NDau Zellen erkennen ließen. Gesunde humane Leukozyten wurden von MBR-8 nicht beeinflusst.

Der Kobalt-Salen-Komplex MBR-60 entwickelte zytotoxische Effekte in Leukämie- und Lymphomzellen in etwas höheren mikromolaren Konzentrationen. Ähnlich wie bei MBR-8 setzte auch MBR-60 das mitochondriale Membranpotential herab. Darüber hinaus aktivierte die Substanz Procaspase-9 und Procaspase-3 in der Western Blot Analyse und wirkte unabhängig von CD95 in BJAB FADDdn Zellen. MBR-60 sensibilisierte Nalm-6 Zellen gegenüber Daunorubicin und Vincristin. Letztlich wurde auch bei dieser Substanz eine Selektivität gegenüber Tumorzellen beobachtet.

Alle drei neuen Wirkstoffe erweisen sich *in vitro* als potentielle neue Chemotherapeutika, insbesondere in multiresistenten Leukämie- und Lymphomzellen, sowie in anderen soliden Tumorzellen. Sie müssen in weiteren Experimenten, auch *in vivo*, präklinisch evaluiert werden.

2. Einleitung

2.1 Leukämien und Lymphome im Kindesalter

Krebserkrankungen im Kindesalter sind selten. Dennoch machen sie, nach Unfällen, die zweithäufigste Todesursache für Kinder aus.[1] Mit über 30 Prozent sind Leukämien die häufigste maligne Erkrankung im Kindesalter, gefolgt von Hirntumoren und Lymphomen.[2] Bei Kindern im Alter von null bis vier Jahren liegt die Inzidenz für eine Leukämie unter den Tumorerkrankungen sogar bei 36,1 Prozent, bei älteren Kindern (15 bis 19 Jahre) nur noch bei 15,4 Prozent. Hingegen sind Jugendliche im Alter von 15 bis 19 Jahren mit einer Inzidenz von 22,5 Prozent häufiger von Lymphomen betroffen als Kleinkinder (5,3 Prozent).[3] Heute liegen die Überlebensraten bei Leukämien und Lymphomen im Kindesalter bei über 80 Prozent.[1,4]

2.2 Therapie der akuten lymphoblastischen Leukämie im Kindesalter

Unter den Leukämien im Kindesalter dominiert mit einem Anteil von 80 Prozent die akute lymphoblastische Leukämie (ALL).[5] Das Therapiekonzept dieser Erkrankung besteht noch heute hauptsächlich aus einer Poly-Chemotherapie.[2] Als Standardchemotherapeutika bei Erstdiagnose der ALL finden sich in den aktuellen Leitlinien für die Induktionsphase verschiedene Zytostatika wieder. Dazu gehören Vincristin, Dexamethason, Asparaginase und Anthrazyklin-Derivate wie Daunorubicin oder Doxorubicin. Darüber hinaus werden in der Konsolidierungsphase je nach Risikogruppe Cyclophosphamid, Cytosin-Arabinosid, 6-Mercaptopurin, Etoposid, Thioguanin und Methotrexat – auch intrathekal - eingesetzt. Die Erhaltungsphase setzt sich aus der oralen Verabreichung von 6-Mercaptopurin täglich und Methotrexat wöchentlich zusammen.[6] Es fällt auf, dass bei der Verabreichung von Chemotherapeutika bei ALL keine Platin-Verbindungen verwendet werden, welche zurzeit die einzigen Metall-Komplexe der auf dem Markt befindlichen Zytostatika sind, die zur Therapie von Krebserkrankungen zugelassen sind. Der Bekannteste von ihnen ist Cisplatin, welches in den 1960er Jahren zum ersten Mal Beachtung in der Therapie von hämatoonkologischen Erkrankungen fand.[7-10] Bisher findet Cisplatin vor allem Verwendung in der Behandlung von Bronchial-, Ovarial- und Mammakarzinomen, sowie Hirntumoren und Keimzell-Tumoren, jedoch nicht in der von Leukämien.[9,11] Auch in der Erstlinientherapie vieler Lymphome werden Platin-Derivate aufgrund mangelnder Wirksamkeit nicht eingesetzt, wohingegen in der Zweitlinientherapie von Lymphomen der Einsatz von Platin-Derivaten erfolgt. Die Ansprechraten in der Zweitlinientherapie mit Cisplatin und Carboplatin liegen zwischen 40 und 80 Prozent.[12]

Die Prognosen der malignen Erkrankungen haben sich dank intensiver Forschung, aus der zahlreiche neue Chemotherapeutika und Therapiekonzepte hervorgingen, deutlich gebessert. Dennoch kommt es durch das Auftreten von Zytostatika-Resistenzen weiterhin zu Rezidiven

der Tumorerkrankung.[1] Die Rezidivrate der ALL liegt bei 15 bis 20 Prozent.[13] Die Überlebensrate bei ALL-Rezidiven liegt nur bei 25 bis 40 Prozent.[14] Herkömmliche Zytostatika-Therapien werden durch die Resistenzen der Leukämiezellen im Rezidiv limitiert, und die Suche nach neuen Zytostatika, die die Resistenzmechanismen überwinden, ist daher sehr präsent in der hämatoonkologischen Forschung.[15]

2.3 Apoptose

Den Resistenzmechanismen von Tumorzellen liegen häufig veränderte Expressionen von Proteinen zugrunde, die an der Apoptoseinduktion der Zelle beteiligt sind.[15] Bei der Untersuchung eines potentiellen Wirkstoffes hinsichtlich seiner Apoptose-induzierenden Wirkung spielt daher der Einfluss in den Apoptose-Signalweg eine große Rolle.

Die Apoptose beschreibt den programmierten Zelltod. In der Apoptose-Signalkaskade existieren ein intrinsischer und ein extrinsischer Pfad, welche in einer gemeinsamen Endstrecke resultieren.[16,17] Wichtig ist der programmierte Zelltod bei der Entstehung neuer Organismen, sowie bei der Aufrechterhaltung des Gleichgewichts von Zellaufbau und -abbau in einem existierenden Organismus.[18] Kommt es zu einer Störung in der Apoptose, so führt dies beispielsweise zu autoimmunen oder malignen Erkrankungen.[19,20] Bereits 1972 wurden erste Publikationen veröffentlicht, die den Zusammenhang von Apoptose und der Entstehung von Krebs belegten.[19,21] Bei der Untersuchung neuer zytostatischer Wirkstoffe ist es neben der Wirksamkeitstestung daher von hoher Bedeutung, den Wirkmechanismus, der den Untergang der Zielzelle auslöst, herauszufinden. Dadurch können Zytostatika gezielt in der Therapie maligner Erkrankungen eingesetzt werden.

2.3.1. Der intrinsische Apoptoseweg

Die intrinsische Apoptose spiegelt den Verlust des mitochondrialen Membranpotentials und damit dessen erhöhte Permeabilität wider.[22,23] Eingeleitet wird dieser Prozess durch intrazellulär erzeugte Signale, welche wiederum zur Aktivierung von Kinasen, Phosphatasen und Transkriptionsfaktoren führen.[24] Reguliert wird die mitochondriale Apoptose von Mitgliedern der Bcl-2-Familie, die die Signale aufnehmen und zu pro- oder anti-apoptotischen Antworten führen.[25] Zu den pro-apoptotischen Proteinen zählen Bak und Bax, die in aktivierter Form das Signal zur Apoptoseeinleitung geben. Gehemmt werden diese beiden Proteine von den anti-apoptotischen Bcl-2-Proteinen, welche wiederum von BH3-only Proteinen (Bim, Bik, Noxa, PUMA, Bid, Bad, Bmf) inhibiert werden. Sind Bak und Bax aktiviert, werden SMAC und Cytochrom c freigesetzt. Der Weg zur Apoptose ist damit eingeleitet.[16,26-30] Eine detailliertere Veranschaulichung der Aktivierungskaskade ist Abb. 1 zu entnehmen.

2.3.2. Der extrinsische Apoptoseweg

Eingeleitet wird die extrinsische Apoptose durch die Bindung von extrazellulären Liganden, wie TNF, FAS-L oder TRAIL, an transmembranäre Todes-Rezeptoren. Dazu gehören TNFR1,

Fas (CD95) und TRAIL Rezeptoren.[31,32] Durch dessen Stimulation bildet sich u.a. aus dem Adapter-Protein FADD und Procaspase-8 der Multiproteinkomplex DISC (Abb. 1). Dies resultiert in einer Autoaktivierung von Caspase-8, wodurch die Effektorcaspasen Caspase-3, -6 und -7 aktiviert werden.[25,32-34]

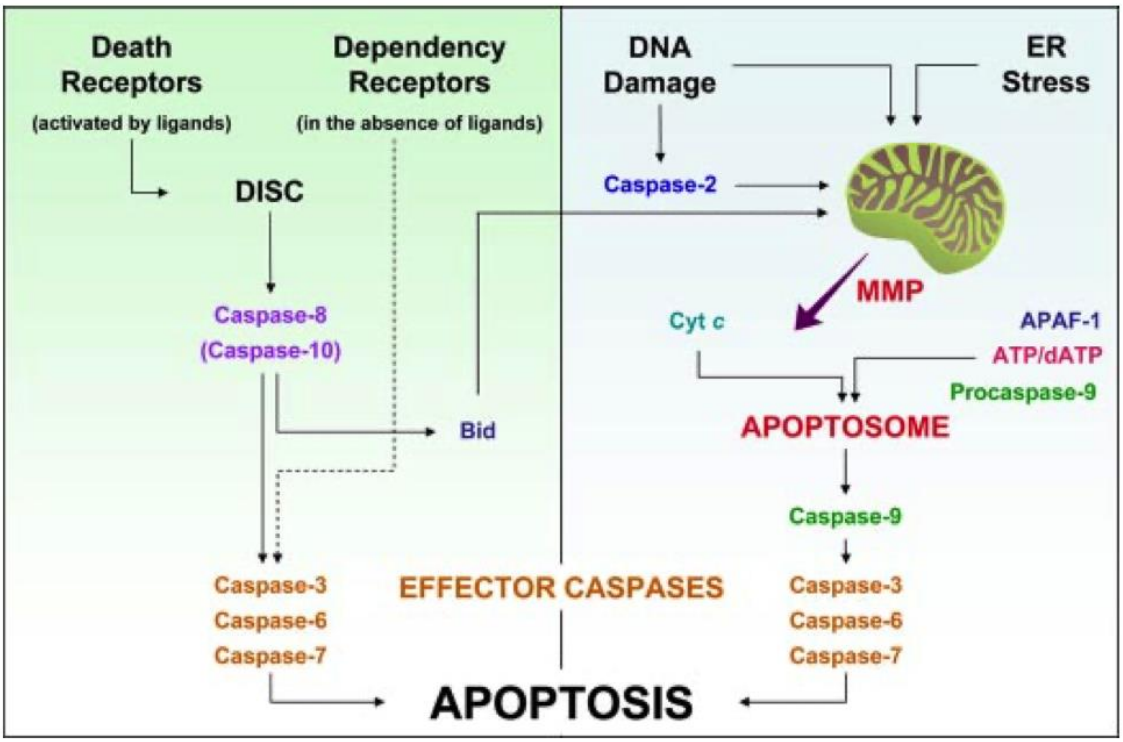

Abb. 1 Extrinsische (links) und intrinsische (rechts) Caspasen-Aktivierungskaskade, skizziert von Kroemer et al. (2007).[24] Auf extrinsischer Seite führen die Liganden-aktivierten Todes-Rezeptoren zur Ausbildung des Multiproteinkomplexes DISC. Dieser wiederum initiiert die Aktivierung von Caspase-8. Das Ergebnis ist die Aktivierung der Effektorcaspasen, darunter Caspase-3, -6 und -7. Gegenübergestellt ist die intrinsische Apoptose, ausgelöst durch DNA-Schädigungen und Zellstress. Über mehrere Schritte wird schließlich Cytochrom c-induziert das Apoptosom gebildet, welches die Spaltung von Procaspase-9 zu Caspase-9 bewirkt. Caspase-9 aktiviert die Effektorcaspasen, womit die gemeinsame Endstrecke der beiden Apoptosewege erreicht ist.

2.4 Metall-Komplexe in der Therapie maligner Erkrankungen

Zu den Wirkstoffen, die in die fehlregulierte Apoptose-Signalkaskade eingreifen, gehören u.a. neuartige Metall-Komplexe.[35] Die Entwicklung dieser metallhaltigen Zytostatika hat seit der Entdeckung der stark Apoptose-induzierenden Platinverbindungen ein großes weltweites Interesse geweckt.[36-38] Insbesondere die fehlende Wirkung durch Ausbildung von Resistenzen in Tumorzellen, auch gegenüber anderen herkömmlichen Zytostatika, und das Auftreten von Nebenwirkungen limitiert die Verwendung von Platinverbindungen zur Therapie diverser Tumorerkrankungen, sodass Interesse an neuen Metall-Komplex-Wirkstoffen besteht.[37,39-43]
Diese Metall-Komplexe beinhalten in ihrer chemischen Zusammensetzung ein entsprechendes Metall und einen Liganden, der als Trägersubstanz des Metalls dient.

Insbesondere Gold-, Platin-, Ruthenium- und Iridium-basierte Komplexe spielten bisher hinsichtlich ihrer Wirkung am mitochondrialen Membranpotential eine Rolle.[35] Vorangegangene Publikationen der Arbeitsgruppe von Prof. Dr. med. Dr. rer. nat. Aram Prokop beschreiben die Apoptose-induzierende Wirksamkeit von Gold-, Ruthenium- und Iridium-Komplexen in Leukämie- und soliden Tumorzellen.[44-51]

2.4.1. Salen-, Salan- und Salalen-Liganden

Salene, Salane und Salalene sind bekannte chemische Liganden von Metall-Komplexen (Abb. 2).[52-55] Bereits 1889 wurde erstmals von Salenen berichtet.[56] Salane und Salalene leiten sich von dem Salen ab.[54] Die Apoptose-induzierende Wirkung der Salane in verschiedenen Tumorzellen wurde bereits mehrfach publiziert.[57-63] Auch von Salenen abgeleitete Komplexe zeigten Anti-Tumor-Aktivitäten.[62,64-69] Salalene hingegen sind hinsichtlich anti-proliferativer und Apoptose-induzierender Wirkungen in Krebszellen bisher nicht untersucht worden.

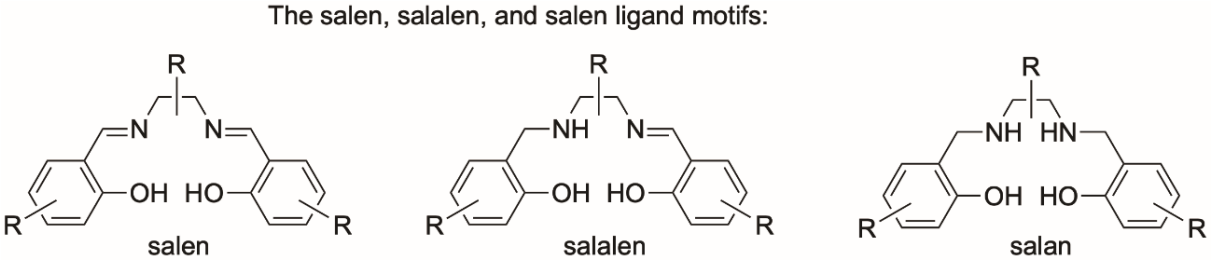

Abb. 2 Chemische Struktur der Salen-, Salalen- und Salan-Liganden.

2.4.2. Wirksamkeitstestung von Titan-Komplexen

Die beschriebenen Liganden können als Trägersubstanz für verschiedene Metalle dienen, darunter die chemisch definierten Übergangsmetalle. Diese stellen eine Reihe von Elementen im Periodensystem dar, die eine unvollständige d-Unterschale ausbilden.[70,71] Die Attraktivität von Übergangsmetall-Komplexen als potentielle Zytostatika ist in den letzten Jahren gestiegen.[39] Auch bei Platin handelt es sich um ein Übergangsmetall.[72] Übergangsmetall-Komplexe greifen insbesondere in die Atmungskette der Mitochondrien ein.[73,74] Dies kann einerseits durch die Liganden selbst geschehen, indem im Mitochondrium vorhandene Metalle heraus komplexiert werden. Andererseits können die im Komplex enthaltenen Übergangsmetalle mit biologischen Liganden wechselwirken und konkurrieren. Beides führt zu einer Abnahme des mitochondrialen Membranpotentials und folglich dem Untergang der Zelle.[75,76]

Ein weiterer interessanter Vertreter der Übergangsmetalle ist Titan. Der Titan-Komplex Budotitan wurde 1996 bereits in einer klinischen Phase I Studie hinsichtlich Antitumoraktivität erprobt.[77] Antiproliferative Wirkungen von Titanocen-Komplexen gegen Tumorzellen wurden *in vitro* und *in vivo* nachgewiesen. So leitete beispielsweise Titanocen C Apoptose in Zellen eines kleinzelligen Bronchialkarzinoms und in Platin-resistenten Zellen einer akuten

myeloischen Leukämie (AML) ein.[78] Titanocen Y induzierte Apoptose in Leukämie-, Lymphom- und soliden Tumorzellen *in vitro*.[79] Carbonyl-substituierte Titanocene zeigten apoptotische Effekte in ALL-Zellen und soliden Tumoren *in vitro*, sowie *in vivo* Wachstumshemmungen von menschlichen Lymphomen in Mäusen.[80] Weitere Titan-Komplexe entwickelten *in vitro* zytotoxische Wirkungen u.a. gegen Platin-resistente Tumorzellen.[81-83] Die oben beschriebenen Salene, Salane und Salalene bilden mit Übergangsmetallen stabile Komplexe. Die Zytotoxizität möglicher Titan-Salan-Komplexe ist bereits beschrieben worden.[58,59] Jedoch gibt es noch keine publizierten Daten zu Titan-Komplexen mit Salalen-Liganden hinsichtlich deren zytostatischer Wirkungen. Frühere Publikationen beschreiben lediglich deren katalytischen Eigenschaften in der Chemie.[84-87]

2.4.3. Kobalt-Komplexe mit zytostatischer Wirkung

Ebenfalls zu den Übergangsmetallen gehört das Element Kobalt. Die Erforschung von Kobalt-Komplexen hinsichtlich ihrer biologischen Aktivität startete bereits 1952.[88] Im zeitlichen Verlauf folgten weitere Studien zur Testung der Zytotoxizität von verschiedenen Kobalt-Komplexen.[89-94] Ali et al. (2016) synthetisierten Kobalt-Komplexe auf Salen-Basis und testeten ihre zytotoxische Wirkung auf solide Tumorzellen. Die apoptotische Wirkung zeigte sich weniger ausgeprägt, als die von Cisplatin, jedoch wiesen die Substanzen eine Selektivität gegenüber Krebszellen im Vergleich zu gesunden humanen Zellen auf.[95]

2.4.4. Aluminium-Komplexe in der Krebsforschung

Neben Übergangsmetall-Komplexen lag der Fokus dieser Arbeit auf einem Aluminium-Komplex. Aluminium ist ein Metall der dritten Hauptgruppe des Periodensystems der Elemente. Zusammen mit Salen-Liganden bildet dieses Metall stabile Komplexe. Aluminium-Salen-Komplexe sind hinsichtlich ihrer chemischen Eigenschaften vielfältig beschrieben worden.[56,96-100] Publikationen zu zytotoxischen Eigenschaften dieser Metall-Komplexe lagen in den Literaturdatenbanken bisher jedoch nicht vor.

2.5 Fragestellungen und Ziel der Arbeit

Mein Forschungsschwerpunkt in der Arbeitsgruppe Experimentelle Onkologie von Prof. Dr. med. Dr. rer. nat. Aram Prokop lag in der Untersuchung neuartiger Metall-Komplexe hinsichtlich der Wirksamkeit und Resistenzüberwindung in multiresistenten Tumorzellen. Daher habe ich im Rahmen meiner Promotionsarbeit verschiedene Metall-Komplexe und dessen Liganden in unterschiedlichen Zelllinien *in vitro* getestet. Alle Substanzen wurden mir von Prof. Dr. rer. nat. Albrecht Berkessel, Department für Organische Chemie der Universität zu Köln, und seinen Mitarbeitern Dr. rer. nat. Qifang Wang und Dr. rer. nat. Marc Brandenburg zur Verfügung gestellt.

Meine erste Publikation beschreibt die anti-proliferative Wirksamkeit des Salalen-Liganden WQF 044 in Leukämie- und soliden Tumorzellen. Darüber hinaus wird dort weitreichender auf

den Apoptosemechanismus der Substanz eingegangen. Dieser wurde mittels geeigneter Verfahren wie Western Blot Analysen, Polymerase-Kettenreaktionen (PCR) und dem Einsatz multiresistenter Zelllinien herausgefunden. Die Substanzen wurden von Dr. rer. nat. Qifang Wang und Prof. Dr. rer. nat. Albrecht Berkessel synthetisiert und mir zur Erforschung ihrer biologischen Aktivität zur Verfügung gestellt.[85,86]

Aufgrund der hoch interessanten Wirkweise von Salenen in Tumorzellen und der Tatsache, dass bisher kaum Kobalt-Salen-Komplexe hinsichtlich ihrer apoptotischen Aktivität untersucht worden sind, synthetisierte Prof. Dr. rer. nat. Albrecht Berkessel zusammen mit Dr. rer. nat. Marc Brandenburg den Kobalt-Salen-Komplex MBR-60 und stellte mir diesen zur Untersuchung seiner biologischen Aktivität bereit. Dessen Stabilität und katalytische Eigenschaften wurden zuvor bereits beschrieben.[101,102] Die Zytotoxizität in Leukämie- und soliden Tumorzellen und der Apoptosemechanismus dieses Komplexes wurden daraufhin von mir untersucht, anfangs zusammen mit Frau Liliane Abodo Onambele. Später führte ich die Arbeit eigenständig fort und verfasste daraus meine zweite Publikation. Ferner sollte gezeigt werden, dass der Ligand von MBR-60 keine Apoptose-induzierende Wirkung in Lymphomzellen hat.

Da die Apoptose-induzierende Wirkung des Kobalt-Salen-Komplexes MBR-60 sehr vielversprechend war, widmete ich mich daraufhin dem von Dr. rer. nat. Marc Brandenburg und Prof. Dr. rer. nat. Albrecht Berkessel zur Verfügung gestellten Aluminium-Salen-Komplex MBR-8. Bislang waren keine Daten zur biologischen Aktivität von Aluminium-Salen-Komplexen in der Literatur zu finden. Dies motivierte mich umso mehr, MBR-8 näher zu untersuchen und damit neue wissenschaftliche Erkenntnisse beizusteuern. Wie im Fall des Kobalt-Komplexes, testete ich auch hier zum Vergleich den passenden metallfreien Liganden. Die ersten Screeninguntersuchungen von MBR-8 habe ich gemeinsam mit Frau Liliane Abodo Onambele durchgeführt. Die anschließenden Experimente zur Untersuchung des Wirkmechanismus führte ich eigenständig durch. Aus den Ergebnissen verfasste ich meine dritte Publikation.

In meiner Arbeit konnte ich somit neuartige Metall-Komplexe und Metall-Komplex-Liganden finden, die im Gegensatz zu Cisplatin auch in Leukämie- und Lymphomzellen wirksam sind. Ferner sind die neuen metallhaltigen Wirkstoffe in der Lage, Zytostatika-multiresistente Tumor- und Leukämiezellen in die Apoptose zu treiben.

3. Material und Methoden

Der Material- und Methodenteil ist den Publikationen zu entnehmen.

4. Ergebnisse

Der Ergebnisteil ist den Publikationen zu entnehmen.

5. Diskussion

In der vorliegenden Arbeit wurde die Wirksamkeit neuartiger Metall-Komplexe und der Liganden in Leukämie- und soliden Tumorzellen getestet. Dadurch sollten neue Wirkstoffe gefunden werden, die insbesondere in Zytostatika-multiresistenten Zelllinien wirksam sind. Eine Übersicht über die Wirksamkeit der getesteten Substanzen in den verwendeten Zelllinien gibt Tab. 1 wieder. Tab. 2 erläutert die verwendeten Zelllinien.

Sub. / Zelll.	WQF 044	WQF-II-394	WQF-II-397	MBR-60	Ligand 5	MBR-8	Ligand 4
Nalm-6	< 3	> 100	50 – 100	< 70		30	
NDau	< 3			< 70		30	
NVCR	< 3						
BJAB	<3			< 50	> 100	< 10	> 100
BiBo	5						
7CCA	> 5			> 50			
BJAB FADDdn	10			< 50			
MCF-7/ mock	10 – 20					70 – 100	
MCF-7/ casp-3	> 20					70 – 100	
MelHO pIRES	60						
MelHO Bcl-2	> 60						
RM82	> 5						
RM82 SiHoVCR	5						

Tab. 1 AC_{50}-Werte der getesteten Substanzen (Sub.) in verschiedenen Zelllinien (Zelll.) in Mikromolar (µM). Die Werte geben die eingesetzten Konzentrationen an, bei denen die Hälfte der Zellen apoptotisch sind. Grau markierte Bereiche zeigen nicht getestete Kombinationen.

Zelllinie	Art der Neoplasie	Zytostatika-Resistenz	Bekannte Zytostatika-Ko-Resistenzen	Veränderter Wirkungs-mechanismus
Nalm-6	B-Zell akute lymphatische Leukämie	n.a.	n.a.	n.a.
NDau	B-Zell akute lymphatische Leukämie	Daunorubicin-resistente Nalm-6-Zellen	Cytarabin, Doxorubicin, Epirubicin, Etoposid, Fludarabin, Idarubicin, Mitoxantron, Paclitaxel, Vinblastin, Vincristin, Vindesin, Vinorelbin	P-Glykoprotein Überexpression
NVCR	B-Zell akute lymphatische Leukämie	Vincristin-resistente Nalm-6-Zellen	Daunorubicin, Doxorubicin, Epirubicin, Etoposid, Fludarabin, Idarubicin, Mitoxantron, Paclitaxel, Vinblastin, Vindesin, Vinorelbin	P-Glykoprotein Überexpression
BJAB	Burkitt-like Lymphom	n.a.	n.a.	n.a.
BiBo	Burkitt-like Lymphom	Vincristin-resistente BJAB-Zellen	Cytarabin, Daunorubicin, Paclitaxel, Vinblastin, Vindesin, Vinorelbin	Bcl-2 Überexpression
7CCA	Burkitt-like Lymphom	Doxorubicin-resistente BJAB-Zellen	Cladribin, Clofarabin, Cytarabin, Daunorubicin, Epirubicin, Etoposid, Fludarabin, Idarubicin, Mitoxantron, Paclitaxel, Vinblastin, Vincristin, Vindesin, Vinorelbin, 4-OH-Cyclophosphamid	Caspase-3 Unterexpression
BJAB FADDdn	Burkitt-like Lymphom	n.a.	n.a.	Expression einer dominant negativen FADD-Mutante
MCF-7/ mock	Adeno-karzinom der Mamma	n.a.	n.a.	n.a.
MCF-7/ casp-3	Adeno-karzinom der Mamma	n.a.	n.a.	Expression von Caspase-3

MelHO pIRES	Malignes Melanom	n.a.	n.a.	n.a.
MelHO Bcl-2	Malignes Melanom	n.a.	n.a.	Bcl-2 Überexpression
RM82	Ewing Sarkom	n.a.	n.a.	n.a.
RM82 SiHoVCR	Ewing Sarkom	Vincristin-resistente RM82-Zellen	Cytarabin, Daunorubicin, Doxorubicin, Epirubicin, Mitoxantron, Paclitaxel, Vinblastin, Vindesin, Vinorelbin	Unterexpression von CD95 und Procaspase-8

Tab. 2 Charakteristika der verwendeten Zelllinien. n.a. = nicht anwendbar.

5.1 Der metallfreie Salalen-Ligand WQF 044 induziert Apoptose über den mitochondrialen Apoptoseweg in resistenten Leukämie- und soliden Tumorzellen

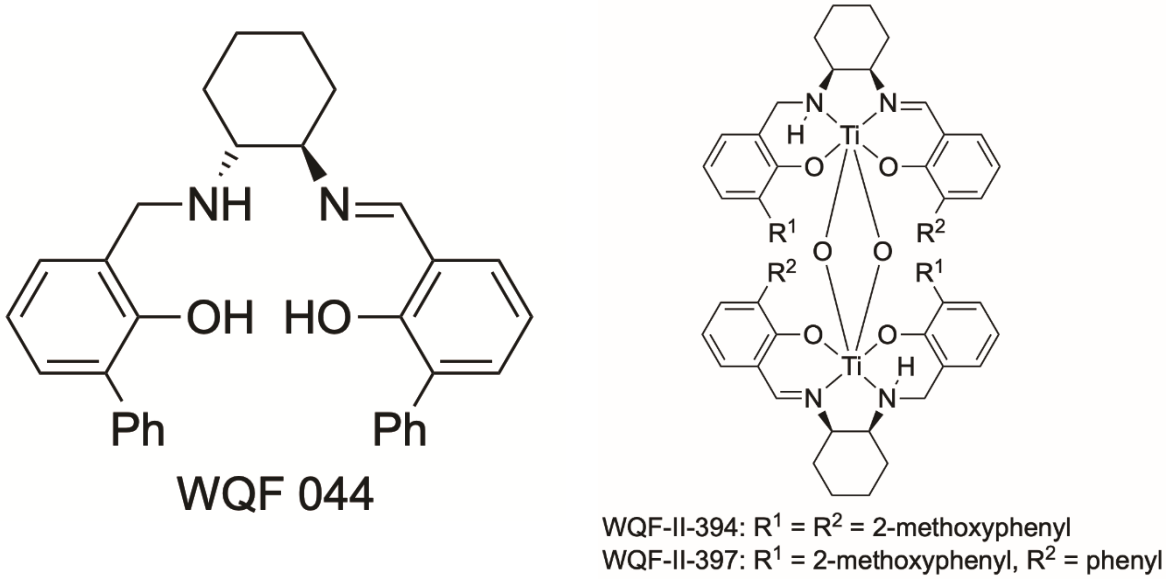

Abb. 3 Strukturformeln des Salalen-Liganden WQF 044 und der Titan-Komplexe WQF-II-394 und WQF-II-397.

5.1.1. Salalen-Ligand WQF 044 übertrifft die Titan-Salalen-Komplexe WQF-II-394 und -397 in seiner zytotoxischen Aktivität

Maligne Tumore entstehen durch eine Fehlregulation in der Zellproliferation und eine gestörte Apoptoseeinleitung in der Zelle. An diesen Mechanismen setzen Chemotherapeutika an, um in den Tumorzellen letztendlich die Apoptose zu induzieren.[103] Bei der Testung der Titan-Salalen-Komplexe WQF-II-394 und WQF-II-397, sowie dessen Salalen-Liganden WQF 044 stellte sich heraus, dass der Ligand die zugehörigen Metall-Komplexe in seiner Apoptose-induzierenden Wirksamkeit deutlich übertraf. Zur Veranschaulichung sind die Strukturformeln

der getesteten Substanzen in Abb. 3 zu finden. Bereits in Konzentrationen von unter 3 µM induzierte WQF 044 in über 50 Prozent der Zellen einer akuten lymphatischen Leukämie (Nalm-6) und eines Burkitt-like Lymphoms (BJAB) Apoptose (Publikation 1, Fig. 3 und Fig. 4a). WQF-II-397 zeigte immerhin einen Wirkbeginn bei einer Konzentration von 50 µM mit rund 30 Prozent apoptotischen Nalm-6-Zellen. Dahingegen blieben die Leukämiezellen durch den Einsatz von bis zu 100 µM von WQF-II-394 unbeeinflusst (Abb. 4). Es ist gut möglich, dass die Titan-Komplexe aufgrund ihrer strukturellen Gegebenheiten im Vergleich zu dem Liganden nicht oder nur erschwert in die Zielzelle gelangen konnten und daher deutlich höhere Konzentrationen zur Apoptoseinduktion nötig waren. Darüber hinaus zeigte diese Erkenntnis, dass nicht das Titan an sich, sondern das Grundgerüst des Liganden für die zytotoxische Wirkung verantwortlich war.

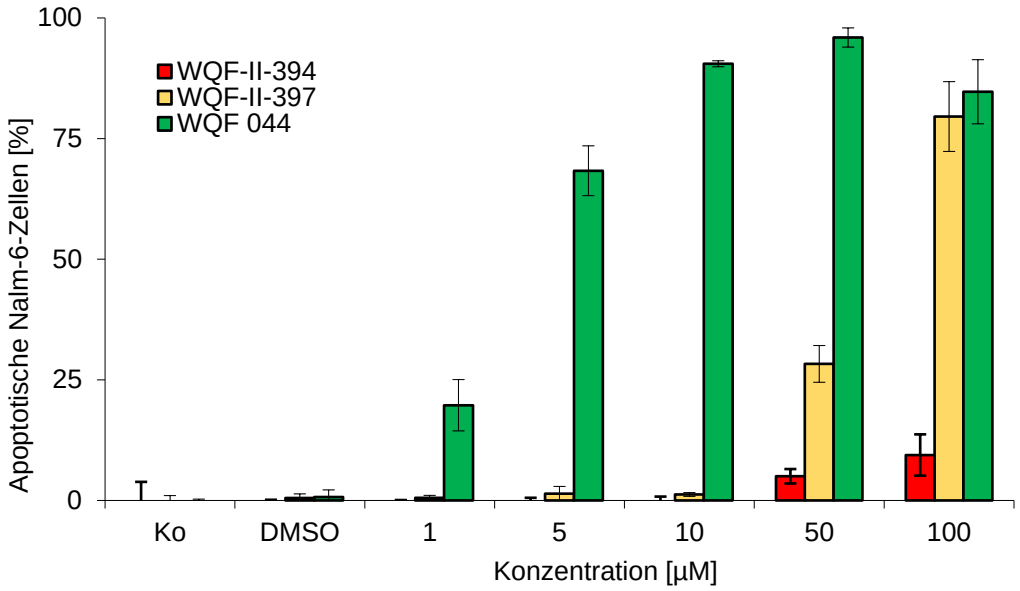

Abb. 4 Apoptoseinduktion von den Titan-Salalen-Komplexen WQF-II-394 und WQF-II-397, sowie dem Salalen-Liganden WQF 044 in Leukämiezellen (Nalm-6). Die Substanzen wurden in aufsteigenden Konzentrationen von 1 µM bis 100 µM auf Nalm-6 Zellen pipettiert und für 72 h bei 37°C inkubiert. Dabei blieben Kontrollzellen (Ko) unbehandelt und DMSO-Zellen (DMSO) lediglich mit dem Lösungsmittel DMSO behandelt. Die DNA-Fragmentierung wurde mittels FACScan Analyse gemessen. Pro eingesetzter Konzentration und Substanz wurden drei Proben verwendet. Die Werte geben den Prozentsatz an apoptotischen Zellen ± der Standardabweichung an. Im Methodenteil der Publikation 1 ist die detaillierte Versuchsbeschreibung zu finden.

Aufgrund der deutlich schwächeren Wirksamkeit der Titan-Komplexe lag der Fokus der ersten Publikation auf der zytostatischen Wirksamkeit des Salalen-Liganden. Es ist nicht vorhersehbar, ob ein Metall-Komplex oder sein Ligand zytostatisch wirksamer ist. Daher ist ein Vergleich der Wirksamkeit von Metall-Komplexen und Liganden sinnvoll. Frühere Publikationen beweisen die unvorhersehbare Wirkung von Liganden im Vergleich zu den

Komplexen. So haben beispielsweise Kilic et al. (2018) vier Hemi-Salen-Liganden und die zugehörigen Tribor-Komplexe in verschiedenen Tumorzellen *in vitro* getestet. Es waren deutlich niedrigere Konzentrationen der Liganden nötig, um vergleichbare zytotoxische Effekte wie die der Tribor-Komplexe zu erzeugen.[104] Dahingegen beschreibt eine weitere Arbeit von Ozbolat et al. (2018), dass ein Fe(III)-Komplex signifikant höhere zytotoxische Effekte in der Harnblasenkarzinom-Zelllinie ECV304 erzeugte als der passende Curcumin-Ligand. Dennoch waren hier beide Substanzen im niedrigen mikromolaren Bereich wirksam.[105] Drei Ruthenium(II) Komplexe waren *in vitro* deutlich zytotoxischer gegenüber Mamma- und Prostatakarzinomzellen als der metallfreie Ligand.[106]

5.1.2. WQF 044 wirkt Apoptose-induzierend in verschiedenen Tumorzellen

Die weiterführenden Experimente mit WQF 044 ergaben, dass der Ligand in Leukämie- (Nalm-6), Lymphom- (BJAB) und Ewing Sarkom Zellen (RM82), sowie in Mammakarzinom- (MCF-7) und Melanomzellen (MelHO) Apoptose induzieren kann (Publikation 1, Fig. 3, 4, 5 und 6). In den beiden zuletzt genannten Zelllinien waren etwas höhere Konzentrationen des Wirkstoffes nötig.[63,79,107]

Neben der Apoptoseinduktion zeigte sich auch eine steigende Inhibition der Zellproliferation bei steigenden Konzentrationen von WQF 044 (Publikation 1, Fig. 2b). Um auszuschließen, dass die Substanz Nekrose-induzierend statt Apoptose-induzierend auf Tumorzellen wirkte, wurde nach drei Stunden Inkubationszeit eine Messung des Enzyms Laktatdehydrogenase (LDH) durchgeführt. LDH wird in den ersten Stunden der Nekrose durch Membranschädigung beim Zellzerfall freigesetzt.[108] Es wurde keine LDH-Freisetzung detektiert, sodass der unspezifische Zelltod durch Nekrose ausgeschlossen werden konnte (Publikation 1, Fig. 2a). Bestätigt wurden die Ergebnisse durch den Nachweis von Früh- und Spätapoptose, sowie den Ausschluss von Nekrose mittels Annexin-Färbung in WQF 044 behandelten Nalm-6 Zellen (Publikation 1, Fig. 2c-e).

Bei den verwendeten Zelllinien ist zu erwähnen, dass ich die Ewing Sarkom Zelllinie RM82 eigenständig gegen Vincristin resistent gezüchtet habe. Ferner konnte ich mittels Western Blot Technik und PCR nachweisen, dass der Resistenzmechanismus dieser Zellen auf einer Unterexpression der Proteine CD95 und Caspase-8 beruht (Publikation 1, Fig. 6c). Die Vincristin-resistenten RM82SiHoVCR Zellen zeigen eine Ko-Resistenz gegenüber folgenden Zytostatika: Cytarabin, Daunorubicin, Doxorubicin, Epirubicin, Mitoxantron, Paclitaxel, Vinblastin, Vindesin und Vinorelbin (Tab.2).

5.1.3. WQF 044 induziert Apoptose über den intrinsischen Weg in resistenten Leukämie- und soliden Tumorzellen

Verschiedene Experimente zeigten, dass WQF 044 die Apoptose über den intrinsischen Signalweg einleitet. So konnte die Abhängigkeit der Substanz von Proteinen des

mitochondrialen Apoptosewegs nachgewiesen werden. In Nalm-6 Zellen wurde nach dem Einsatz der Substanz und einer Inkubationszeit von 48 Stunden ein Abfall des mitochondrialen Membranpotentials beobachtet (Publikation 1, Fig. 5a).

Darüber hinaus wirkt WQF 044 in Vincristin-resistenten BJAB Zellen (BiBo) und modifizierten MelHO-Zellen (MelHO Bcl-2) schwächer im Vergleich zu dessen Ausgangszellen (BJAB, MelHO pIRES) (Publikation 1, Fig. 4). BiBo und MelHO Bcl-2 Zellen zeichnen sich durch eine Überexpression des anti-apototischen Proteins Bcl-2 aus.[109] In BiBo-Zellen war noch eine geringe Wirksamkeit von WQF-044 zu beobachten, welche jedoch deutlich schwächer als in den BJAB Zellen war (Publikation 1, Fig. 4a). In den MelHO Bcl-2 Zellen löste WQF 044 im relevanten Konzentrationsbereich keine Apoptose aus, wohingegen die MelHO pIRES Zellen bei 20 bis 40 µM WQF 044 apoptotisch waren (Publikation 1, Fig. 4b). Im Gegensatz dazu zeigte sich in der PCR-Analyse von WQF 044-behandelten Nalm-6 Zellen eine 18-fache Unterexpression von Bcl-2 (Publikation 1, Tab. 2). Die fehlende Wirksamkeit in den MelHO Bcl-2 Zellen könnte auf die bekannte 30-fache Bcl-2 Überexpression dieser Zellen zurückzuführen sein, welche eine Aufhebung der zytostatischen Wirksamkeit von WQF 044 erzeugte. Die Überexpression von Bcl-2 ist ein häufiges Phänomen in Zytostatika-resistenten humanen Melanomen und limitiert auch hier den Einsatz von WQF 044.[110]

Unterstützt wurde die Bcl-2-Abhängigkeit von WQF 044 durch die Detektion einer fünffachen BAX-, einer 43-fachen Cytochrom c und einer 15-fachen SMAC-Überexpression in der PCR-Analyse von WQF 044 behandelten Nalm-6 Zellen (Publikation 1, Tab. 2). Aktiviertes Bax sendet vermehrt pro-apoptotische Signale aus, folglich werden Cytochrom c und SMAC freigesetzt.[111-113] Das anschließend gebildete Apoptosom induziert die Prozessierung von Procaspase-9, um die Caspasenkaskade zu aktivieren.[24] Die Procaspase-9-Prozessierung wurde in der Western Blot Analyse von WQF 044 behandelten Nalm-6 Zellen gezeigt (Publikation 1, Fig. 5e). Auffällig war, dass auch Procaspase-8 durch WQF 044 aktiviert wurde (Publikation 1, Fig. 5e), wohingegen weiterführende Experimente gegen eine Beteiligung des extrinsischen Signalwegs sprachen. Es ist anzunehmen, dass Procaspase-8 von Caspase-3 aktiviert wurde, wie es auch Wieder et al. (2001) beschrieben haben: die Procaspase-8-Prozessierung wurde in BJAB-Zellen postmitochondrial von Caspase-3 induziert – ohne den Einfluss von Proteinen des extrinsischen Apoptosewegs.[114] Gestützt wurde diese Tatsache im Zusammenhang mit WQF 044 durch die Detektion einer deutlichen Unterexpression von FADD und Fas (Publikation 1, Tab. 2).

Darüber hinaus wurde keine signifikant unterschiedliche Apoptoseinduktion durch WQF 044 in BJAB und BJAB/FADDdn Zellen beobachtet (Publikation 1, Fig. 6a). Letztgenannte Zellen wurden so modifiziert, dass sie kein FADD exprimieren. Die Wirkung von WQF 044 auf BJAB/FADDdn Zellen war daher unbeeinflusst von dem Fehlen von FADD. Dies unterstützte die Annahme, dass die Substanz unabhängig vom extrinsischen Signalweg ihre Wirkung

entfaltete. Noch beeindruckender war dies in den Vincristin-resistenten Ewing Sarkom Zellen (RM82SiHoVCR) zu sehen. Die Apoptose setzte in diesen Zellen bereits in deutlich niedrigeren Konzentrationen von WQF 044 ein als in der Ausgangszelllinie RM82 (Publikation 1, Fig. 6b). Diese Beobachtung bewies zum einen erneut die Unabhängigkeit der Substanz von dem extrinsischen Signalweg, da RM82SiHoVCR Zellen eine Unterexpression von CD95 und Procaspase-8 zeigten (Publikation 1, Fig. 6c). Zum anderen unterstrich sie die Wirkung von WQF 044 gegen Zytostatika-multiresistente Zellen, da die Zellen neben Vincristin auch gegen andere Vincaalkaloide, Anthrazykline und vor allem Platin-Derivate resistent sind (Tab. 2; Publikation 1, Tab. 1). Diese Daten zeigen, dass WQF 044 interessant im Hinblick auf den Einsatz als Chemotherapeutikum gegen Tumor-Rezidive ist, da ausgebildete Zytostatika-Resistenzen immer noch ein großes Problem bei der Behandlung von kindlichen Tumoren darstellen.[115,116]

Weiterführende Experimente bekräftigten die Annahme, dass WQF 044 die Apoptose Caspasen-abhängig induziert. Dies setzt eine korrekte Funktion der Caspasen, z.B. der von Caspase-3, voraus.[117] Die Abhängigkeit des Wirkstoffs von Caspase-3 wurde anhand von modifizierten Zelllinien bewiesen. Doxorubicin-resistente BJAB Zellen (7CCA) zeichnen sich durch eine Unterexpression von Caspase-3 aus.[63] Von den MCF-7 Zellen ist bekannt, dass sie keine Caspase-3 besitzen (MCF-7/mock).[118] In die modifizierten MCF-7 Zellen (MCF-7/casp-3) wurde Caspase-3 nachträglich inkorporiert. WQF 044 zeigte in den 7CCA und MCF-7/mock Zelllinien nahezu keine Apoptose-induzierende Wirkung im relevanten Konzentrationsbereich (Publikation 1, Fig. 5c, d), was den Beweis für eine Caspase-3-abhängige Wirksamkeit von WQF 044 darstellt. Zusätzlich verdeutlichte der Einsatz des Pancaspasen-Inhibitors zVAD-fmk, dass eine Blockade multipler Caspasen die Wirkungsentfaltung von WQF 044 in BJAB Zellen verhinderte (Publikation 1, Fig. 5b).

5.1.4. Apoptoseinduktion in multiresistenten Tumorzellen durch WQF 044

Die Entwicklung verschiedenster Resistenzmechanismen führt zu multiresistenten Tumor-Rezidiven.[119-121] 15 bis 20 Prozent der Kinder mit einer ALL entwickeln ein Rezidiv mit einer Entwicklung von Zytostatika-Multiresistenzen.[115] Die Heilungsraten bei einem ALL-Rezidiv sind deutlich niedriger als bei der Erstdiagnose einer ALL.[13,122] Die Suche nach neuartigen Zytostatika, welche Multiresistenzen überwinden, ist daher groß. Es gibt verschiedene Ursachen der Resistenzen. Dazu zählen Defekte in der Apoptose-Signalkaskade der Tumorzellen, die die Apoptoseinduktion verhindern und in der Expression von ABC-Transportern, die Zytostatika unter ATP-Verbrauch wieder aus der Zelle herausschleusen.[123-125] Die Fähigkeit von WQF 044 unabhängig von dem extrinsischen Apoptoseweg zu agieren, wurde in Kapitel 5.1.3. beschrieben. Diese kann als Überbrückungsmechanismus in der Therapie resistenter Tumore dienen, die aufgrund eines Defekts in diesem Signalweg entstanden sind und in vielfältiger Weise beschrieben wurden. So wurde beispielsweise eine

FADD-Überexpression in AML-Zellen mehrerer Patienten gefunden, die zu einem schlechteren Therapieoutcome führte.[126,127] Des Weiteren sind hohe Caspase-8-Level in Glioblastomen nachgewiesen worden, die mit einem schlechteren Therapieansprechen assoziiert waren. Es wurde angenommen, dass Caspase-8 an dieser Stelle seine apoptotische Aktivität verlor und neue anti-apoptotische Fähigkeiten annahm.[128] Dieses Phänomen zeigte sich in Zusammenhang mit einer FADD-Überexpression auch in Plattenepithelkarzinomen des Kopf- und Halsbereiches, Bronchial-, Larynx-, Pharynx-, Mamma- und Ovarialkarzinomen.[129-132]

Das Membranprotein P-gp ist ein ABC-Transporter. In der Chemotherapie führt die Überexpression von P-gp zu einer verminderten Zytostatikakonzentration in der Zelle und limitiert damit die Behandlung.[133] Zu den P-gp-abhängigen Zytostatika zählen Taxane, Anthrazykline und Vincaalkaloide, gegen die Tumorzellen mit P-gp Überexpression folglich resistent sind.[116,134,135] Der Resistenzmechanismus der Vincristin- und Daunorubicin-resistenten Nalm-6 Zellen (NVCR, NDau) beruht auf genau dieser P-gp Überexpression.[51,107] Beide resistenten Zelllinien weisen Ko-Resistenzen zu Fludarabin, Paclitaxel, Mitoxantron, Idarubicin, Doxorubicin, Epirubicin, Etoposid und den Vincaalkaloiden auf und zeigen damit einen ausgeprägten multiresistenten Charakter (Tab. 2; Publikation 1, Tab. 1). DNA-Fragmentierungs-Messungen in mit WQF 044 behandelten Nalm-6, NVCR und NDau Zellen resultierten in signifikant höheren Apoptosewerten der resistenten Zelllinien im Vergleich zu den ursprünglichen Nalm-6 Zellen (Publikation 1, Fig. 3). Damit war WQF 044 in der Lage, P-gp zu übergehen und die Apoptose in resistenten Leukämiezellen erfolgreich einzuleiten.

5.1.5. WQF 044 als Alternative zu Platin-Derivaten

Cisplatin wird zur Therapie einiger solider Tumoren verwendet. Da Platin-Derivate nicht in der Therapie der Leukämien und Lymphome eingesetzt werden, wurden keine vergleichenden Experimente mit WQF 044 und Cisplatin in Nalm-6 und BJAB Zellen durchgeführt. Stattdessen lag der Fokus auf der Resistenzüberwindung in Zellen, die gegen leitliniengerechte Zytostatika wie Vincristin, Doxorubicin und Daunorubicin resistent waren.

Beim Ewing Sarkom gibt es hingegen Studien, die auf eine Wirksamkeit von Platin-Derivaten in diesen Tumoren hinweisen.[136-139] In der Erstlinientherapie werden die Platin-Komplexe nicht standardmäßig eingesetzt. Erst bei Rezidiven oder refraktären Ewing Sarkomen kommen diese zum Einsatz. Generell liegt die 5-Jahres-Überlebensrate bei Patienten, die innerhalb von zwei Jahren ein Rezidiv eines Ewing Sarkoms erleiden, bei nur vier Prozent.[140] Eine retrospektive Studie mit 107 Patienten, die entweder eine Therapierefraktärität aufwiesen oder ein Rezidiv erlitten, zeigte das Potential von Platin-Derivaten. Die Patienten wurden mit einer Kombination aus Etoposid und Carboplatin (Etop-Carb) oder Etoposid und Cisplatin (Etop-Cis) behandelt. Das 5-Jahres-Überleben lag in der Etop-Carb Gruppe (24,5 Prozent) nur gering

über dem der Etop-Cis Gruppe (20 Prozent). Insbesondere schwere Nebenwirkungen limitierten die Therapie.[136]

Um das Potential von WQF 044 mit dem der Platin-Derivate zu vergleichen, wurden WQF 044, Cisplatin, Oxaliplatin und Carboplatin in den RM82 Zellen und in den Vincristin-resistent gezüchteten RM82SiHoVCR Zellen getestet. Vincristin gehört neben Ifosfamid, Doxorubicin und Etoposid zum Standardregime des sogenannten VIDE-Schemas der (neo-)adjuvanten Therapie von Ewing Sarkomen.[141] Eine Vincristin-Resistenz kann daher ein Grund für ein Nicht-Ansprechen auf die Therapie sein oder die Therapie bei Rezidiven limitieren.

Der Wirkbeginn von WQF 044 in RM82 Zellen lag wie in Kapitel 5.1.3. beschrieben bei 3 bis 5 µM mit einem AC_{50}-Wert von > 5 µM (Tab 1; Publikation 1, Fig. 6b). Dahingegen waren in den RM82SiHoVCR Zellen bei einer WQF 044 Konzentration von 3 µM bereits 36,1 Prozent der Zellen apoptotisch (AC_{50} = 5 µM). Im Vergleich dazu zeigt Abb. 5, dass die Platin-Derivate in deutlich höheren Konzentrationen eingesetzt werden müssen, um eine Induktion der Apoptose bewirken zu können. Cisplatin ergibt die insgesamt besten Ergebnisse unter den Platin-Verbindungen mit einem AC_{50}-Wert von 10 µM (Abb. 5a). Es fällt jedoch auf, dass Cisplatin in den Vincristin-resistenten Zellen schlechter wirkt als in den Wildtyp-Zellen. Eine Verdopplung der Cisplatin Konzentration von 5 auf 10 µM führt zu keinem Anstieg der Apoptosewerte in den RM82SiHoVCR Zellen. Daher kann von einer gewissen Resistenz der Zellen gegenüber Cisplatin gesprochen werden. Vergleicht man die Anzahl der apoptotischen Zellen durch Cisplatin bei 5 µM mit denen von WQF 044, wird ersichtlich, dass die Werte in den RM82 Zellen nahezu identisch sind. Dagegen weist WQF 044 eine deutlich bessere Wirksamkeit in den Vincristin-resistenten RM82 Zellen auf als Cisplatin.

Der Einsatz von Oxaliplatin in den Ewing Sarkom Zelllinien ergab einen Wirkbeginn bei 10 µM und damit deutlich später als in den mit WQF 044 behandelten Zellen (Abb. 5b). Nachdem mit 20 µM nochmals doppelt so viel Oxaliplatin auf die Zellen pipettiert wurde, ließ sich keine Erhöhung des Apoptose-induzierenden Effekts in den RM82SiHoVCR Zellen erkennen.

Am wenigsten wirksam ist Carboplatin (Abb. 5c). Nach dem Pipettieren von 10 µM zeigte sich in beiden Zelllinien noch keine eindeutige Apoptoseinduktion, weshalb die eingesetzte Konzentration auf 30 µM verdreifacht wurde. Auch in dieser Konzentration blieb die Apoptose in RM82SiHoVCR Zellen mit 11,74 Prozent sehr gering. In RM82 Zellen stieg sie immerhin auf 29,75 Prozent an. Weil die Apoptoseinduktion durch Carboplatin deutlich geringer war als die durch WQF 044, wurde keine weitere Konzentrationserhöhung vorgenommen.

Insgesamt übertrifft WQF 044 die Wirkung von Platinderivaten sowohl in ursprünglichen Ewing Sarkom Zellen, als auch in den multiresistent-gezüchteten Zellen. Damit könnte WQF 044 als eine aussichtsreiche Alternative für die Platin-Derivate bei der Behandlung der Therapie-refraktären und rezidivierten Ewing-Sarkome in Frage kommen, wenn die präklinischen und klinischen Testungen erfolgreich verlaufen sollten.

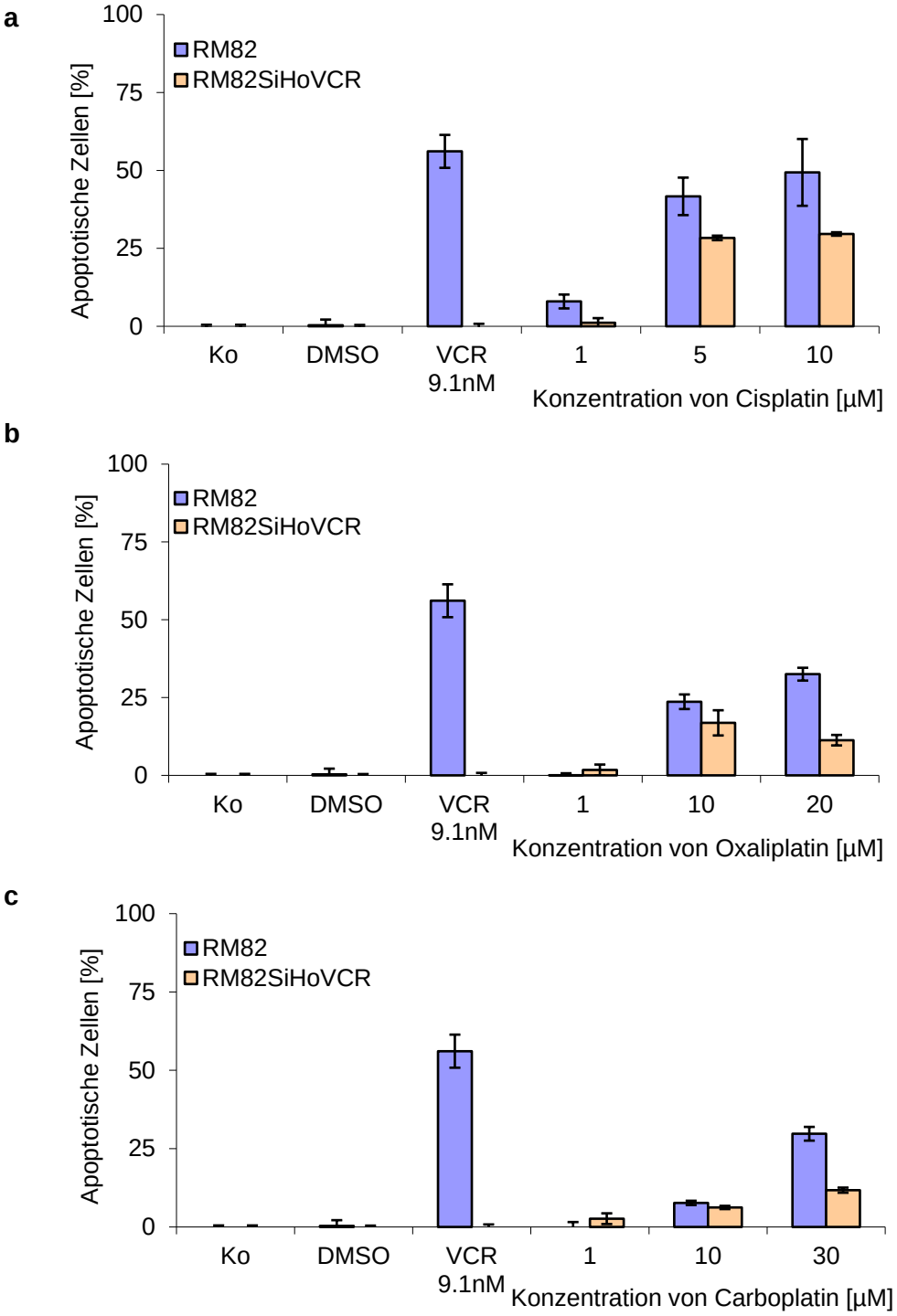

Abb. 5 Apoptoseinduktion von Platin-Derivaten in multiresistenten Ewing Sarkom Zellen. RM82 und RM82SiHoVCR Zellen wurden mit unterschiedlichen Konzentrationen von Platin-Derivaten behandelt und für 72 Stunden bei 37°C inkubiert. Kontrollzellen (Ko) blieben unbehandelt. Die DNA-Fragmentierung wurde mittels FACScan Analyse gemessen. Die Werte geben den Prozentsatz an apoptotischen Zellen ± der Standardabweichung an (n = 3). Eine genaue Methodenbeschreibung ist dem Methodenteil der Publikation 1 zu entnehmen. **a** Cisplatin in RM82 und RM82SiHoVCR **b** Oxaliplatin in RM82 und RM82SiHoVCR **c** Carboplatin in RM82 und RM82SiHoVCR.

5.2 Der Kobalt-Salen-Komplex MBR-60 induziert Apoptose in Burkitt-like Lymphom- und Leukämiezellen und überwindet Zytostatika-Multiresistenzen *in vitro*

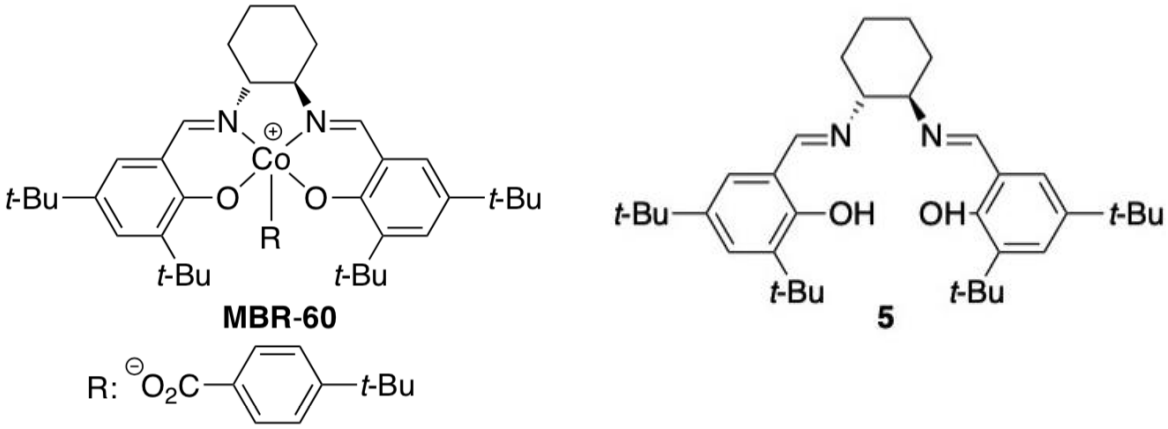

Abb. 6 Strukturformeln des Kobalt-Salen-Komplexes MBR-60 und des Liganden 5.

Salene spielen schon lange eine interessante Rolle bei der Entwicklung neuer Zytostatika, da sie die Fähigkeit haben, Metall-Komplexe zu bilden. [67,95,142] Der Kobalt-Salen-Komplex MBR-60 wurde zuvor noch nicht hinsichtlich seiner Aktivität in Tumorzellen getestet. Einige wenige andere Kobalt-Komplexe mit Anti-Tumor-Aktivität sind bereits beschrieben. Hauptsächlich in soliden Tumorzellen sind zytotoxische Aktivitäten beobachtet worden. Beispielsweise hemmte ein Kobalt(II) Salen Komplex die Zellproliferation in Zervixkarzinomzellen (HeLa) *in vitro*.[95] Ein weiterer Kobalt(II) Komplex wies eine *in vitro* Zytotoxizität in Zellen einer akuten T-Zell Leukämie (Jurkat-Zellen), eines Ovarialkarzinoms (SKOV3) und eines Glioblastoms (U87) auf.[143] Auch ein beschriebener Kobalt(III) Komplex induzierte Apoptose in niedrigen mikromolaren Konzentrationen in verschiedenen Tumorzellen, darunter HeLa und SKOV3 Zellen.[144]

5.2.1. Kobalt-Komplex MBR-60 oder Ligand 5: Wer wirkt besser?

Bei Betrachtung der zytostatischen Wirkung des Kobalt-Salen-Komplexes MBR-60 fällt auf, dass höhere Konzentrationen von MBR-60 im Vergleich zu WQF 044 nötig waren, um die Apoptose in BJAB Zellen zu induzieren (Publikation 2, Fig. 2a). Der AC_{50}-Wert der mit MBR-60 behandelten BJAB-Zellen lag bei rund 50 µM, für WQF bei unter 3 µM (Tab. 1). Dabei muss beachtet werden, dass die Inkubationszeit der MBR-60 behandelten Zellen mit 96 Stunden länger gewählt wurde als zuvor mit WQF 044 (72 Stunden), da erst nach dieser Zeit eine gute Wirksamkeit beobachtet wurde. Dies spricht für eine langsame Apoptose durch MBR-60 und ist ein Indiz für eine Transkriptionsabhängigkeit. Darüber hinaus wurde gezeigt, dass der Ligand 5 keine Apoptose-induzierende Wirksamkeit in den untersuchten

Konzentrationsbereichen aufwies (Publikation 2, Fig. 2a). Die chemischen Strukturformeln des Metall-Komplexes und des Liganden sind in Abb. 6 veranschaulicht. Anders als im Fall des Salalen-Liganden WQF 044 liegt hier der weitere Fokus auf dem Metall-Komplex.

5.2.2. MBR-60 wirkt anti-proliferativ und Apoptose-induzierend in Lymphom- und Leukämiezellen

Mittels Messung der LDH-Freisetzung nach einer Stunde wurde eine Nekrose-induzierende Wirkung von MBR-60 ausgeschlossen (Publikation 2, Fig. 2c). In den Lymphomzellen (BJAB) startete die Hemmung der Zellproliferation bei 10 µM von MBR-60. Bei einer Konzentration von 50 µM zeigte MBR-60 eine Hemmung der Proliferation von über 80 Prozent (Publikation 2, Fig. 2b). Neben der Wirkung in Lymphomzellen wurde auch eine Apoptoseinduktion in den Leukämiezellen (Nalm-6) nachgewiesen, wobei der AC_{50}-Wert bei 50 bis 70 µM lag (Publikation 2, Fig. 4).

5.2.3. Der Kobalt-Komplex MBR-60 induziert Apoptose über den intrinsischen Apoptoseweg

Der Wirkmechanismus von MBR-60 ähnelt dem von WQF 044. Das mitochondriale Membranpotential wird unter dem Einfluss des Kobalt-Komplexes in Nalm-6 Zellen herabgesetzt (Publikation 2, Fig. 6). Darüber hinaus wirkt die Substanz in Caspase-3 unterexprimierten 7CCA Zellen schlechter als in den ursprünglichen BJAB-Zellen und zeigt damit eine Caspase-3-abhängige Apoptoseinduktion (Publikation 2, Fig. 5). Die Aktivierung von Procaspase-3 durch MBR-60 spiegelt sich zudem in der Western Blot Analyse wider (Publikation 2, Fig. 7). Zusätzlich ist dort eine Aktivierung von Procaspase-9 und -8 zu sehen. Die Procaspase-9-Aktivierung unterstreicht zusätzlich die Apoptoseeinleitung über den mitochondrialen Weg. Die Aktivierung von Procaspase-8 mit gleichzeitiger CD95-Unabhängigkeit lässt sich durch die oben beschriebene Erkenntnis von Wieder et al. (2001) erklären (Publikation 2, Fig. 3 und 7).[114] Eine Apoptoseinduktion über den extrinsischen Weg ließ sich als primärer Wirkmechanismus ausschließen, denn MBR-60 induzierte gleichermaßen in BJAB und BJAB FADDdn Zellen unabhängig von CD95 Apoptose (Publikation 2, Fig. 3).

5.2.4. MBR-60 wirkt in multiresistenten Leukämiezellen

Der Kobalt-Salen-Komplex MBR-60 induziert gleichermaßen Apoptose in resistenten (NDau) und nicht-resistenten (Nalm-6) Leukämiezellen und überwindet dabei die P-gp Expression der NDau-Zellen (Publikation 2, Fig. 4). Damit ist auch MBR-60 ein neuer potentieller Wirkstoff gegen Zytostatika-resistente Leukämien.

5.3 Der Aluminium-Salen-Komplex MBR-8 sensibilisiert multiresistente Leukämiezellen gegenüber bekannten Zytostatika und wirkt apoptotisch in Leukämie-, Lymphom- und Mammakarzinomzellen

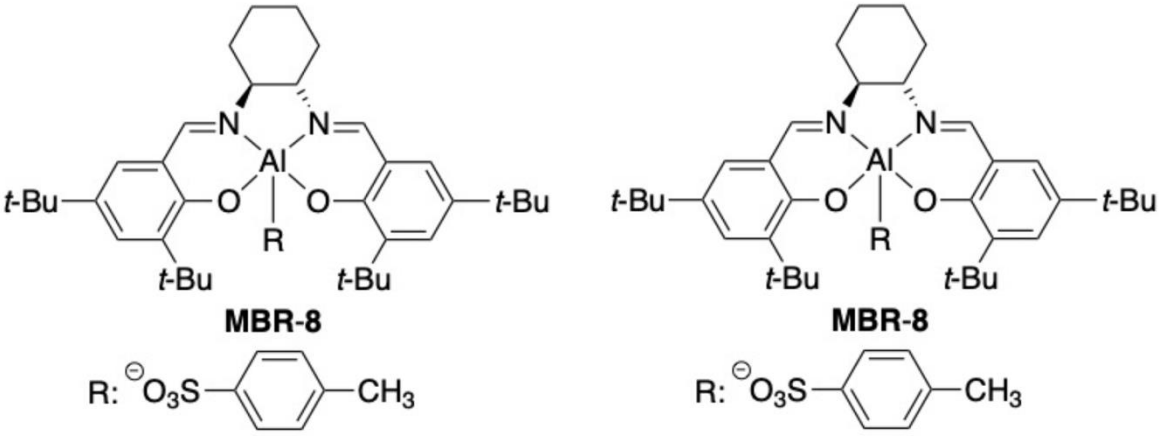

Abb. 7 Strukturformeln des Aluminium-Salen-Komplexes MBR-8 und des Liganden 4.

Ähnlich wie der Kobalt-Komplex basiert der Aluminium-Komplex MBR-8 auch auf einem speziellen Salen-Liganden (Ligand 4), der sich von trans-1,2-Diaminocyclohexan ableitet (Abb. 7). Aufgrund der Unwirksamkeit von Ligand 5 auf Tumorzellen, war bei Ligand 4 mit vergleichbaren Ergebnissen zu rechnen (Publikation 2, Fig. 2a). Dies bestätigte sich bei der Testung von Ligand 4 auf BJAB Zellen (Publikation 3, Fig. 3). Bei einer Konzentration von 100 µM konnte nur in zehn Prozent der Zellen die Apoptose induziert werden. Dagegen lag der AC_{50}-Wert des Aluminium-Salen-Komplexes MBR-8 in BJAB Zellen bei unter 10 µM (Tab. 1).

5.3.1. MBR-8 wirkt Apoptose-induzierend in verschiedenen Tumorzellen

Neben der Apoptose-induzierenden Wirkung in BJAB Zellen wirkt MBR-8 auch in den Leukämiezellen (Nalm-6) zytostatisch. Der AC_{50}-Wert liegt mit 30 µM etwas über dem in BJAB Zellen (Tab 1; Publikation 3, Fig. 4). Das Wirkspektrum von MBR-8 wird erweitert um Mammakarzinomzellen (MCF-7), in denen bei einer Konzentration von 70 bis 100 µM das Wirkmaximum erreicht wurde (Publikation 3, Fig. 5). Die Kinetik der Apoptoseinduktion ähnelt der des Kobalt-Salen-Komplexes MBR-60, da diese ebenfalls 96 Stunden dauerte.

Im Gegensatz zu Kobalt-Komplexen sind Aluminium-Komplexe im Hinblick auf zytotoxische Aktivitäten nahezu unerforscht. 2017 wurde eine Studie veröffentlicht, in der eine Aluminium-haltige Substanz erfolgreich als Photosensibilisator bei der Phototherapie von malignen Melanomen eingesetzt wurde.[145] *In vitro* Experimente, die die Apoptoseinduktion von Aluminium-Komplexen in Tumorzellen beschreiben, sind in der Literaturdatenbank Pubmed kaum zu finden. 1971 ist die Anti-Tumor-Aktivität von verschiedenen Metallen der dritten Hauptgruppe des Periodensystems näher erforscht worden.[146] Aluminium-, Gallium-, Indium-

und Thallium-Salze konnten die Tumoraktivität reduzieren, jedoch stellte sich damals nur Gallium-Salz als erfolgsversprechend heraus. Weitere Studien zu Gallium-Komplexen bewiesen die zytotoxische Aktivität dieses Metalls: Beschrieben ist beispielsweise Gallium-Pyridoxal, das proliferationshemmend in Gallium-Nitrat-resistenten AML-Zellen (HL60) und in T-ALL-Zellen (CCRF-CEM) wirkt.[147,148] Gallium-Nitrat selbst wirkt nachweislich antiproliferativ in Non-Hodgkin-Lymphom- und Harnblasenkarzinomzellen. Neben *in vitro* und *in vivo* Experimenten sind bereits klinische Studien mit Gallium-Nitrat durchgeführt worden.[149-153]
Die neuen Erkenntnisse der Wirksamkeit von MBR-8 sind daher sehr bemerkenswert und sollen ein Augenmerk auf dieses interessante Metall in der Entwicklung neuer Chemotherapeutika legen. Es wurde gezeigt, dass MBR-8 eine bessere zytostatische Wirksamkeit in Leukämie- (Nalm-6) und Lymphomzellen (BJAB) aufweist als MBR-60.

5.3.2. MBR-8 aktiviert Caspase-3 und senkt das mitochondriale Membranpotential

Um den durch MBR-8 induzierten Apoptosemechanismus näher zu verstehen, wurde MBR-8 in den MCF-7/mock und den Caspase-3-inkorporierten MCF-7/casp-3 Zellen getestet. Dabei ließ sich eine bessere Wirksamkeit in den MCF-7/casp-3 Zellen erkennen, sodass MBR-8 offenbar in Abhängigkeit von Caspase-3 Apoptose induziert (Publikation 3, Fig. 5). Dennoch induziert MBR-8 auch in den MCF-7/mock Zellen Apoptose, sodass von einem weitreichenderen Wirkungspotential ausgegangen werden kann. Die Aktivierung von Caspase-3 spiegelt sich ebenfalls in der Western Blot Analyse mit einer Verringerung der 32 kDa Procaspase-3 Bande und einer deutlichen Bande der prozessierten Caspase-3 bei 17 kDa wider (Publikation 3, Fig. 6). Mithilfe der JC-1-Messung konnte ein Verlust der mitochondrialen Membrandepolarisation von bis zu 42 Prozent bei 50 µM von MBR-8 in Nalm-6 Zellen nachgewiesen werden (Publikation 3, Fig. 7). Auch MBR-8 wirkt somit über den intrinsischen Apoptosesignalweg.

5.3.3. MBR-8 überwindet die P-gp Überexpression in Zytostatika-multiresistenten Leukämiezellen und sensibilisiert diese gegenüber herkömmlichen Zytostatika

Nach der Behandlung mit MBR-8 beginnt die Apoptoseinduktion in Daunorubicin-resistenten Nalm-6 Zellen (NDau) bei niedrigeren Konzentrationen als bei den Ursprungszellen (Publikation 3, Fig. 4). Die AC_{50}-Werte liegen in beiden Zelllinien bei einer Konzentration von 30 µM. Der Aluminium-Komplex MBR-8 überwindet die P-gp-Überexpression in NDau Zellen, die eine häufige Ursache für Resistenzen gegen gängige Chemotherapeutika darstellt.[154]
Bei der Nalm-6 Zelllinie handelt es sich um Zellen einer akuten lymphatischen Leukämie der B-Vorläufer-Zellen (BCP-ALL). Bei dieser Form der Leukämie ist das Outcome der Patienten stark abhängig von chromosomalen Translokationen.[155,156] So sprechen beispielsweise BCP-

ALL Patienten mit der Translokation t(17;19) extrem schlecht auf eine Hochdosis-Chemotherapie an.[157,158] Eine experimentelle Studie mit P-gp positiven t(17;19)-ALL Zellen ergab, dass die Wirksamkeit von Daunorubicin und Vincristin in diesen Zellen durch Nilotinib und Verapamil erhöht wurde, da diese zu einer Sensibilisierung der Tumorzellen führten.[159] Die Chemo-Sensibilisierung spielt eine immer größere Rolle, da durch den gezielten Zusatz von Wirkstoffen zur eigentlichen Chemotherapie eine Dosisminderung und gleichzeitige Wirkungsverstärkung geschaffen werden kann.[160-163] Dies reduziert unter anderem die Nebenwirkungsrate der Chemotherapeutika, die häufig die Therapie limitiert.[164] Im Hinblick auf die BCP-ALL sind weitere Daten zur Chemo-Sensibilisierung veröffentlicht. Die Kombination eines Pafah1b Inhibitors mit Tyrosinkinaseinhibitoren erhöhte die Therapieeffektivität in BCR-ABL1-positiven BCP-ALL-Zellen.[165] RAS-Signalweg-mutierte Prednisolon-resistente BCP-ALL-Zellen konnten durch den MEK-Inhibitor Trametinib gegenüber Prednisolon sensibilisiert werden.[166] Der Galektin-1-Inhibitor PTX008 sensibilisierte BCP-ALL-Zellen gegenüber Vincristin.[167] Auch SMAC-Mimetika wiesen synergistische Effekte mit Vincristin, Dexamethason und Asparaginase in BCP-ALL-Zellen auf.[168] Die zahlreichen Studien verdeutlichen den hohen therapeutischen Stellenwert von synergistischen Wirkstoffen in der ALL-Therapie.[169-172]

MBR-8 weist ebenfalls das Potential auf, Leukämiezellen gegenüber Zytostatika zu sensibilisieren. Die Kombination von niedrigen Konzentrationen von MBR-8 und Vincristin, in denen in Monotherapie keine apoptotischen Effekte erzielt werden, führt in Nalm-6 Zellen zu einer Wirkverstärkung um bis zu 853 Prozent (Publikation 3, Fig. 9b). Ähnliche synergistische Effekte wurden mit MBR-8 und Doxorubicin in Nalm-6 Zellen beobachtet. Die Apoptoserate wurde durch den gemeinsamen Einsatz der Substanzen von 13,1 Prozent auf über 75 Prozent gesteigert (Publikation 3, Fig. 9c). Noch beeindruckender zeigte sich die Sensibilisierung der Nalm-6 Zellen durch MBR-8 in der Kombination mit Vincristin. Die Addition der apoptotischen Zellen beim einzelnen Einsatz von 1 µM MBR-8 und 8 nM Daunorubicin ergab lediglich 2,3 Prozent Apoptose. Setzt man die beiden Substanzen gemeinsam auf den Zellen ein, so liegt die Apoptoseinduktion bei über 56 Prozent. Dies entspricht einem synergistischen Effekt von 2465 Prozent (Publikation 3, Fig. 9a). Aufgrund dieses hohen Effekts wurde die Kombination von MBR-8 und Daunorubicin zusätzlich auf den Daunorubicin-resistenten NDau Zellen getestet. Eingesetzt wurden Daunorubicin Konzentrationen von 53 nM und 55 nM, bei denen auf den Nalm-6 Zellen im Vergleich zu den NDau Zellen bekanntlich ein deutlicher apoptotischer Effekt zu erkennen ist. Erstaunlicherweise war das Ergebnis auf den NDau Zellen vergleichbar mit dem auf den Nalm-6 Zellen. Der synergistische Effekt lag bei der höheren Daunorubicin Konzentration in Kombination mit 1 µM MBR-8 sogar bei wahnsinnigen 5790 Prozent (Publikation 3, Fig. 9d). MBR-8 zeigte damit ein großes Potential zur Sensibilisierung Zytostatika-multiresistenter Leukämiezellen für die Chemotherapie.

5.4 MBR-8 zeigte die besten Synergien mit bekannten Zytostatika im Vergleich zu MBR-60 und WQF 044

Vergleicht man die synergistischen Effekte des Aluminium-Komplexes MBR-8 mit denen der anderen beiden neu entdeckten Wirkstoffe WQF 044 und MBR-60, so übertrifft MBR-8 diese in seinem Potential. Die wirkungsverstärkenden Effekte erreichten bis zu 2465 Prozent bei der Kombination von MBR-8 und Daunorubicin in Nalm-6 Zellen (Publikation 3, Fig. 9a-c). Dennoch zeigten auch MBR-60 und WQF 044 eine deutliche Sensibilisierung von Tumorzellen gegen Chemotherapien. Die kombinierte Behandlung von Nalm-6 Zellen mit MBR-60 und Daunorubicin ergab einen synergistischen Effekt von 378 Prozent (Publikation 2, Fig. 9); die von MBR-60 und Vincristin führte immerhin zu 161 Prozent mehr Apoptose im Vergleich zur Einzeltherapie (Publikation 2, Fig. 10). WQF 044 ist in Kombination mit Vincristin auf den BJAB-Lymphomzellen getestet worden. Dabei resultierte der gemeinsame Einsatz der Substanzen in niedrigen Konzentrationen in einer Wirkungsverstärkung um 352 bzw. 375 Prozent (Publikation 1, Fig. 7). Damit haben alle drei Substanzen das Potential, synergistische Effekte mit gängigen Zytostatika zu entwickeln und die Wirksamkeit von Chemotherapien zu verstärken.

5.5 Selektivität der Wirkstoffe in gesunden humanen Leukozyten

Einen ersten Hinweis auf eine selektive Wirkung der neuen Agentien in malignen Zellen zeigte ein Selektivitätstest mit gesunden humanen Leukozyten. Im für Leukämie- und Lymphomzellen relevanten Wirkbereich wurden verschiedene Konzentrationen der neuen Wirkstoffe eingesetzt und dessen Toxizität auf die Leukozyten getestet. Bei einer WQF 044 Konzentration von 3 µM, wo der AC_{50}-Wert in Nalm-6 und BJAB Zellen bereits erreicht war, wurde keine Apoptose in Leukozyten nachgewiesen (Publikation 1, Fig. 8). Erhöhte man die Wirkstoffkonzentration auf 5 µM, befanden sich lediglich zehn Prozent der humanen Leukozyten in Apoptose.

Der Kobalt-Salen-Komplex MBR-60 wurde in Konzentrationen von 50 bis 70 µM auf den Leukozyten eingesetzt. Dabei stieg die Apoptoserate von 12,5 Prozent bei 50 µM auf 19,7 Prozent bei 100 µM leicht an (Publikation 2, Fig. 8). Vergleicht man aber die Werte mit denen in Nalm-6-Zellen (75,5 Prozent Apoptose bei 100 µM MBR-60), so ist von einer deutlichen Selektivität zu sprechen.

MBR-8 ist mit einer Konzentration von 30 µM untersucht worden: Nur vier Prozent der Leukozyten befanden sich dabei in Apoptose (Publikation 3, Fig. 8). Erhöhte man die MBR-8 Konzentration auf 50 µM, blieb die Apoptoseinduktion in den gesunden Zellen unverändert niedrig. Alle drei Substanzen weisen somit eine Selektivität gegenüber malignen Zellen auf. Die Ergebnisse sind beim Einsatz von WQF 044 und MBR-8 jedoch besser als bei MBR-60.

5.6 Ausblick

Abschließend zeigt diese Arbeit die erfolgreiche präklinische Evaluation von Metall-Komplexen und Metall-Komplex-Liganden im Hinblick auf die zytostatische Wirksamkeit in Leukämie- und soliden Tumorzellen. Die Untersuchung von neuartigen Metall-Komplexen spielt seit der Entdeckung von Cisplatin eine immer größere Rolle in der hämatoonkologischen Forschung. In den vorliegenden *in vitro* Testungen des Salalen-Liganden WQF 044, des Kobalt-Salen-Komplexes MBR-60 und des Aluminium-Salen-Komplexes MBR-8 wird das zytostatische Potential aller drei Wirkstoffe deutlich. Die neuartigen Zytostatika induzieren Apoptose über den mitochondrialen Apoptose-Signalweg in multiresistenten Leukämie-, Lymphom- und anderen soliden Tumorzellen in niedrigen mikromolaren Konzentrationen. In Leukämie- und Lymphomzellen sind synergistische Effekte mit herkömmlichen Zytostatika gezeigt worden.

Die ersten *in vitro* Ergebnisse zeigen neue Metall-Komplexe als potentielle Zytostatika in Zytostatika-resistenten Tumor- und Leukämiezellen. Erste *ex vivo* Ergebnisse in gesunden humanen Leukozyten belegen bereits eine Selektivität der neuen Wirkstoffe gegenüber Tumorzellen. Als weitere *ex vivo* Versuche könnten Wirkstoff-Testungen in entnommenem Tumormaterial von Patienten durchgeführt werden. Das biologische Material wird dabei außerhalb des Patienten kultiviert und den Zytostatika in unterschiedlichen Konzentrationen ausgesetzt.

Der nächste Schritt in der Erforschung von WQF 044, MBR-60 und MBR-8 liegt in der *in vivo* Testung. Anhand von Maus-Modellen wird die Wirksamkeit in lebenden Organismen getestet und dient damit als Grundlage für die darauffolgende klinische Erforschung. Hierzu werden klinisch relevante und molekular charakteristische Maus-Modelle verwendet. Künftige *in vivo* Studien sind zur Testung der *in vivo* Wirksamkeit und Aufdeckung möglicher Nebenwirkungen der Wirkstoffe erforderlich. Zusätzlich können die beeindruckenden synergistischen Effekte der drei Wirkstoffe anhand kombinierter Zytostatika-Therapien in den Mäusen überprüft werden. Die *in vivo* Versuche können sowohl die Limitationen der Wirkstoffe aufzeigen, als auch bisher nicht bekanntes Potential hervorbringen.

6. Literaturverzeichnis

1. Ward E, DeSantis C, Robbins A, Kohler B, Jemal A. Childhood and adolescent cancer statistics, 2014. *CA Cancer J Clin* 2014; **64**(2): 83-103.
2. Seth R, Singh A. Leukemias in Children. *Indian J Pediatr* 2015; **82**(9): 817-24.
3. Steliarova-Foucher E, Colombet M, Ries LAG, et al. International incidence of childhood cancer, 2001-10: a population-based registry study. *Lancet Oncol* 2017; **18**(6): 719-31.
4. Mori T. Childhood lymphoma. *Rinsho Ketsueki* 2016; **57**(10): 2285-93.
5. Madhusoodhan PP, Carroll WL, Bhatla T. Progress and Prospects in Pediatric Leukemia. *Curr Probl Pediatr Adolesc Health Care* 2016; **46**(7): 229-41.
6. Hoelzer D, Bassan R, Dombret H, et al. Acute lymphoblastic leukaemia in adult patients: ESMO Clinical Practice Guidelines for diagnosis, treatment and follow-up. *Ann Oncol* 2016; **27**(suppl 5): v69-v82.
7. Rosenberg B, VanCamp L, Trosko JE, Mansour VH. Platinum compounds: a new class of potent antitumour agents. *Nature* 1969; **222**(5191): 385-6.
8. Rosenberg B, Vancamp L, Krigas T. Inhibition of Cell Division in Escherichia Coli by Electrolysis Products from a Platinum Electrode. *Nature* 1965; **205**: 698-9.
9. Dasari S, Tchounwou PB. Cisplatin in cancer therapy: molecular mechanisms of action. *Eur J Pharmacol* 2014; **740**: 364-78.
10. Prestayko AW, D'Aoust JC, Issell BF, Crooke ST. Cisplatin (cis-diamminedichloroplatinum II). *Cancer Treat Rev* 1979; **6**(1): 17-39.
11. Amable L. Cisplatin resistance and opportunities for precision medicine. *Pharmacol Res* 2016; **106**: 27-36.
12. Mi M, Zhang C, Liu Z, Wang Y, Li J, Zhang L. Gemcitabine, cisplatin, and dexamethasone and ifosfamide, carboplatin, and etoposide regimens have similar efficacy as salvage treatment for relapsed/refractory aggressive lymphoma: A retrospectively comparative study. *Medicine (Baltimore)* 2020; **99**(49): e23412.
13. Vrooman LM, Silverman LB. Treatment of Childhood Acute Lymphoblastic Leukemia: Prognostic Factors and Clinical Advances. *Curr Hematol Malig Rep* 2016; **11**(5): 385-94.
14. Raetz EA, Bhatla T. Where do we stand in the treatment of relapsed acute lymphoblastic leukemia? *Hematology Am Soc Hematol Educ Program* 2012; **2012**: 129-36.
15. Pierro J, Hogan LE, Bhatla T, Carroll WL. New targeted therapies for relapsed pediatric acute lymphoblastic leukemia. *Expert Rev Anticancer Ther* 2017; **17**(8): 725-36.
16. Zaman S, Wang R, Gandhi V. Targeting the apoptosis pathway in hematologic malignancies. *Leuk Lymphoma* 2014; **55**(9): 1980-92.
17. Hassen S, Ali N, Chowdhury P. Molecular signaling mechanisms of apoptosis in hereditary non-polyposis colorectal cancer. *World J Gastrointest Pathophysiol* 2012; **3**(3): 71-9.

18. Meier P, Finch A, Evan G. Apoptosis in development. *Nature* 2000; **407**(6805): 796-801.
19. Cotter TG. Apoptosis and cancer: the genesis of a research field. *Nat Rev Cancer* 2009; **9**(7): 501-7.
20. Plati J, Bucur O, Khosravi-Far R. Apoptotic cell signaling in cancer progression and therapy. *Integr Biol (Camb)* 2011; **3**(4): 279-96.
21. Kerr JF, Wyllie AH, Currie AR. Apoptosis: a basic biological phenomenon with wide-ranging implications in tissue kinetics. *Br J Cancer* 1972; **26**(4): 239-57.
22. Kroemer G, Dallaporta B, Resche-Rigon M. The mitochondrial death/life regulator in apoptosis and necrosis. *Annu Rev Physiol* 1998; **60**: 619-42.
23. Lambert IH, Hoffmann EK, Jorgensen F. Membrane potential, anion and cation conductances in Ehrlich ascites tumor cells. *J Membr Biol* 1989; **111**(2): 113-31.
24. Kroemer G, Galluzzi L, Brenner C. Mitochondrial membrane permeabilization in cell death. *Physiol Rev* 2007; **87**(1): 99-163.
25. Goldar S, Khaniani MS, Derakhshan SM, Baradaran B. Molecular mechanisms of apoptosis and roles in cancer development and treatment. *Asian Pac J Cancer Prev* 2015; **16**(6): 2129-44.
26. Deveraux QL, Roy N, Stennicke HR, et al. IAPs block apoptotic events induced by caspase-8 and cytochrome c by direct inhibition of distinct caspases. *EMBO J* 1998; **17**(8): 2215-23.
27. Chen HC, Kanai M, Inoue-Yamauchi A, et al. An interconnected hierarchical model of cell death regulation by the BCL-2 family. *Nat Cell Biol* 2015; **17**(10): 1270-81.
28. Chipuk JE, Moldoveanu T, Llambi F, Parsons MJ, Green DR. The BCL-2 family reunion. *Mol Cell* 2010; **37**(3): 299-310.
29. Shamas-Din A, Brahmbhatt H, Leber B, Andrews DW. BH3-only proteins: Orchestrators of apoptosis. *Biochim Biophys Acta* 2011; **1813**(4): 508-20.
30. Youle RJ, Strasser A. The BCL-2 protein family: opposing activities that mediate cell death. *Nat Rev Mol Cell Biol* 2008; **9**(1): 47-59.
31. Guicciardi ME, Gores GJ. Life and death by death receptors. *FASEB J* 2009; **23**(6): 1625-37.
32. Jin Z, El-Deiry WS. Overview of cell death signaling pathways. *Cancer Biol Ther* 2005; **4**(2): 139-63.
33. Cohen GM. Caspases: the executioners of apoptosis. *Biochem J* 1997; **326 (Pt 1)**: 1-16.
34. Baud V, Karin M. Signal transduction by tumor necrosis factor and its relatives. *Trends Cell Biol* 2001; **11**(9): 372-7.
35. Erxleben A. Mitochondria-Targeting Anticancer Metal Complexes. *Curr Med Chem* 2019; **26**(4): 694-728.

36. Kelland L. The resurgence of platinum-based cancer chemotherapy. *Nat Rev Cancer* 2007; **7**(8): 573-84.
37. Milosavljevic N, Duranton C, Djerbi N, et al. Nongenomic effects of cisplatin: acute inhibition of mechanosensitive transporters and channels without actin remodeling. *Cancer Res* 2010; **70**(19): 7514-22.
38. Bruijnincx PC, Sadler PJ. New trends for metal complexes with anticancer activity. *Curr Opin Chem Biol* 2008; **12**(2): 197-206.
39. Liang JX, Zhong HJ, Yang G, Vellaisamy K, Ma DL, Leung CH. Recent development of transition metal complexes with in vivo antitumor activity. *J Inorg Biochem* 2017; **177**: 276-86.
40. Ott I, Gust R. Non platinum metal complexes as anti-cancer drugs. *Arch Pharm (Weinheim)* 2007; **340**(3): 117-26.
41. Galanski M, Jakupec MA, Keppler BK. Update of the preclinical situation of anticancer platinum complexes: novel design strategies and innovative analytical approaches. *Curr Med Chem* 2005; **12**(18): 2075-94.
42. Ott I, Gust R. [Special qualities of inorganic cytostatics. Medicinal chemistry of platinum complexes]. *Pharm Unserer Zeit* 2006; **35**(2): 124-33.
43. Rabik CA, Dolan ME. Molecular mechanisms of resistance and toxicity associated with platinating agents. *Cancer Treat Rev* 2007; **33**(1): 9-23.
44. Geldmacher Y, Splith K, Kitanovic I, et al. Cellular impact and selectivity of half-sandwich organorhodium(III) anticancer complexes and their organoiridium(III) and trichloridorhodium(III) counterparts. *J Biol Inorg Chem* 2012; **17**(4): 631-46.
45. Dobroschke M, Geldmacher Y, Ott I, et al. Cytotoxic rhodium(III) and iridium(III) polypyridyl complexes: structure-activity relationships, antileukemic activity, and apoptosis induction. *ChemMedChem* 2009; **4**(2): 177-87.
46. Meggers E, Atilla-Gokcumen GE, Grundler K, Frias C, Prokop A. Inert ruthenium half-sandwich complexes with anticancer activity. *Dalton Trans* 2009; (48): 10882-8.
47. Schmidt C, Albrecht L, Balasupramaniam S, et al. A gold(i) biscarbene complex with improved activity as a TrxR inhibitor and cytotoxic drug: comparative studies with different gold metallodrugs. *Metallomics* 2019; **11**(3): 533-45.
48. Serebryanskaya TV, Lyakhov AS, Ivashkevich LS, et al. Gold(I) thiotetrazolates as thioredoxin reductase inhibitors and antiproliferative agents. *Dalton Trans* 2015; **44**(3): 1161-9.
49. Schmidt C, Karge B, Misgeld R, Prokop A, Bronstrup M, Ott I. Biscarbene gold(i) complexes: structure-activity-relationships regarding antibacterial effects, cytotoxicity, TrxR inhibition and cellular bioavailability. *Medchemcomm* 2017; **8**(8): 1681-9.

50. Schmidt C, Karge B, Misgeld R, et al. Gold(I) NHC Complexes: Antiproliferative Activity, Cellular Uptake, Inhibition of Mammalian and Bacterial Thioredoxin Reductases, and Gram-Positive Directed Antibacterial Effects. *Chemistry* 2017; **23**(8): 1869-80.
51. Rubbiani R, Kitanovic I, Alborzinia H, et al. Benzimidazol-2-ylidene gold(I) complexes are thioredoxin reductase inhibitors with multiple antitumor properties. *J Med Chem* 2010; **53**(24): 8608-18.
52. Canali L, Sherrington DC. Utilisation of homogeneous and supported chiral metal(salen) complexes in asymmetric catalysis. *Chemical Society Reviews* 1999; **28**(2): 85-93.
53. Matsumoto K, Saito B, Katsuki T. Asymmetric catalysis of metal complexes with non-planar ONNO ligands: salen, salalen and salan. *Chem Commun (Camb)* 2007; (35): 3619-27.
54. Cozzolino M, Leo V, Tedesco C, Mazzeo M, Lamberti M. Salen, salan and salalen iron(iii) complexes as catalysts for CO2/epoxide reactions and ROP of cyclic esters. *Dalton Trans* 2018; **47**(37): 13229-38.
55. Larrow JF, Jacobsen EN. Asymmetric Processes Catalyzed by Chiral (Salen)Metal Complexes. Organometallics in Process Chemistry; 2004: 123-52.
56. Gualandi A, Calogero F, Potenti S, Cozzi PG. Al(Salen) Metal Complexes in Stereoselective Catalysis. *Molecules* 2019; **24**(9).
57. Peri D, Meker S, Manna CM, Tshuva EY. Different ortho and para electronic effects on hydrolysis and cytotoxicity of diamino bis(phenolato) "salan" Ti(IV) complexes. *Inorg Chem* 2011; **50**(3): 1030-8.
58. Immel TA, Grutzke M, Batroff E, Groth U, Huhn T. Cytotoxic dinuclear titanium-salan complexes: structural and biological characterization. *J Inorg Biochem* 2012; **106**(1): 68-75.
59. Immel TA, Groth U, Huhn T, Ohlschlager P. Titanium salan complexes displays strong antitumor properties in vitro and in vivo in mice. *PLoS One* 2011; **6**(3): e17869.
60. Immel TA, Grutzke M, Spate AK, Groth U, Ohlschlager P, Huhn T. Synthesis and X-ray structure analysis of a heptacoordinate titanium(IV)-bis-chelate with enhanced in vivo antitumor efficacy. *Chem Commun (Camb)* 2012; **48**(46): 5790-2.
61. Meker S, Manna CM, Peri D, Tshuva EY. Major impact of N-methylation on cytotoxicity and hydrolysis of salan Ti(IV) complexes: sterics and electronics are intertwined. *Dalton Trans* 2011; **40**(38): 9802-9.
62. Luna-Garcia R, Damian-Murillo BM, Barba V, Hopfl H, Beltran HI, Zamudio-Rivera LS. Structure and conformational motion of seven-coordinate diorganotin(IV) complexes derived from salen and salan type ligands. *J Organomet Chem* 2009; **694**(24): 3965-72.
63. Dragoun M, Gunther T, Frias C, Berkessel A, Prokop A. Metal-free salan-type compound induces apoptosis and overcomes multidrug resistance in leukemic and lymphoma cells in vitro. *J Cancer Res Clin Oncol* 2018; **144**(4): 685-95.

64. Mir JM, Jain N, Jaget PS, Maurya RC. Density functionalized [Ru(II)(NO)(Salen)(Cl)] complex: Computational photodynamics and in vitro anticancer facets. *Photodiagnosis Photodyn Ther* 2017; **19**: 363-74.

65. Terenzi A, Lotsch D, van Schoonhoven S, et al. Another step toward DNA selective targeting: Ni(II) and Cu(II) complexes of a Schiff base ligand able to bind gene promoter G-quadruplexes. *Dalton Trans* 2016; **45**(18): 7758-67.

66. Ghanbari Z, Housaindokht MR, Izadyar M, et al. Structure-activity relationship for Fe(III)-salen-like complexes as potent anticancer agents. *ScientificWorldJournal* 2014; **2014**: 745649.

67. Woldemariam GA, Mandal SS. Iron(III)-salen damages DNA and induces apoptosis in human cell via mitochondrial pathway. *J Inorg Biochem* 2008; **102**(4): 740-7.

68. Mohammadi M, Yazdanparast R. Methoxy VO-salen complex: in vitro antioxidant activity, cytotoxicity evaluation and protective effect on CCl4-induced oxidative stress in rats. *Food Chem Toxicol* 2009; **47**(4): 716-21.

69. Herchel R, Sindelar Z, Travnicek Z, Zboril R, Vanco J. Novel 1D chain Fe(III)-salen-like complexes involving anionic heterocyclic N-donor ligands. Synthesis, X-ray structure, magnetic, (57)Fe Mossbauer, and biological activity studies. *Dalton Trans* 2009; (44): 9870-80.

70. Szumera M. Structural investigations of silicate-phosphate glasses containing MoO3 by FTIR, Raman and 31P MAS NMR spectroscopies. *Spectrochim Acta A Mol Biomol Spectrosc* 2014; **130**: 1-6.

71. Li CY, Li XY, Shen L, Ji HF. Regulatory effects of transition metals supplementation/deficiency on the gut microbiota. *Appl Microbiol Biotechnol* 2021; **105**(3): 1007-15.

72. Johnstone TC, Suntharalingam K, Lippard SJ. Third row transition metals for the treatment of cancer. *Philos Trans A Math Phys Eng Sci* 2015; **373**(2037).

73. Silvestri S, Cirilli I, Marcheggiani F, et al. Evaluation of anticancer role of a novel ruthenium(II)-based compound compared with NAMI-A and cisplatin in impairing mitochondrial functionality and promoting oxidative stress in triple negative breast cancer models. *Mitochondrion* 2021; **56**: 25-34.

74. Kleih M, Bopple K, Dong M, et al. Direct impact of cisplatin on mitochondria induces ROS production that dictates cell fate of ovarian cancer cells. *Cell Death Dis* 2019; **10**(11): 851.

75. Green DR, Galluzzi L, Kroemer G. Cell biology. Metabolic control of cell death. *Science* 2014; **345**(6203): 1250256.

76. Tomas-Gamasa M, Martinez-Calvo M, Couceiro JR, Mascarenas JL. Transition metal catalysis in the mitochondria of living cells. *Nat Commun* 2016; **7**: 12538.

77. Schilling T, Keppler KB, Heim ME, et al. Clinical phase I and pharmacokinetic trial of the new titanium complex budotitane. *Invest New Drugs* 1996; **13**(4): 327-32.

78. Olszewski U, Claffey J, Hogan M, et al. Anticancer activity and mode of action of titanocene C. *Invest New Drugs* 2011; **29**(4): 607-14.
79. Kater L, Claffey J, Hogan M, et al. The role of the intrinsic FAS pathway in Titanocene Y apoptosis: The mechanism of overcoming multiple drug resistance in malignant leukemia cells. *Toxicol In Vitro* 2012; **26**(1): 119-24.
80. Gansauer A, Winkler I, Worgull D, et al. Carbonyl-substituted titanocenes: a novel class of cytostatic compounds with high antitumor and antileukemic activity. *Chemistry* 2008; **14**(14): 4160-3.
81. Mokdsi G, Harding MM. Inhibition of human topoisomerase II by the antitumor metallocenes. *J Inorg Biochem* 2001; **83**(2-3): 205-9.
82. Kostova I. Titanium and vanadium complexes as anticancer agents. *Anticancer Agents Med Chem* 2009; **9**(8): 827-42.
83. Melendez E. Titanium complexes in cancer treatment. *Crit Rev Oncol Hematol* 2002; **42**(3): 309-15.
84. Talsi EP, Bryliakova AA, Bryliakov KP. Titanium Salan/Salalen Complexes: The Twofaced Janus of Asymmetric Oxidation Catalysis. *Chem Rec* 2016; **16**(2): 924-39.
85. Berkessel A, Gunther T, Wang Q, Neudorfl JM. Titanium salalen catalysts based on cis-1,2-diaminocyclohexane: enantioselective epoxidation of terminal non-conjugated olefins with H2O2. *Angew Chem Int Ed Engl* 2013; **52**(32): 8467-71.
86. Wang Q, Neudorfl JM, Berkessel A. Titanium cis-1,2-diaminocyclohexane (cis-DACH) salalen catalysts for the asymmetric epoxidation of terminal non-conjugated olefins with hydrogen peroxide. *Chemistry* 2015; **21**(1): 247-54.
87. Press K, Cohen A, Goldberg I, Venditto V, Mazzeo M, Kol M. Salalen titanium complexes in the highly isospecific polymerization of 1-hexene and propylene. *Angew Chem Int Ed Engl* 2011; **50**(15): 3529-32.
88. Dwyer FP, Gyarfas EC, Rogers WP, Koch JH. Biological activity of complex ions. *Nature* 1952; **170**(4318): 190-1.
89. Jung M, Kerr DE, Senter PD. Bioorganometallic chemistry--synthesis and antitumor activity of cobalt carbonyl complexes. *Arch Pharm (Weinheim)* 1997; **330**(6): 173-6.
90. Ott I, Kircher B, Gust R. Investigations on the effects of cobalt-alkyne complexes on leukemia and lymphoma cells: cytotoxicity and cellular uptake. *J Inorg Biochem* 2004; **98**(3): 485-9.
91. Schmidt K, Jung M, Keilitz R, Schnurr B, Gust R. Acetylenehexacarbonyldicobalt complexes, a novel class of antitumor drugs. *Inorganica Chimica Acta* 2000; **306**(1): 6-16.
92. Munteanu CR, Suntharalingam K. Advances in cobalt complexes as anticancer agents. *Dalton Trans* 2015; **44**(31): 13796-808.

93. Singh VK, Kadu R, Roy H, Raghavaiah P, Mobin SM. Phenolate based metallomacrocyclic xanthate complexes of Co(II)/Cu(II) and their exclusive deployment in [2 : 2] binuclear N,O-Schiff base macrocycle formation and in vitro anticancer studies. *Dalton Trans* 2016; **45**(4): 1443-54.

94. Obermoser V, Baecker D, Schuster C, Braun V, Kircher B, Gust R. Chlorinated cobalt alkyne complexes derived from acetylsalicylic acid as new specific antitumor agents. *Dalton Trans* 2018; **47**(12): 4341-51.

95. Ali A, Kamra M, Bhan A, Mandal SS, Bhattacharya S. New Fe(iii) and Co(ii) salen complexes with pendant distamycins: selective targeting of cancer cells by DNA damage and mitochondrial pathways. *Dalton Trans* 2016; **45**(22): 9345-53.

96. Beattie C, North M. Mechanistic investigation of the reaction of epoxides with heterocumulenes catalysed by a bimetallic aluminium salen complex. *Chemistry* 2014; **20**(26): 8182-8.

97. Taylor MS, Jacobsen EN. Enantioselective Michael additions to alpha,beta-unsaturated imides catalyzed by a Salen-Al complex. *J Am Chem Soc* 2003; **125**(37): 11204-5.

98. Clegg W, Harrington RW, North M, Pasquale R. Cyclic carbonate synthesis catalysed by bimetallic aluminium-salen complexes. *Chemistry* 2010; **16**(23): 6828-43.

99. Gurian PL, Cheatham LK, Ziller JW, Barron AR. Aluminium complexes of N,N′-ethylenebis(salicylideneimine)(H2salen). X-Ray crystal structures of [{Al(salen)}2(μ-O)]·MeCN and [Al(OC6H2Me3-2,4,6)(salen)]. *J Chem Soc, Dalton Trans* 1991; (6): 1449-56.

100. Rutherford D, Atwood DA. Five-Coordinate Aluminum Amides. *Organometallics* 1996; **15**(21): 4417-22.

101. Schaus SE, Brandes BD, Larrow JF, et al. Highly selective hydrolytic kinetic resolution of terminal epoxides catalyzed by chiral (salen)Co(III) complexes. Practical synthesis of enantioenriched terminal epoxides and 1,2-diols. *J Am Chem Soc* 2002; **124**(7): 1307-15.

102. Nielsen LP, Stevenson CP, Blackmond DG, Jacobsen EN. Mechanistic investigation leads to a synthetic improvement in the hydrolytic kinetic resolution of terminal epoxides. *J Am Chem Soc* 2004; **126**(5): 1360-2.

103. Herr I, Debatin KM. Cellular stress response and apoptosis in cancer therapy. *Blood* 2001; **98**(9): 2603-14.

104. Kilic A, Koyuncu I, Durgun M, Ozaslan I, Kaya IH, Gonel A. Synthesis and Characterization of the Hemi-Salen Ligands and Their Triboron Complexes: Spectroscopy and Examination of Anticancer Properties. *Chem Biodivers* 2018; **15**(1).

105. Ozbolat G, Yegani AA, Tuli A. Synthesis, characterization and electrochemistry studies of iron(III) complex with curcumin ligand. *Clin Exp Pharmacol Physiol* 2018; **45**(11): 1221-6.

106. Correa RS, da Silva MM, Graminha AE, et al. Ruthenium(II) complexes of 1,3-thiazolidine-2-thione: Cytotoxicity against tumor cells and anti-Trypanosoma cruzi activity enhanced upon combination with benznidazole. *J Inorg Biochem* 2016; **156**: 153-63.

107. Lee SY, Peckermann I, Abinet E, Okuda J, Henze G, Prokop A. The rare-earth yttrium complex [YR(mtbmp)(thf)] triggers apoptosis via the extrinsic pathway and overcomes multiple drug resistance in leukemic cells. *Med Oncol* 2012; **29**(1): 235-42.

108. Van Cruchten S, Van Den Broeck W. Morphological and biochemical aspects of apoptosis, oncosis and necrosis. *Anat Histol Embryol* 2002; **31**(4): 214-23.

109. Letai A, Bassik MC, Walensky LD, Sorcinelli MD, Weiler S, Korsmeyer SJ. Distinct BH3 domains either sensitize or activate mitochondrial apoptosis, serving as prototype cancer therapeutics. *Cancer Cell* 2002; **2**(3): 183-92.

110. Helmbach H, Rossmann E, Kern MA, Schadendorf D. Drug-resistance in human melanoma. *Int J Cancer* 2001; **93**(5): 617-22.

111. Kuwana T, Mackey MR, Perkins G, et al. Bid, Bax, and lipids cooperate to form supramolecular openings in the outer mitochondrial membrane. *Cell* 2002; **111**(3): 331-42.

112. Wolter KG, Hsu YT, Smith CL, Nechushtan A, Xi XG, Youle RJ. Movement of Bax from the cytosol to mitochondria during apoptosis. *J Cell Biol* 1997; **139**(5): 1281-92.

113. Hsu YT, Wolter KG, Youle RJ. Cytosol-to-membrane redistribution of Bax and Bcl-X(L) during apoptosis. *Proc Natl Acad Sci U S A* 1997; **94**(8): 3668-72.

114. Wieder T, Essmann F, Prokop A, et al. Activation of caspase-8 in drug-induced apoptosis of B-lymphoid cells is independent of CD95/Fas receptor-ligand interaction and occurs downstream of caspase-3. *Blood* 2001; **97**(5): 1378-87.

115. Vrooman LM, Silverman LB. Childhood acute lymphoblastic leukemia: update on prognostic factors. *Curr Opin Pediatr* 2009; **21**(1): 1-8.

116. Pieters R, Klumper E, Kaspers GJ, Veerman AJ. Everything you always wanted to know about cellular drug resistance in childhood acute lymphoblastic leukemia. *Crit Rev Oncol Hematol* 1997; **25**(1): 11-26.

117. Men LJ, Liu JZ, Chen HY, et al. Down regulation of G protein-coupled receptor 137 expression inhibits proliferation and promotes apoptosis in leukemia cells. *Cancer Cell Int* 2018; **18**: 13.

118. Engels IH, Totzke G, Fischer U, Schulze-Osthoff K, Janicke RU. Caspase-10 sensitizes breast carcinoma cells to TRAIL-induced but not tumor necrosis factor-induced apoptosis in a caspase-3-dependent manner. *Mol Cell Biol* 2005; **25**(7): 2808-18.

119. Chan HSL, Thorner PS, Haddad G, Deboer G, Gallie BL, Ling V. Multidrug-Resistance in Malignancies of Children. *Int J Pediat Hem Onc* 1995; **2**(1): 11-29.

120. Styczynski J. Drug resistance in childhood acute myeloid leukemia. *Curr Pharm Biotechnol* 2007; **8**(2): 59-75.

121. Pogorzala M, Kubicka M, Rafinska B, Wysocki M, Styczynski J. Drug-resistance Profile in Multiple-relapsed Childhood Acute Lymphoblastic Leukemia. *Anticancer Res* 2015; **35**(10): 5667-70.
122. Hunger SP, Mullighan CG. Acute Lymphoblastic Leukemia in Children. *N Engl J Med* 2015; **373**(16): 1541-52.
123. Prokop A, Wieder T, Sturm I, et al. Relapse in childhood acute lymphoblastic leukemia is associated with a decrease of the Bax/Bcl-2 ratio and loss of spontaneous caspase-3 processing in vivo. *Leukemia* 2000; **14**(9): 1606-13.
124. Chapuy B, Koch R, Radunski U, et al. Intracellular ABC transporter A3 confers multidrug resistance in leukemia cells by lysosomal drug sequestration. *Leukemia* 2008; **22**(8): 1576-86.
125. de Jonge-Peeters SD, Kuipers F, de Vries EG, Vellenga E. ABC transporter expression in hematopoietic stem cells and the role in AML drug resistance. *Crit Rev Oncol Hematol* 2007; **62**(3): 214-26.
126. Zhang R, Liu Y, Hammache K, et al. The role of FADD in pancreatic cancer cell proliferation and drug resistance. *Oncol Lett* 2017; **13**(3): 1899-904.
127. Tourneur L, Delluc S, Levy V, et al. Absence or low expression of fas-associated protein with death domain in acute myeloid leukemia cells predicts resistance to chemotherapy and poor outcome. *Cancer Res* 2004; **64**(21): 8101-8.
128. Fianco G, Contadini C, Ferri A, Cirotti C, Stagni V, Barila D. Caspase-8: A Novel Target to Overcome Resistance to Chemotherapy in Glioblastoma. *Int J Mol Sci* 2018; **19**(12).
129. Fantl V, Smith R, Brookes S, Dickson C, Peters G. Chromosome 11q13 abnormalities in human breast cancer. *Cancer Surv* 1993; **18**: 77-94.
130. Gibcus JH, Menkema L, Mastik MF, et al. Amplicon mapping and expression profiling identify the Fas-associated death domain gene as a new driver in the 11q13.3 amplicon in laryngeal/pharyngeal cancer. *Clin Cancer Res* 2007; **13**(21): 6257-66.
131. Prapinjumrune C, Morita K, Kuribayashi Y, et al. DNA amplification and expression of FADD in oral squamous cell carcinoma. *J Oral Pathol Med* 2010; **39**(7): 525-32.
132. Rasamny JJ, Allak A, Krook KA, et al. Cyclin D1 and FADD as biomarkers in head and neck squamous cell carcinoma. *Otolaryngol Head Neck Surg* 2012; **146**(6): 923-31.
133. Mollazadeh S, Sahebkar A, Hadizadeh F, Behravan J, Arabzadeh S. Structural and functional aspects of P-glycoprotein and its inhibitors. *Life Sci* 2018; **214**: 118-23.
134. Wang Y, Cui J, Dai Y, et al. Reversal of P-glycoprotein-mediated multidrug resistance and pharmacokinetics study in rats by WYX-5. *Can J Physiol Pharmacol* 2017; **95**(5): 580-5.
135. Juliano RL, Ling V. A surface glycoprotein modulating drug permeability in Chinese hamster ovary cell mutants. *Biochim Biophys Acta* 1976; **455**(1): 152-62.

136. van Maldegem AM, Benson C, Rutkowski P, et al. Etoposide and carbo-or cisplatin combination therapy in refractory or relapsed Ewing sarcoma: a large retrospective study. *Pediatr Blood Cancer* 2015; **62**(1): 40-4.

137. Van Winkle P, Angiolillo A, Krailo M, et al. Ifosfamide, carboplatin, and etoposide (ICE) reinduction chemotherapy in a large cohort of children and adolescents with recurrent/refractory sarcoma: the Children's Cancer Group (CCG) experience. *Pediatr Blood Cancer* 2005; **44**(4): 338-47.

138. Baum ES, Gaynon P, Greenberg L, Krivit W, Hammond D. Phase II trail cisplatin in refractory childhood cancer: Children's Cancer Study Group Report. *Cancer Treat Rep* 1981; **65**(9-10): 815-22.

139. Luksch R, Grignani G, D'Angelo P, et al. Front-line window therapy with cisplatin in patients with primary disseminated Ewing sarcoma: A study by the Associazione Italiana di Ematologia ed Oncologia Pediatrica and Italian Sarcoma Group. *Pediatr Blood Cancer* 2017; **64**(12).

140. Cotterill SJ, Ahrens S, Paulussen M, et al. Prognostic factors in Ewing's tumor of bone: analysis of 975 patients from the European Intergroup Cooperative Ewing's Sarcoma Study Group. *J Clin Oncol* 2000; **18**(17): 3108-14.

141. Ladenstein R, Potschger U, Le Deley MC, et al. Primary disseminated multifocal Ewing sarcoma: results of the Euro-EWING 99 trial. *J Clin Oncol* 2010; **28**(20): 3284-91.

142. Bhattacharya S, Mandal SS. Ambient oxygen activating water soluble cobalt-salen complex for DNA cleavage. *J Chem Soc Chem Comm* 1995; (24): 2489-90.

143. Shokohi-Pour Z, Chiniforoshan H, Sabzalian MR, Esmaeili SA, Momtazi-Borojeni AA. Cobalt (II) complex with novel unsymmetrical tetradentate Schiff base (ON) ligand: in vitro cytotoxicity studies of complex, interaction with DNA/protein, molecular docking studies, and antibacterial activity. *J Biomol Struct Dyn* 2018; **36**(2): 532-49.

144. Zou BQ, Wang SL, Qin QP, Bai YX, Tan MX. Synthesis, Characterization, and Cytotoxicity of the Cobalt (III) Complex with N,N-Diethyl-4-(2,2':6',2''-terpyridin-4'-yl)aniline. *Chem Biodivers* 2018; **15**(10): e1800215.

145. Ndhundhuma IM, Abrahamse H. Susceptibility of In Vitro Melanoma Skin Cancer to Photoactivated Hypericin versus Aluminium(III) Phthalocyanine Chloride Tetrasulphonate. *Biomed Res Int* 2017; **2017**: 5407012.

146. Hart MM, Adamson RH. Antitumor activity and toxicity of salts of inorganic group 3a metals: aluminum, gallium, indium, and thallium. *Proc Natl Acad Sci U S A* 1971; **68**(7): 1623-6.

147. Chitambar CR, Boon P, Wereley JP. Evaluation of transferrin and gallium-pyridoxal isonicotinoyl hydrazone as potential therapeutic agents to overcome lymphoid leukemic cell resistance to gallium nitrate. *Clin Cancer Res* 1996; **2**(6): 1009-15.

148. Knorr GM, Chitambar CR. Gallium-pyridoxal isonicotinoyl hydrazone (Ga-PIH), a novel cytotoxic gallium complex. A comparative study with gallium nitrate. *Anticancer Res* 1998; **18**(3A): 1733-7.

149. Chitambar CR. Gallium-containing anticancer compounds. *Future Med Chem* 2012; **4**(10): 1257-72.

150. Collery P, Keppler B, Madoulet C, Desoize B. Gallium in cancer treatment. *Crit Rev Oncol Hematol* 2002; **42**(3): 283-96.

151. Foster BJ, Clagettcarr K, Hoth D, Leylandjones B. Gallium Nitrate - the 2nd Metal with Clinical Activity. *Cancer Treatment Reports* 1986; **70**(11): 1311-9.

152. Chitambar CR. Gallium nitrate for the treatment of non-Hodgkin's lymphoma. *Expert Opin Investig Drugs* 2004; **13**(5): 531-41.

153. Chitambar CR. Gallium compounds as antineoplastic agents. *Curr Opin Oncol* 2004; **16**(6): 547-52.

154. Klumper E, Pieters R, Veerman AJ, et al. In vitro cellular drug resistance in children with relapsed/refractory acute lymphoblastic leukemia. *Blood* 1995; **86**(10): 3861-8.

155. Mullighan CG. Molecular genetics of B-precursor acute lymphoblastic leukemia. *J Clin Invest* 2012; **122**(10): 3407-15.

156. Tasian SK, Hunger SP. Genomic characterization of paediatric acute lymphoblastic leukaemia: an opportunity for precision medicine therapeutics. *Br J Haematol* 2017; **176**(6): 867-82.

157. Raimondi SC, Privitera E, Williams DL, et al. New recurring chromosomal translocations in childhood acute lymphoblastic leukemia. *Blood* 1991; **77**(9): 2016-22.

158. Inukai T, Hirose K, Inaba T, et al. Hypercalcemia in childhood acute lymphoblastic leukemia: frequent implication of parathyroid hormone-related peptide and E2A-HLF from translocation 17;19. *Leukemia* 2007; **21**(2): 288-96.

159. Watanabe A, Inukai T, Kagami K, et al. Resistance of t(17;19)-acute lymphoblastic leukemia cell lines to multiagents in induction therapy. *Cancer Med* 2019; **8**(11): 5274-88.

160. De Keersmaecker K, Lahortiga I, Mentens N, et al. In vitro validation of gamma-secretase inhibitors alone or in combination with other anti-cancer drugs for the treatment of T-cell acute lymphoblastic leukemia. *Haematologica* 2008; **93**(4): 533-42.

161. Mishra D, Singh S, Narayan G. Curcumin Induces Apoptosis in Pre-B Acute Lymphoblastic Leukemia Cell Lines Via PARP-1 Cleavage. *Asian Pac J Cancer Prev* 2016; **17**(8): 3865-9.

162. Weston VJ, Wei W, Stankovic T, Kearns P. Synergistic action of dual IGF1/R and MEK inhibition sensitizes childhood acute lymphoblastic leukemia (ALL) cells to cytotoxic agents and involves downregulation of STAT6 and PDAP1. *Exp Hematol* 2018; **63**: 52-63 e5.

163. Hulleman E, Kazemier KM, Holleman A, et al. Inhibition of glycolysis modulates prednisolone resistance in acute lymphoblastic leukemia cells. *Blood* 2009; **113**(9): 2014-21.
164. Pui CH, Robison LL, Look AT. Acute lymphoblastic leukaemia. *Lancet* 2008; **371**(9617): 1030-43.
165. Fiedler ERC, Bhutkar A, Lawler E, Besada R, Hemann MT. In vivo RNAi screening identifies Pafah1b3 as a target for combination therapy with TKIs in BCR-ABL1(+) BCP-ALL. *Blood Adv* 2018; **2**(11): 1229-42.
166. Jerchel IS, Hoogkamer AQ, Aries IM, et al. RAS pathway mutations as a predictive biomarker for treatment adaptation in pediatric B-cell precursor acute lymphoblastic leukemia. *Leukemia* 2018; **32**(4): 931-40.
167. Paz H, Joo EJ, Chou CH, et al. Treatment of B-cell precursor acute lymphoblastic leukemia with the Galectin-1 inhibitor PTX008. *J Exp Clin Cancer Res* 2018; **37**(1): 67.
168. Schirmer M, Trentin L, Queudeville M, et al. Intrinsic and chemo-sensitizing activity of SMAC-mimetics on high-risk childhood acute lymphoblastic leukemia. *Cell Death Dis* 2016; **7**: e2052.
169. Toscan CE, Failes T, Arndt GM, Lock RB. High-throughput screening of human leukemia xenografts to identify dexamethasone sensitizers. *J Biomol Screen* 2014; **19**(10): 1391-401.
170. Aries IM, Jerchel IS, van den Dungen RE, et al. EMP1, a novel poor prognostic factor in pediatric leukemia regulates prednisolone resistance, cell proliferation, migration and adhesion. *Leukemia* 2014; **28**(9): 1828-37.
171. Toscan CE, Rahimi M, Bhadbhade M, Pickford R, McAlpine SR, Lock RB. Thioimidazoline based compounds reverse glucocorticoid resistance in human acute lymphoblastic leukemia xenografts. *Org Biomol Chem* 2015; **13**(22): 6299-312.
172. Zinngrebe J, Schlichtig F, Kraus JM, et al. Biomarker profile for prediction of response to SMAC mimetic monotherapy in pediatric precursor B-cell acute lymphoblastic leukemia. *Int J Cancer* 2020; **146**(11): 3219-31.

7. Anhang

7.1 Abbildungsverzeichnis

7.2 Tabellenverzeichnis

8. Vorabveröffentlichungen von Ergebnissen

Publikation 1

Sina M. Hopff, Qifang Wang, Corazon Frias, Marie Ahrweiler, Nicola Wilke, Nathalie Wilke, Albrecht Berkessel, Aram Prokop. *A metal-free salalen ligand with anti-tumor and synergistic activity in resistant leukemia and solid tumor cells via mitochondrial pathway*. Journal of Cancer Research and Clinical Oncology (2021) 147: 2591–2607.
DOI: 10.1007/s00432-021-03679-3
Impact Factor: 4,553 (2020)

Publikation 2

Sina M. Hopff, Liliane A. Onambele, Marc Brandenburg, Albrecht Berkessel, Aram Prokop. *Discovery of a cobalt (III) salen complex that induces apoptosis in Burkitt like lymphoma and leukemia cells, overcoming multidrug resistance in vitro*. Bioorganic Chemistry (2020) 104: 104193.
DOI: 10.1016/j.bioorg.2020.104193
Impact Factor: 5,275 (2020)

Publikation 3

Sina M. Hopff, Liliane A. Onambele, Marc Brandenburg, Albrecht Berkessel, Aram Prokop. *Sensitizing multidrug-resistant leukemia cells to common cytostatics by an aluminium-salen complex that has high-apoptotic effects in leukemia, lymphoma and mamma carcinoma cells*. Biometals (2021) 34: 211-220.
DOI: 10.1007/s10534-020-00273-x
Impact Factor: 2,949 (2020)

Journal of Cancer Research and Clinical Oncology (2021) 147:2591–2607
https://doi.org/10.1007/s00432-021-03679-3

ORIGINAL ARTICLE – CANCER RESEARCH

A metal-free salalen ligand with anti-tumor and synergistic activity in resistant leukemia and solid tumor cells via mitochondrial pathway

Sina M. Hopff[1] · Qifang Wang[2] · Corazon Frias[1] · Marie Ahrweiler[1] · Nicola Wilke[1] · Nathalie Wilke[1] · Albrecht Berkessel[2] · Aram Prokop[1,3,4]

Received: 3 December 2020 / Accepted: 27 May 2021 / Published online: 2 July 2021

Abstract

Purpose Since the discovery of the well-known cis-platin, transition metal complexes are highly recognized as cytostatic agents. However, toxic side effects of the metal ions present in the complexes may pose significant problems for their future development. Therefore, we investigated the metal-free salalen ligand WQF 044.

Methods DNA fragmentations in leukemia (Nalm6) and solid tumor cells (BJAB, MelHO, MCF-7, RM82) proved the apoptotic effects of WQF 044, its overcoming of resistances and the cellular pathways that are affected by the substance. The apoptotic mechanisms finding were supported by western blot analysis, measurement of the mitochondrial membrane potential and polymerase chain reactions.

Results A complex intervention in the mitochondrial pathway of apoptosis with a Bcl-2 and caspase dependence was observed. Additionally, a wide range of tumors were affected by the ligand in a low micromolar range in-vitro. The compound overcame multidrug resistances in P-gp over-expressed acute lymphoblastic leukemia and CD95-downregulated Ewing's sarcoma cells. Quite remarkable synergistic effects with vincristine were observed in Burkitt-like lymphoma cells.

Conclusion The investigation of a metal-free salalen ligand as a potential anti-cancer drug revealed in promising results for a future clinical use.

Keywords Metal-free ligand · Salalen · Mitochondrial pathway · Apoptosis · Synergistic effects · Multidrug resistance

Introduction

Developing new anti-cancer targets, especially against resistant tumors, is very challenging in cancer research (Kelland 2007). The discovery of the well-known cisplatin was pioneering on this field, but severe side effects limit the use of platin derivates (Bruijnincx and Sadler 2008; Kelland 2007; Rabik and Dolan 2007; Wild2012). Therefore finding new substances without a metal ion in its center is of high interest.

Salans, salalens and in particular salens are most prominent ligands in coordination chemistry, and many of their metal complexes have shown potent antitumor activity (Scheme 1, top) (Grutzke et al. 2015; Hopff et al. 2020; Immel et al. 2011, 2012a, b; Lee 2010, 2011; Meker et al. 2011; Mir et al. 2017; Peri et al. 2011; Terenzi 2016). However, earlier work of ours on Mo-complexes had revealed that the biological activity may actually reside in the ligand. For example, the metal-free salan ligand THG 1213 (Scheme 1, bottom right) was in fact much more active than the corresponding Mo-complexes (Dragoun et al. 2018). Another striking observation was that the corresponding salen ligand THG 1212 (Scheme 1, bottom left) was inactive (Dragoun et al. 2018).

With this in mind, we decided to also investigate the metal-free salalen ligand WQF 044 (Scheme 1, bottom

✉ Sina M. Hopff
sina.hopff@uk-koeln.de

1 Department of Pediatric Hematology/Oncology, Municipal Clinics of Cologne, Children's Hospital of the City Cologne, Amsterdamer Straße 59, 50735 Cologne, Germany

2 Department of Chemistry, University of Cologne, Greinstraße 4, 50939 Cologne, Germany

3 Department of Pediatric Hematology/Oncology, Helios Clinic Schwerin, Wismarsche Straße 393-397, 19055 Schwerin, Germany

4 Medical School Hamburg (MSH), University of Applied Sciences and Medical University, Am Kaiserkai 1, 20457 Hamburg, Germany

Scheme 1 Top: General structures of the salen, the salalen, and the salan motifs. Bottom: Explicit structures of the salen THG 1212, the salalen WQF 044 (this work), and of the salan THG 1213

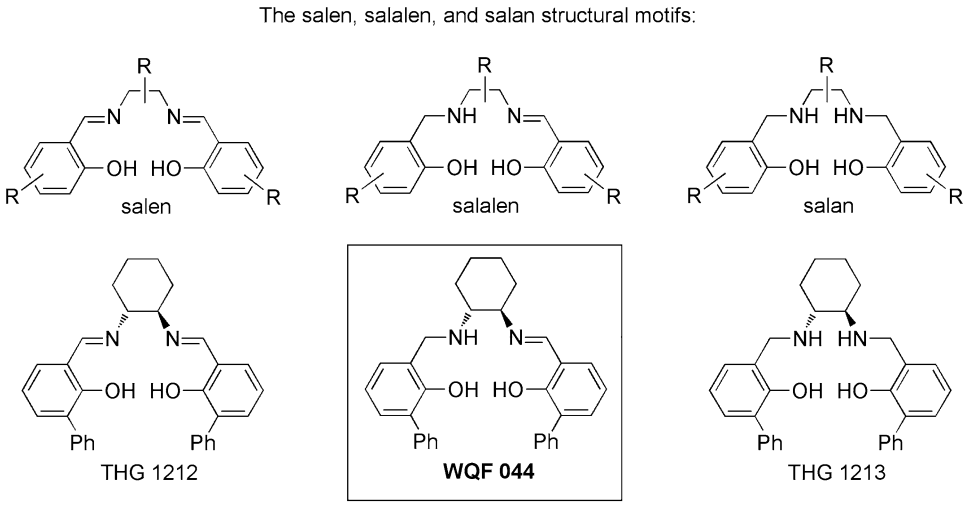

middle). The catalytic activity and characterization of the compound is already known (Berkessel et al. 2007). Please note that the salalen WQF 044 is the direct salalen analogue of the salan THG 1213 investigated earlier (Dragoun et al. 2018). Additionally, no biological data representing the apoptotic activity of salalan ligands have been published so far. We were delighted to see that the salalen WQF 044 affected leukemia, lymphoma, mamma carcinoma and melanoma cells in a low micromolar range. We extended the number of cell lines to a human Ewing's sarcoma cell line that we recently made resistant to vincristine. The main focus of interest was to find out the in-vitro cytotoxicity in resistant tumor cells and to compare the apoptotic activity of the compound with cytostatics including salans and salens that were published before. In fact, a proposal for the apoptotic mechanism of action of WQF 044 could be derived from our studies on a wide range of different tumor cells and modified cell lines.

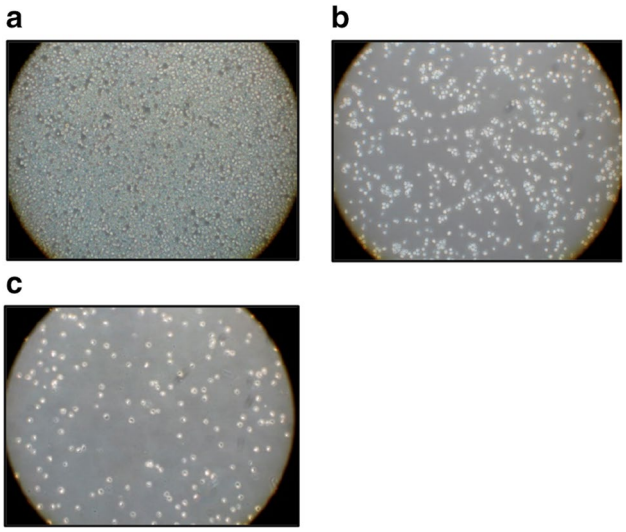

Fig. 1 **a–c** Morphology of Nalm6 cells under the microscope after 72 h of incubation at 37 °C. **a** Control cells were left untreated. **b** Nalm6 cells were treated with 1 µM of WQF 044. **c** 10 µM of WQF 044 was pipetted on these cells

Results

Proof of anti-proliferative effects of WQF 044 and cell death via apoptosis

The salalen ligand WQF 044 inhibits proliferation and induces apoptosis in human B cell precursor leukemia cells (Nalm6). The following microscopic photos visualize the effect of WQF 044 on the Nalm6 cells after 72 h of incubation. In the control (Fig. 1a), a large number of Nalm6 cells can be observed. The cells are not apoptotic as they appear clear and round. Leukemia cells that were treated with 1 µM of WQF 044 are shown in Fig. 1b. Conspicuous is the lower number of cells. It is apparent that the cells look significantly damaged. They lost their circular and light appearance. Figure 1c clearly illustrates the high apoptotic effect on the cells after pipetting 10 µM of the compound. The few cells remaining are all damaged.

The anti-proliferative potency of WQF 044 was proved by using the CASY cell counter. After pipetting 1–20 µM of the substance, an inhibited proliferation of over 95 percent was observed (Fig. 2b). IC_{50}, the concentration of WQF 044 necessary to affect half maximal growth inhibition, is lower than 3 µM in Nalm6 cells. Furthermore, it is important that the cell death, triggered by WQF 044, is due to apoptosis and not necrosis. A lactate dehydrogenase (LDH) release measurement gives information about this fact. During necrosis, the cells lose their membrane integrity so that LDH can easily migrate out of the cells. This process does not happen during apoptosis within the first hours (Van Cruchten

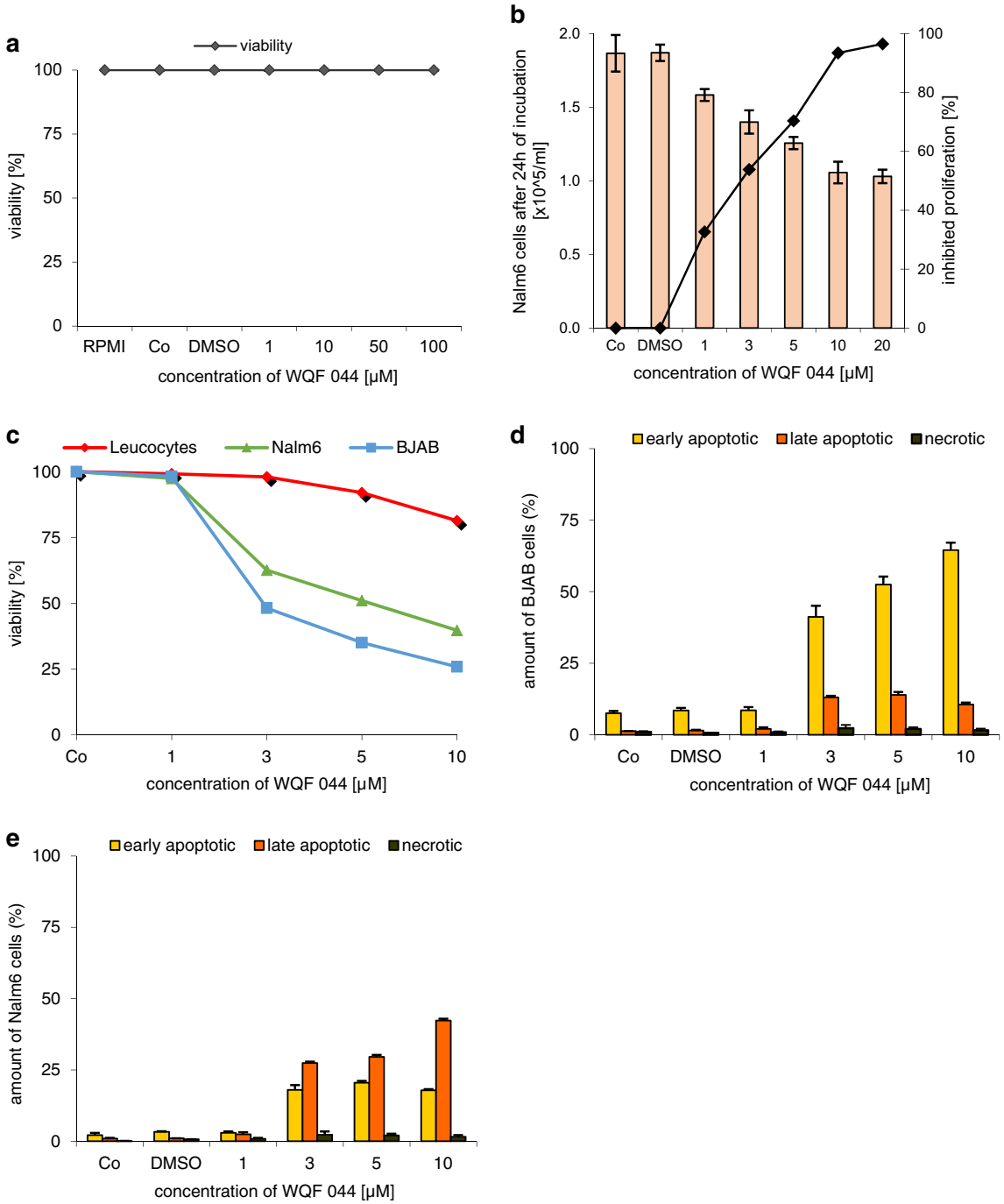

Fig. 2 Inhibition of proliferation and excluding of necrosis. **a** Different concentrations of WQF 044 were pipetted on Nalm6 cells. After 3 h of incubation at 37 °C, an LDH release assay was made to determine the viability. Values are given as percentage of control (Co) ($n=3$). **b** Nalm6 cells were treated with different concentrations of WQF 044 and incubated for 24 h. The CASY cell counter and analyzer system was used to measure the proliferation with three batches per concentration. The number of untreated control cells (Co) was set as 0% growth inhibition. Values are given as percentage of inhibition of cell proliferation ($n=3$). **c–e** BJAB and Nalm6 cells and leucocytes were incubated with different concentrations of WQF 044 for 48 h. The viability, early and late apoptosis and necrosis were measured after Annexin V/PI staining by using flow cytometry. In the Annexin V/PI assay, vital cells (AnnV−/PI−) can be distinguished from early apoptotic (AnnV+/PI−), late apoptotic (AnnV+/PI+), and necrotic (AnnV−/PI+) cells. Three batches per concentration were used

and Van Den Broeck 2002). We incubated WQF 044-treated Nalm6 cells for 3 h and made a LDH release assay that revealed no significant detection of LDH outside the cells (Fig. 2a) (Wieder et al. 1998). To specify the stage of apoptosis induced by WQF 044 an Annexin-V/propidium iodide (PI) assay was made. Annexin V binds to phosphatidylserine that is released in an early stage of apoptosis (Fadok et al. 2001; Schlegel and Williamson 2001). This exposure lasts until the final stage of apoptosis. PI is membrane impermeable. Therefore, cells that are devoid of PI staining show an intact membrane (van Engeland et al. 1998).

Next to the leukemic Nalm6 cells, Burkitt-like lymphoma cells (BJAB) were used for this experiment. First of all the data underlined that cell death induced by WQF 044 was due to apoptosis and not necrosis (Fig. 2d, e). After 48 h of incubation with WQF 044, it turned out that the highest amount of BJAB cells was in an early stage of apoptosis (Annexin V-positive, PI-negative) (Fig. 2d) whereas Nalm6 cells showed more late apoptosis after the same time (Annexin V/PI-double-positive), but still some early apoptotic cells (Fig. 2e). Furthermore, at a concentration of 10 µM, WQF 044 reduced the number of vital BJAB cells by approximately 75 percent and Nalm6 cells by 60 percent (Fig. 2c).

WQF 044 overcomes multidrug resistance in leukemia cells

The overcoming of multidrug resistance (MDR) is an important quality of a new substance because MDR poses a huge problem in the treatment of relapsed malignant diseases (Uderzo et al. 2001). Various cellular-based mechanisms are responsible for the development of MDR in tumor cells. The excretion of P-glycoprotein (P-gp), encoded by the MDR1/ACBC1 gene, is one of these mechanisms (Gottesman et al. 2002; Krishna and Mayer 2000; Marques 2019). It is an efflux pump in the cell membrane that transports drugs out of the cells resulting in a decrease of the cellular drug concentration (Gottesman and Pastan 1988; Lin and Yamazaki 2003; Mukhametov and Raevsky 2017). It has been proven that P-gp over-expression causes resistances to taxanes, anthracyclines and vinca-alkaloids because they are substrates of this transporter (Pieters et al. 1997; Wang et al. 2017). In our lab, we generated a vincristine resistant (NVCR) and a daunorubicin-resistant (NDau) Nalm6 cell line that are both characterized by an over-expression of P-gp (Rubbiani 2010). They are additionally resistant to fludarabine, paclitaxel and colchicine (Kater et al. 2011; Kater 2012). Only recently, we found out that NDau cells are also resistant to cytarabine, mitoxantrone, idarubicin, doxorubicin, epirubicin, etoposide and the vinca alkaloids. Except of a cytarabine sensibility, NVCR cells have the same tested co-resistances as the NDau cells (Table 1).

DNA fragmentations effected by WQF 044 in the resistant cell lines compared to the Nalm6 cell line revealed that this ligand has the potential to overcome the MDR. The apoptotic effects were even significantly higher in the resistant cell lines than in the control Nalm6 cells after exposing them to 1 to 5 µM of WQF 044 (Fig. 3a, b).

Bcl-2 over-expression in Burkitt-like lymphoma and human melanoma cells reduces activity of WQF 044

Another mechanism of MDR is the over-expression of the anti-apoptotic protein Bcl-2 in tumor cells (Krishna and Mayer 2000). At this point, BJAB cells and its vincristine-resistant cells (BiBo) played a main role because the BiBo cells are characterized by an Bcl2-over-expression (Kater et al. 2011). The cells further have co-resistances to cytarabine, daunorubicin, vindesine, vinorelbine, vinblastine and paclitaxel (Table 1). A DNA fragmentation with WQF 044 in these two cell lines gave further information about the working mechanism of the substances. First of all, it can be said that WQF 044 induces apoptosis in BJAB cells in a dose-dependent manner (Fig. 4a). In comparison to that the apoptotic effects in BiBo cells were significantly lower than in the BJAB cells, but at least values up to 50 percent at 5 µM of WQF 044 could be reached. The same phenomenon was observed in the analysis of a DNA fragmentation with special human melanoma cells (MelHO). The MelHO pIRES cell line was stably transfected with the pIRES vector. Compared to this the MelHO Bcl-2 cells had the pIRES-Bcl-2-vector included. They strongly over-express the anti-apoptotic Bcl-2 protein (Jesse et al. 2009). Figure 4b clearly demonstrates that WQF 044 had no effect on the MelHO Bcl-2 cell line, but induced apoptosis in the MelHO pIRES cells with a high significance compared to the MelHO Bcl-2 cells, respectively.

WQF 044 regulates mitochondria-related Bcl-2 family proteins, DIABLO and cytochrome c

Even though a dependence of WQF 044 on the Bcl-2 over-expression can be observed, we found several gene expressions, including members of the Bcl-2 family, in a polymerase chain reaction (PCR) analysis of WQF 044 treated Nalm6 cells. The analysis revealed a downregulation of the anti-apoptotic Bcl-2 by 18-fold and a 5-times upregulation of the Bcl-2-associated X protein (BAX) that is pro-apoptotic (Table 2) (Edlich 2018; Garner et al. 2017). Thus, we assume that WQF 044 has an influence on Bcl-2 even though higher concentrations are needed to reach apoptotic effects.

The PCR array analysis also produced other gene expressions that lead to the pathway in which WQF 044 intervened. An over-expression of the IAP-binding mitochondrial

Table 1 Co-Resistances of different tumor cell lines

	NVCR	NDau	BiBo	7CCA	RM82SiHoVCR
Cytarabine	S	R	R	R	R
Fludarabine	R	R	S	R	S
Cladribine	S	S	S	R	S
Clofarabine	S	S	S	R	S
Mitoxantrone	R	R	I	R	R
Idarubicin	R	R	S	R	S
Daunorubicin	R	**R**	R	R	R
Doxorubicin	R	R	S	**R**	R
Epirubicin	R	R	I	R	R
Etoposide	R	R	S	R	I
4-OH-Cyclophosphamide	S	S	S	R	S
Methotrexate	S	S	S	S	S
Vindesine	R	R	R	R	R
Vinorelbine	R	R	R	R	R
Paclitaxel	R	R	R	R	R
Vinblastine	R	R	R	R	R
Vincristine	**R**	R	**R**	R	**R**
Fluoruracil	S	S	S	S	I
Resistant mechanisms	P-gp over-expression	P-gp over-expression	Bcl-2 over-expression	Caspase-3 under-expression	CD95 under-expression, caspase-8 downregulation

DNA-fragmentation was measured as described with the wild-type cell lines and its resistant cell line. The written cytostatics were pipetted on the cells in different concentrations ($n=3$). Apoptotic effects were compared. Cells were resistant (R) if the apoptotic effect in the resistant cell line was half times lower than in the main cell line in a dose-dependent manner. Intermediate (I) stadium was chosen if apoptosis was significantly lower in the resistant cell line, but still higher than the half-value of the non-resistant cell line. Otherwise the cells were sensible (S) to the cytostatic. The primary resistant mechanisms of the cell lines are written with an R in bold

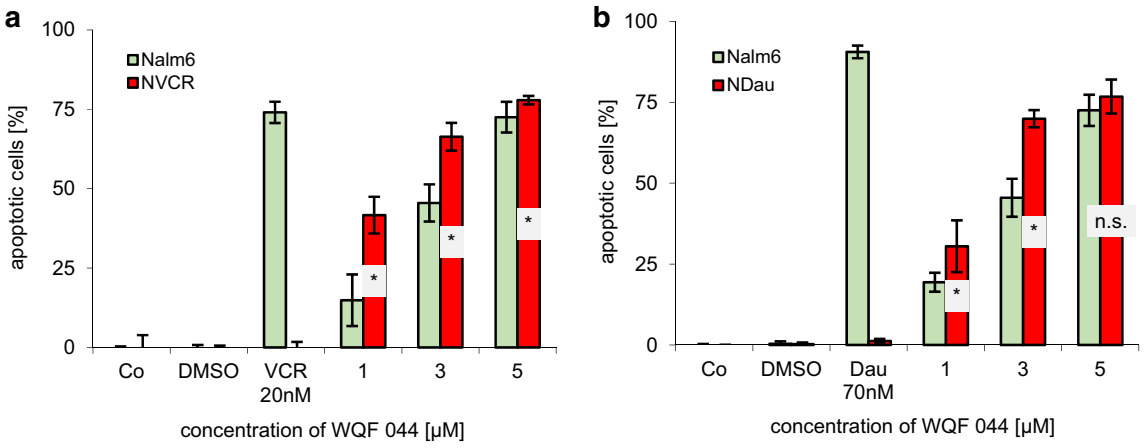

Fig. 3 Overcoming of MDR is proved by treating resistant cells and control Nalm6 cells with different concentrations of WQF 044. Untreated cells were left as control (Co). Incubation time was 72 h at 37 °C. DNA fragmentation was measured by flow cytometric analysis. Values are given in percent ± SD ($n=3$). **a** DNA fragmentation of Nalm6 cells was compared with vincristine-resistant Nalm6 cells (NVCR). To prove the resistance, both cell lines were treated with vincristine (VCR). **b** The experiment was repeated with Nalm6 cells and daunorubicin-resistant NDau cells and resistance is shown by comparing the apoptotic effects in daunorubicin (Dau) treated cells. Comparison of data was calculated by a one-tail *t* test: $*p<0.05$; *ns* not significant

protein (DIABLO) and cyctochrom c, somatic (CYCS) was observed (Table 2). These proteins, including Bcl-2 family members, are part of the intrinsic apoptotic pathway that is mitochondria-dependent (Won 2018). However, apoptosis

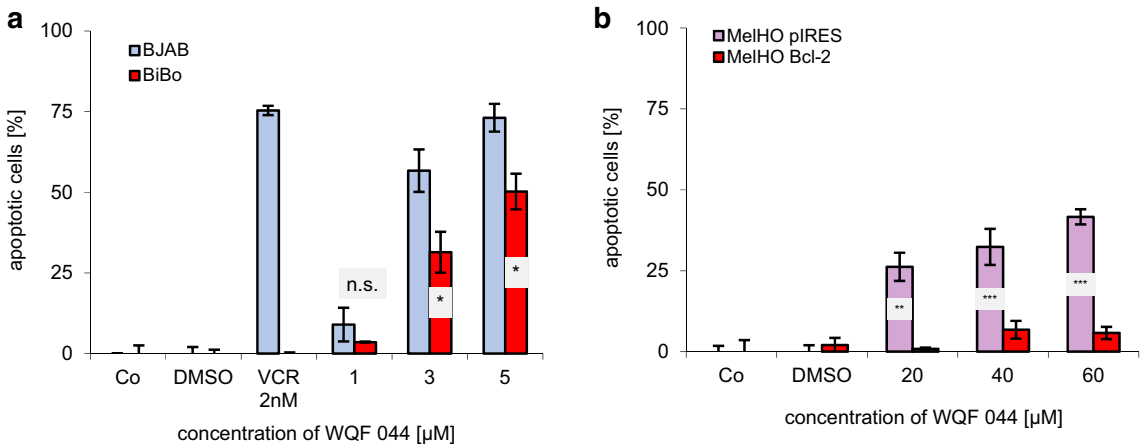

Fig. 4 Dependence of a Bcl-2 over-expression in vincristine-resistant BiBo cells and pIRES-Bcl-2-vector transfected MelHO cells. After 72 h of incubating the cells at 37 °C, DNA fragmentation was measured by flow cytometric analysis. Control cells were left untreated (Co). Apoptotic cells were displayed as percentage of the means of three separate samples ± SD. Comparison of data was calculated by a one-tail t-test. Results have been asterisked as follows: $*p < 0.05$; $**p < 0.01$; $***p < 0.001$; *ns* not significant. **a** BJAB and BiBo cells were treated with different concentrations of WQF 044. Additionally, both cell lines were treated with vincristine (VCR) to prove the resistance. **b** WQF 044 was pipetted on MelHO pIRES und MelHO Bcl-2 cells in three different concentrations. Higher concentrations than in Nalm6 and BJAB cells were used due to the lower sensitivity of these adherent cells

Table 2 PCR analysis of WQF 044 treated Nalm6 cells

Genes over-/under-expressed	Fold-change	Fold-regulation
Bcl-2	0.0545	− 18.3537
BAX	4.6332	4.6332
CD95	0.0236	− 42.459
Cytochrome C	42.5769	42.5769
DIABLO	15.9115	15.9115
FADD	0.1758	− 5.6883

WQF 044 treated Nalm6 cells were incubated for 16 h at 37 °C. For PCR analysis the apoptosis-specific RT2 profiler PCR expression array (SuperArray PAHS-012Z; SABiosciences Corporation, Frederick, MD, USA) was used. Fold-Change (2^(−ΔΔCt)) is the normalized gene expression (2^(−ΔCt)) in the Test Sample (WQF 044 treated Nalm6 cells) divided the normalized gene expression (2^(−ΔCt)) in the Control Sample (untreated Nalm6 cells). Fold-Regulation represents fold-change results in a biologically meaningful way. Fold-change values greater than one indicate a positive- or an up-regulation, and the fold-regulation is equal to the fold-change. Fold-change values less than one indicate a negative or down-regulation, and the fold-regulation is the negative inverse of the fold-change

can also be triggered by the death receptor-dependent extrinsic pathway (Nair et al. 2014).

The mitochondrial membrane potential is reduced by WQF 044

The activation of the intrinsic pathway results in a loss of the mitochondrial membrane potential (Lambert et al. 1989). To investigate the influence of WQF 044 on the mitochondrial permeability transition that can already be seen in the results of the PCR array analysis, Nalm6 cells were stained with a JC-1 dye. Flow cytometric determination showed a decreased fluorescence of Nalm6 cells, reflecting mitochondrial permeability. Figure 5a clearly illustrates the loss of mitochondrial membrane depolarization, beginning from 3 µM of WQF 044.

Caspase-dependence of WQF 044

The protease caspase-3 is a key component of the apoptotic pathway. During apoptosis, it is taking part in the proteolytic cleavage of many key proteins (Cohen 1997). To investigate whether WQF 044 develops its apoptotic effects via an activation of caspase-3, we tested the substance on special cell lines. One cell line is the doxorubicin-resistant BJAB cell line (7CCA) that is characterized by a caspase-3 underexpression (Dragoun et al. 2018). Multiple co-resistances of 7CCA were found to cytarabine, fludarabine, cladribine, clofarabine, mitoxantrone, idarubicin, daunorubicin, epirubicin, etoposide, 4-OH-cyclophosphamide, vindesine, vinorelbine, paclitaxel, vinblastine and vincristine (Table 1). Figure 5c clearly illustrates that WQF 044 could not affect the 7CCA cells, whereas the regular BJAB cells were highly apoptotic at WQF 044 concentrations of 3 to 5 µM.

To further support that WQF 044 is dependent of caspase-3, we used the human breast adenocarcinoma cell line MCF-7/mock and its modified cells called MCF-7/casp-3. It is known that MCF-7/mock cells lack the enzyme caspase-3 (Engels et al. 2005). The second one has caspase-3 later incorporated in the cells so that they stably express this

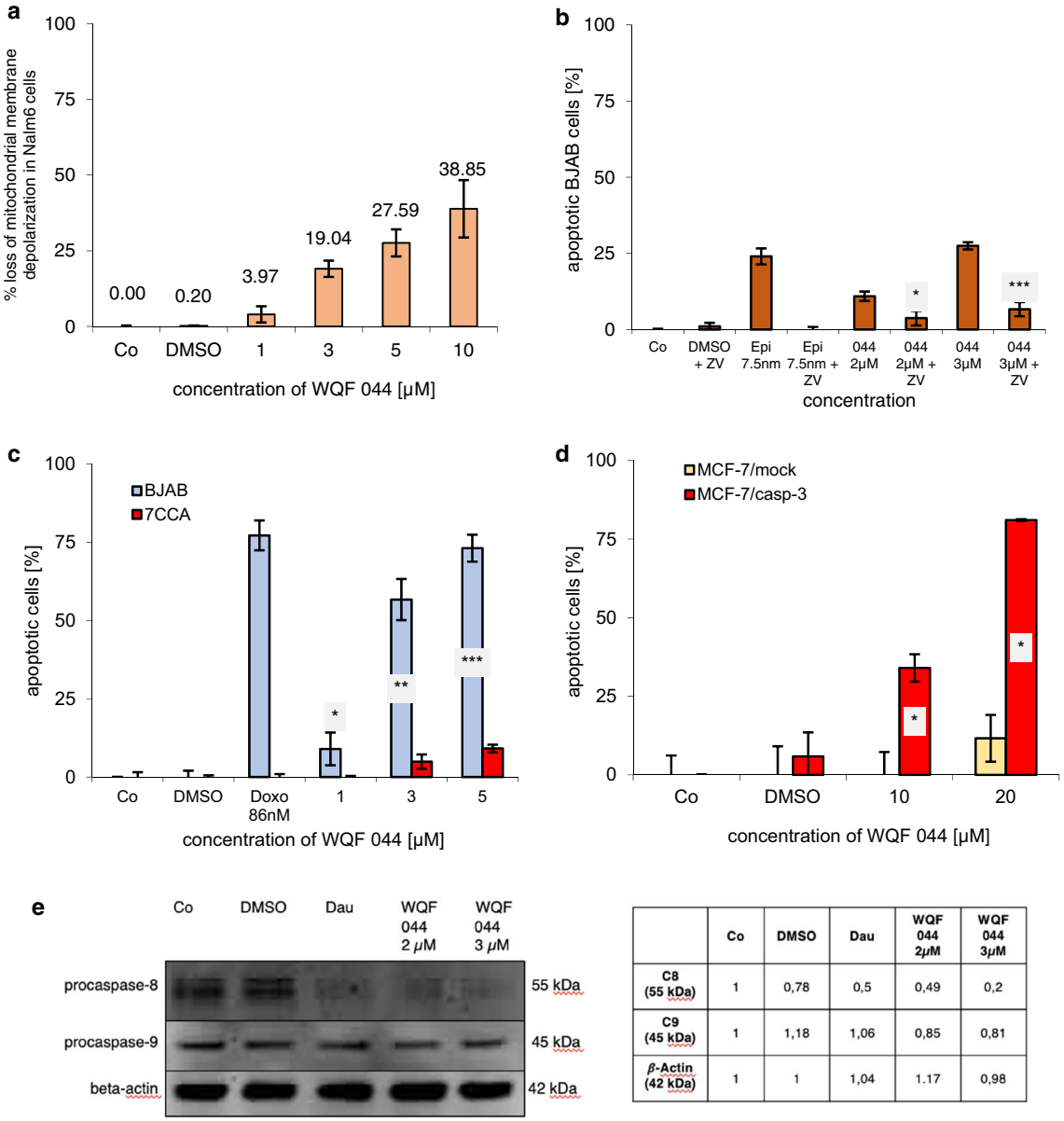

	Co	DMSO	Dau	WQF 044 2µM	WQF 044 3µM
C8 (55 kDa)	1	0,78	0,5	0,49	0,2
C9 (45 kDa)	1	1,18	1,06	0,85	0,81
β-Actin (42 kDa)	1	1	1,04	1.17	0,98

Fig. 5 Caspase dependence of WQF 044. Control cells (Co) were left untreated or treated with DMSO. Comparison of data was calculated by a one-tail *t* test. Results have been asterisked as followed: $*p<0.05$; $**p<0.01$; $***p<0.001$. **a** After incubating Nalm6 cells for 48 h hours with different concentrations of WQF 044, the mitochondrial permeability transition was measured by flow cytometric analysis. Values are given as percentage of cells with low $\Delta\Psi_m \pm$ SD ($n=3$). **b** BJAB cells were treated with 2 µM and 3 µM of WQF 044, alone and in combination with the pancaspase-inhibitor zVAD-fmk (ZV). As control 7.5 nM of epirubicin (Epi) were pipetted alone and in combination with ZVAD-fmk. After 72 h of incubation at 37 °C, DNA fragmentation was measured by flow cytometric analysis. Values were given in percentage of apoptotic cells ± SD ($n=3$). Statistical comparison of data was between the single WQF 044 group and the combined treatment with ZV, respectively. **c** BJAB and 7CCA cells were incubated with different concentrations of WQF 044 for 72 h. DNA fragmentation was measured by flow cytometric analysis. Apoptotic cells were displayed as percentage of the means of three separate samples ± SD. Doxorubicin (Doxo) was applied at 86 nM to show the resistance. **d** MCF-7/mock cells were compared with MCF-7/casp-3 cells in their induction of apoptosis after incubating them with 10 and 20 µM of WQF 044 for 72 h ($n=3$). As in the MelHO cells, higher concentrations than in Nalm6 and BJAB cells were used due to the lower sensitivity of these adherent cells. **e** WQF 044 induces caspase-8 (C8) and caspase-9 (C9) activation in Nalm6 cells. Daunorubicin (Dau) was used as positive control. Nalm6 cells were treated with 2 µM and 3 µM of WQF 044. All cells were incubated for 48 h at 37 °C. The separation of 20 µg cytosolic proteins was done by SDS-PAGE, followed by subjecting them to the western blot analysis. Immunblotting was then done with an anti-C8 and anti-C9 antibody. 43 kDa β-actin was detected to prove equal loading. The western blot quantification was calculated using GeneTools (Syngene). The control was set as 1. DMSO, Dau and WQF 044 2 and 3 µM were compared with the control, respectively

protease. In these MCF-7/casp-3 cells, the DNA fragmentation grade increased from 34 percent at 10 µM of WQF 044 to 81 percent at 20 µM (Fig. 5d). In comparison, exposing MCF-7/mock cells to WQF 044 resulted in no induction of apoptosis. At 20 µM of WQF 044, less than 12 percent of the cells were apoptotic.

Our investigations of WQF 044 in caspase-3 over- and under-expressed cell lines were supported by using the pan-caspase-inhibitor zVAD-fmk. The treatment of BJAB cells with WQF 044 and zVAD-fmk, alone and in combination, revealed an inactivation of the salalen ligand. WQF 044 could not induce apoptosis under the influence of the inhibitor in a dose-dependent manner (Fig. 5b). The apoptotic effects were significantly lower in the combination treatment with the inhibitor and 2 µM of WQF 044, and even very significantly reduced further when using 3 µM of WQF 044 with zVAD-fmk. This result underlines the dependence of WQF 044 on the broad caspase-induced cell-death.

A western blot analysis, after treating Nalm6 cells with 2 and 3 µM of WQF 044 for 48 h, revealed smaller procaspase-9 (49 kDa) and procaspase-8 (55 kDa) bands in the exposed cells compared to the control cells (Fig. 5e). The western blot quantification illustrated the lower number of proteins of inactivated caspase-8 and caspase-9 in comparison to the control cells. The processing of caspase-9 underlined the activation of the mitochondrial pathway by WQF 044.

WQF 044-induced apoptosis is independent of the extrinsic pathway

Significant involvement of the extrinsic pathway, characterized by an activation of caspase-8, was excluded in different ways. BJAB/FADDdn cells were transfected with pcDNA3-FADD−/−. They are expressing a dominant negative FADD mutant that is lacking the death domain. The BJAB/mock cells have a pcDNA3-Primer without the FADDdn gene. The values of WQF 044-treated apoptotic BJAB/FADDdn cells were not significantly higher than these in BJAB/mock cells (Fig. 6a).

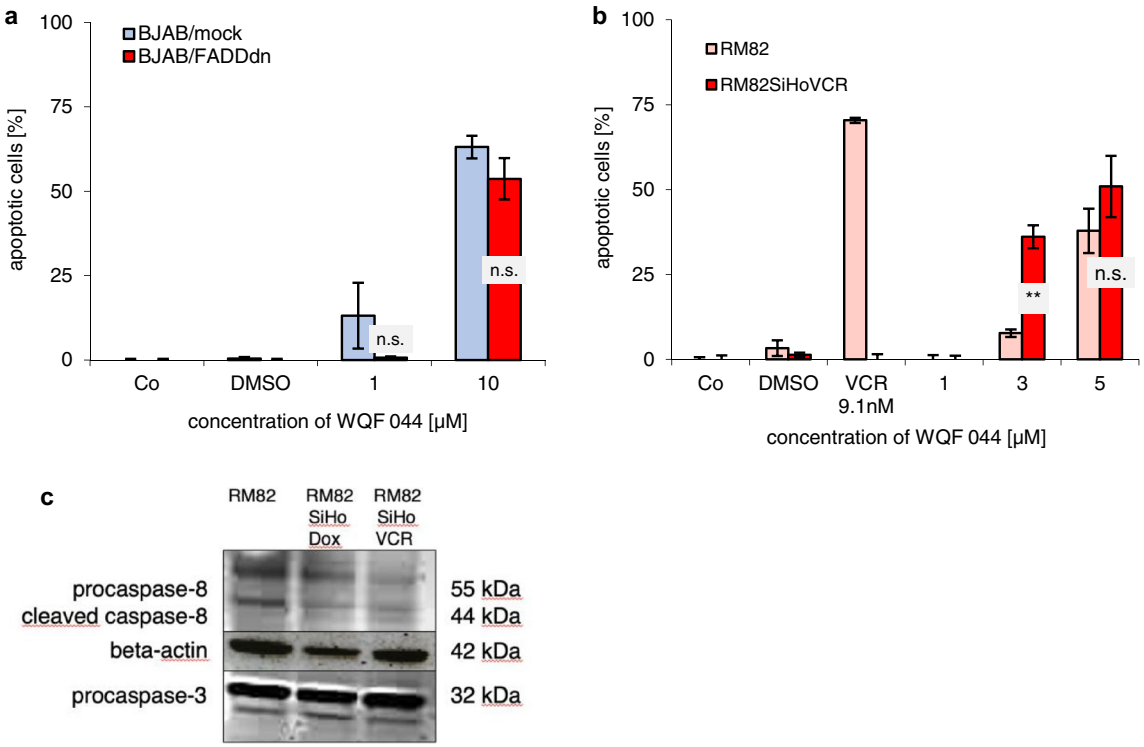

Fig. 6 Exclusion of the extrinsic apoptotic pathway. Incubation time for DNA fragmentation was 72 h at 37 °C. It was measured by flow cytometric analysis. Values were given in percentage of apoptotic cells ± SD ($n = 3$). Control cells (Co) were left untreated. **a** BJAB mock and BJAB/FADDdn cells were exposed with 1 and 10 µM of WQF 044. The differences between the values of WQF 044-treated BJAB/mock and BJAB/FADDdn cells in the two concentrations were not significant (n.s.) with $p > 0.05$. **b** RM82 and vincristine (VCR)-resistant RM82SiHoVCR cells were treated with different concentrations of WQF 044. Comparison of data was performed using a one-tail t test. Results have been asterisked as $^{**}p < 0.01$; *ns* not significant. **c** Presence of caspase-8 and -3 in untreated Ewing's sarcoma cells. For this paper, we focus on the RM82 and RM82SiHoVCR cell line. The separation of 20 µg cytosolic proteins was done by SDS-PAGE, followed by subjecting them to western blot analysis. Immunoblotting was then done with anti-caspase-3 and anti-caspase-8 antibodies. 42 kDa β-actin was detected to prove equal loading

Superficially, an activation of caspase-8 in the western blot analysis was inconsistent with the results of the BJAB/FADDdn cells. However, a previous study demonstrated that caspase-8 can be activated by caspase-3 over the intrinsic pathway; hence its activation is independent of the CD95 death-inducing signaling complex (Wieder 2001).

These results were further supported by a DNA-fragmentation with a Ewing's sarcoma cell line from a primary tumor in the femur, called RM82, that we newly made resistant to vincristine (RM82SiHoVCR) (Ottaviano 2010; van Valen et al. 1992). Polymerase chain reactions and western blot analysis revealed a sixfold CD95-underexpression (data not shown) and a downregulation of procaspase-8 (Fig. 6c) in the vincristine-resistant RM82 cells, whereas caspase-3 bands did not distinguish between the primary tumor and the resistant cell line. Next to their vincristine-resistance, RM82SiHoVCR cells are resistant to several vinca alkaloids, anthracyclines (Table 1) and platins. CD95, also called Fas, is a pro-apoptotic member of the extrinsic pathway (Lavrik and Krammer 2012; Schmidt et al. 2015; Strasser et al. 2009). Thus, apoptosis of RM82SiHoVCR seems to be blocked over the extrinsic pathway. Van Valen et al. earlier described that wild-type RM82 cells can be affected by tumor necrosis factor-related apoptosis-inducing ligand (TRAIL), a member of the extrinsic pathway of apoptosis (Van Valen et al. 2000). Figure 4b clearly demonstrates that the induction of apoptosis by WQF 044 was not disrupted by the CD95-under-expression in vincristine-resistant Ewing's sarcoma cells. At a WQF 044 concentration of 3 µM, the value of apoptotic RM82SiHoVCR cells was even significantly higher than in regular RM82 cells.

WQF 044 sensitizes BJAB cells to vincristine

The use of polychemotherapy results in lower side effects of the selected cytostatic drugs during cancer treatment. Therefore, the compound WQF 044 was tested in combination with vincristine to see if it had the potential to sensitize BJAB cells. Vincristine is a main chemotherapeutic in the fight against Burkitt lymphoma (Dunleavy 2013; Painschab 2019). Thus, the cells were exposed separately to WQF 044 and vincristine and to a combination of both cytostatic agents. Very low concentrations were used that did not affect the cells in single use. The effects are shown in Fig. 7. Synergistic effects of 352 percent after combining 1 µM of WQF 044 with 0.4 µM of vincristine were observed. An even stronger synergism appeared after pipetting 1 µM of WQF 044 plus 0.5 µM of vincristine on BJAB cells (375 percent).

WQF 044 is highly selective to tumor cells

Remarkably, we found out that WQF 044 had nearly no apoptotic effect in healthy human leucocytes. We compared a DNA fragmentation of the substance in leucocytes with those in BJAB and Nalm6 cells. While the cancer cells were highly affected by WQF 044 in a dose-dependent manner, leucocytes showed no significant levels of apoptosis in WQF 044 concentrations from 1 to 5 µM (Fig. 8a). As it turned out in the measurement of early/late apoptosis and necrosis, WQF 044 did not affect the leucocytes in a dose-dependent manner (Fig. 8b). At a WQF 044 concentration of 5 µM, less than 10 percent of the cells were either apoptotic or necrotic whereas the viability of the cells was at 92 percent (Figs. 2c, 8b).

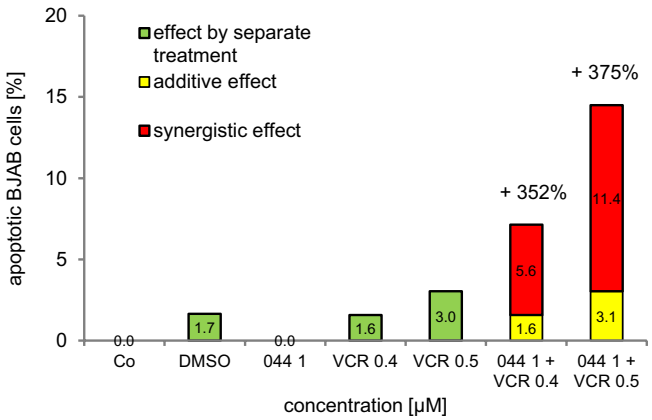

Fig. 7 Synergistic effects of WQF 044 (044) and vincristine (VCR). BJAB cells were treated with 1 µM of WQF 044 and 0.4/0.5 µM of vincristine, alone and in combination. Control cells (Co) were left untreated or with DMSO. After 72 h of incubation at 37 °C, induction of apoptosis was measured by flow cytometric analysis of nuclear DNA fragmentation. Values were given in percentage of apoptotic cells and were expressed at means ± SD ($n = 3$). To determine synergistic effects, the fractional product was calculated

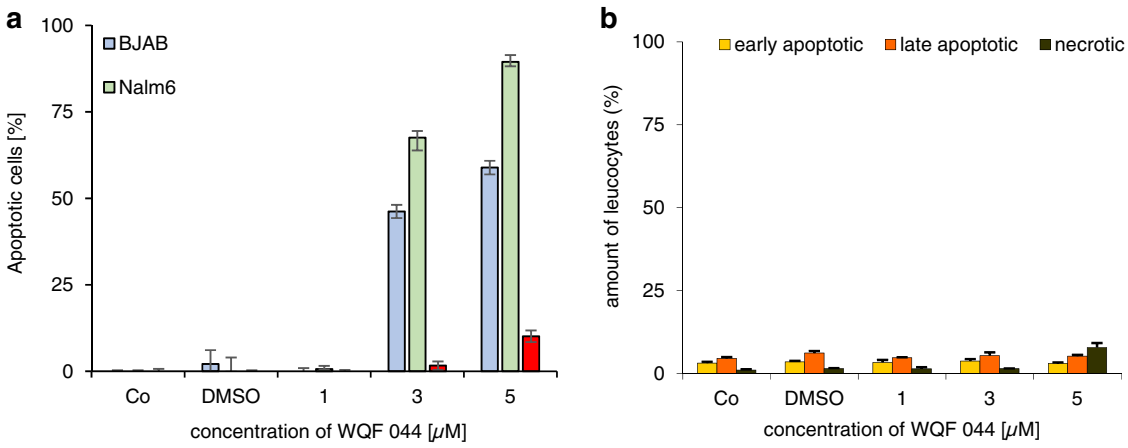

Fig. 8 Selectivity of WQF 044 to cancer cells. **a** A DNA fragmentation of treated BJAB, Nalm6 and non-malignant leucocytes was done. Cells were treated with 1 to 5 µM of WQF 044 and incubated for 72 h at 37 °C. The number of apoptotic cells was measured by flow cytometric analysis using three batches per concentration. Values were given in percentage and were expressed at means ± SD. **b** After incubation at 37 °C for 48 h with 1 to 5 µM of WQF 044, early and late apoptosis and necrosis were measured in leucocytes after Annexin V/PI staining by using flow cytometry ($n = 3$). AnnV+/PI– cells were defined as early apoptotic, AnnV+/PI+ as late apoptotic and AnnV–/PI+ as necrotic cells

Discussion

The discovery of novel organic compounds is of high interest since the discovery of the high cytostatic metal complex cisplatin. Severe side effects such as nephrotoxicity, allergic reactions and gastrointestinal symptoms often limit chemotherapy with cisplatin (Dasari and Tchounwou 2014). Therefore, the metal-free salalen ligand WQF 044 might be a potential alternative with less toxicity.

Especially after long-term chemotherapy, MDR represents a huge problem that causes therapy failure (Baguley 2010). In clinical use, cytostatic agents that modulate ABC transporters have not always proven as efficient as they seemed during their laboratory investigations (Li 2017). Thus, finding new substances with the potential to overcome MDR is a very important goal in oncology research. The examination of the metal-free ligand WQF 044 revealed very promising characteristics of the substance as a future cytostatic drug. An impressive overcoming of MDR in daunorubicin- and vincristine-resistant Nalm6 cells was observed (Fig. 3a, b). The substance defeated the over-expression of P-gp. Moreover, quite remarkable anti-proliferative effects of WQF 044 in leukemia cells were detected in a low micromolar range (Fig. 2b).

The synergetic effects of WQF 044 and vincristine in BJAB cells make the compound even more attractive as a substance that overcomes the defense barrier of the acute lymphoblastic leukemia and Burkitt-lymphoma that cannot be successfully treated with typical common therapies (Fig. 7).

Potential anti-cancer substances often fail in clinical use due to high toxicity. For example, colchicine was used in low concentrations to treat gout and familial Mediterranean fever, but the higher concentrations, that are necessary for anti-cancer treatment, resulted in too many side effects (Kumar et al. 2017). Furthermore, several metal complexes were very promising for anti-cancer treatment, but their *in-vivo* toxicity often limited their use (Liang et al. 2017). In contrast, the substance WQF 044 is a metal-free ligand, thus avoiding metal-induced toxicity. As a most exciting consequence, no apoptotic effects were seen upon treating the healthy human leucocytes with WQF 044, compared to the high apoptotic values in leukemia and lymphoma cells (Figs. 2c, 8a, b). In comparison, leukemia and lymphoma cells lost their viability and showed early and late apoptosis after treating them with WQF 044 (Fig. 2c–e).

Other metal ligands have already been tested in tumor cells. As mentioned in the introduction, the metal-free salan-type compound THG 1213 has been examined and showed anti-proliferative and apoptotic effects in Nalm6 and solid tumor cells and their resistant cell lines in low micromolar concentrations. In contrast, the salen ligand THG 1212 did not affect tumor cells (Dragoun et al. 2018).

Next to the experiments that were done with THG 1213, we widened the examination of WQF 044 with several experiments. Due to our high interest in new metal complexes and their ligands, we focused on cells of a Ewing's sarcoma. The well-known platin derivate cisplatin is used in relapsed treatment of Ewing's sarcoma patients, but strong side effects limit their use (van Maldegem 2015). Therefore, the impressive apoptotic effects of WQF 044, even in resistant Ewing's sarcoma cells, are an important finding (Fig. 6b). The substance may be an alternative treatment in

relapsed Ewing's sarcoma that still has a very frustrating survival-prognosis (Cotterill et al. 2000).

We further observed that the working mechanisms of WQF 044 and THG 1213 are different: THG 1213 could not affect the BJAB/FADDdn cells in the same way than regular BJAB cells, underlining their dependence of the extrinsic pathway, whereas WQF 044 showed a clear independence of the extrinsic pathway of apoptosis as it was not dependent of CD95 (Fig. 6a) (Dragoun et al. 2018). CD95 (APO-1/Fas) is a death receptor and part of the death-including complex that activates caspase-8 over the adapter molecule FADD (Krammer 2000). The independence of the WQF 044-induced apoptosis on the extrinsic pathway was supported by the results of the PCR array analysis: a sixfold under-expression of FADD and a 42-fold under-expression of CD95 were observed what is a clear point against the main involvement of the extrinsic pathway (Table 2).

Especially the fact that the salan THG 1213 induced apoptosis in a low micromolar range, but the salen THG 1212 did not affect the cells made the exploration of the corresponding salalen WQF 044 most interesting. The different results of THG 1213 and WQF 044 underline that even small differences in the chemical structure of a compound can cause completely different results in human cells. Earlier studies on other salans showed that these compounds developed anti-proliferative effects in MCF-7 and other human breast cancer cells at concentrations of 1–2 µM (Gao et al. 2007), whereas WQF 044 needed higher concentrations to affect MCF-7 cells. THG 1213 could not affect MCF-7 cells at all in this micromolar range (Dragoun et al. 2018). Future in-vivo experiments are intended to probe whether the metal-free ligands WQF 044 and THG 1213 show different efficiency on this level.

The examination of other substances illustrates that it cannot be predicted a priori whether a ligand or a metal complex cause better anti-cancer effects. For example, Kilic et al. (2018) found that different hemi-salen ligands showed higher anticancer activity in four different cancer cell lines, whereas related triboron complexes did not affect the cells in the same way (Kilic et al. 2018). Interestingly, Ghanbari (2014) observed that the increase in aromatic rings on the bridge between D-amino groups caused more apoptotic activity of their Fe(III)-salen-like complexes (Ghanbari et al. 2014). Once again, both the ligand structure and the position of the substituent of the salen ligand can modify the effects on cancer cells.

In the case of the molybdenum complexes described by Dragoun et al. (2018), the complexes did not affect the tumor cells in the same way the ligands THG 1213 and WQF 044 did (Dragoun et al. 2018). In comparison to that, another study illustrated that a cobalt(III) salen complex had cytotoxic effects in BJAB and Nalm6 cells, but the corresponding ligand could not induce apoptosis in the tumor cells (Hopff et al. 2020). Furthermore, ruthenium(II) complexes had cytotoxicity effects in MCF-7 and human prostate tumor cells (DU-145) in a low micromolar range, whereas their metal-free-ligand did not provoke the same outcome (Correa 2016).

Due to its high anti-cancer potential, we were very interested in the mode of action of WQF 044 and found out that the intrinsic pathway played a main role. The mitochondrial membrane potential was reduced in WQF 044 influenced Nalm6 cells (Fig. 5a). The high permeability of the mitochondria membrane results in a release of cytochrome c into the cytosol (Kroemer and Reed 2000). This activates procaspase-9, among other proteins. The downstream caspases, especially caspase-3 and caspase-8, are stimulated, so that they lead to DNA fragmentation and apoptosis (Hengartner 2000; Herr and Debatin 2001; Nagata 2000). The consumption of procaspase-8 and procaspase-9 after treating Nalm6 cells with WQF 044 was detected in the western blot analysis (Fig. 5e). The fact that caspase-8 was activated by WQF 044, but the substance did not mainly act over the extrinsic pathway was explained by the phenomenon of a caspase-3 induced caspase-8 activation as described (Wieder et al. 2001).

Furthermore, besides the blocking of P-gp, the compound acted caspase dependent. The extremely low apoptotic effects in caspase-3 under-expressed 7CCA and caspase-3 defective MCF-7/mock cells clearly illustrated that the protease is necessary for WQF 044 to develop its effects on the cells (Fig. 5c, d).

The strong inhibition of WQF 044-induced apoptotic effects by the pancaspase-inhibitor zVAD-fmk clearly supported the caspase-dependent apoptotic mechanism of the compound (Fig. 5b). The zVAD-fmk inhibitor did not completely block apoptosis in WQF 044 treated BJAB cells, whereas the positive control with epirubicin showed no apoptosis. This result points to the involvement of other members of the apoptotic pathway in the mechanism of action of the compound WQF 044.

A 43-fold over-expression of cytochrome c was detected in the PCR array analysis (Table 2). WQF 044 also over-expressed the direct IAP (inhibitor of apoptosis)-binding protein (DIABLO) by 15-fold (Table 2). DIABLO is part of the intrinsic pathway as it is released from the mitochondria. It neutralizes the anti-apoptotic activity of IAP family members (Herr and Debatin 2001). The release of pro-apoptotic components like cytochrome c and DIABLO from the mitochondria is regulated by members of the Bcl-2 family. They influence apoptosis by changing the mitochondria membrane permeability (Antonsson and Martinou 2000; Liu and Hengartner 1999). We found that WQF 044 is dependent on the anti-apoptotic Bcl-2. The over-expression of Bcl-2 in BiBo and MelHO-Bcl2 cells reduced the apoptotic effects

of WQF 044, underlining the involvement of the intrinsic pathway of apoptosis (Fig. 4a, b). Even though WQF 044 did not have the same apoptotic effects in BiBo cells compared to BJAB cells, it still induced apoptosis and overcame the Bcl-2 over-expression (Fig. 4a). This can be explained by the fact that WQF 044 inhibited Bcl-2, as the compound evoked an 18-fold under-expression of this anti-apoptotic protein (Table 2). However, WQF 044 did not break the over-expression of Bcl-2 by 30-fold, existing in the MelHO/Bcl-2 cells, in a dose-dependent manner (Fig. 4b) (Onambele 2010). Another interesting observation was the fivefold over-expression of BAX in the PCR array analysis (Table 2). This is in line with the inhibition of the WQF 044-induced apoptotic effects when anti-apoptotic Bcl-2 is predominant because then it inhibits BAX. Once activated, BAX directly supports the mitochondrial outer membrane permeabilization resulting in a release of killing effectors into the cytosol (Renault et al. 2013).

With our investigations of the salalen ligand WQF 044, we clearly detected the apoptotic mechanisms in different tumor cells and pointed out a main involvement of the intrinsic pathway of apoptosis. Next to the control of the intrinsic pathway of apoptosis by releasing proapoptotic factors, mitochondria own other functions to influence cell death (Orrenius et al. 2003). Therefore, the exact way of how a substance activates the mitochondrial mechanisms of apoptosis can differ. The metal ion reservoir can be depleted or the production of reactive oxygen species (ROS) can be increased above a cytotoxic threshold (Bao 2019; Nam et al. 2018; Yang et al. 2016). Further investigations in this direction are beyond the focus of this manuscript. It will surely to address these issues in future experiments.

Conclusion

Overall, our investigations revealed that salalen ligands, exemplified by compound WQF 044, are quite promising for anti-cancer treatment. Especially the low cytotoxic effects in healthy human leucocytes and the wide range of tumors, that WQF 044 can combat, make the substance highly interesting for future use as a chemotherapeutic. Additionally, we gained new insights into the in-vitro activity of this compound by underlining the mitochondrial function in cancer cells, resulting in a new approach to fight against resistant cancers, especially in childhood.

Methods

Materials

Rnase A was from Qiagen (Hilden, Germany). Propidium iodide (50 µg/ml) was from Serva (Heidelberg, Germany). Further the zVAD-fmk (pancaspase/ panprotease) inhibitor was used. All common cytostatics were provided by the Children's Hospital of the City Cologne, Amsterdamer Straße. The cytostatic agents were freshly dissolved as stock solutions in DMSO prior to the experiments. They were diluted with the respective cell culture media or buffer during the assay procedures. The substance WQF 044 was dissolved in a 40-mM stock solution of DMSO. Next to the regular control cells in the experiments, some cells were incubated with an equal amount of DMSO only, as DMSO control. The results showed similar effects to those obtained in the untreated controls.

WQF 044 was synthesized and characterized according to Berkessel et al. (2007).

Cell lines and cell cultures

We used the human b cell precursor leukemia cell line Nalm6 (AG Henze, Charité, Berlin), the Burkitt-like lymphoma BJAB/mock cells (Prof. Dr. S. Fulda, University of Ulm), the BJAB/FADDdn cells (Peter Daniel, Charité Berlin), the breast adenocarcinoma MCF-7/mock and MCF-7/casp-3 cells (Prof. Dr. R. Jänicke, University of Düsseldorf) and the human melanoma MelHO pIRES and MelHO Bcl-2 cells (Dr. Eberle, Charité, Berlin). Nalm6 and BJAB cells were made resistant in our lab by exposing them to increasing concentrations of the current cytostatic drug. RM82 is a human Ewing's sarcoma cell line from F. Van Valen, University of Muenster, Germany that was exposed to increasing concentrations of vincristine to make the cells resistant (RM82SiHoVCR).

The cell lines were incubated in 250 ml cell culture bottles at 37 °C. RPMI 1640 medium (GIBCO, Invitrogen, Karlsruhe, Germany) was used for the suspension cells. Heat inactivated fetal calf serum (FCS, 10%, v/v), L-glutamine (0.56 g/l), penicillin (100,000 i.u.) and streptomycin (0.1 g/l) were added. The adherent cells were grown in DMEM supplemented with FCS (10%, v/v) and geniticine (0.4 mg/ml). We took care of the cell cultures twice a week and diluted them to a concentration of 1×10^5 cells/ml. 24 h before using the cells for experiments, they were adjusted to 3×10^5 cells/ml to have standard conditions in growing. Immediately before the start of experiments, cells were diluted to 1×10^5 cells/ml.

Measuring the inhibition of cell proliferation by CASY cell counter and analyzer system

CASY cell counter and analyzer system from Roche were used to determine cell count and viability with specifically defined settings for the current cell lines. The system measures the cell concentration in three different size ranges that include cell debris, dead cells and viable cells (Voisard et al. 1991). Before measuring, all cells were treated with different concentrations of WQF 044. Some cells were left untreated or with DMSO as control. Incubation time was 24 h at 37 °C. Then, cells were resuspended and 100 µl of each well was diluted in 10 ml of CASYton (ready-to-use isotonic saline solution) for an immediate automated count of the cells. We defined the control group of the cells as 100% growth meaning that a cell concentration not higher than at the beginning of the experiment reveals maximum inhibition of cell proliferation.

LDH release assay for excluding necrosis

To make sure that cell death was due to apoptosis and not necrosis, a measurement of the lactate dehydrogenase (LDH) release was made. Nalm6 cells were exposed to different concentrations of WQF 044 and incubated for 3 h. With the help of the Cytotoxicity Detection Kit from Roche (Mannheim, Germany), the release of LDH out of the cells was measured in the cell culture supernatants. After centrifugation at 350*g* for 5 min, 20 µl of cell-free supernatants was diluted with 80 µl phosphate-buffered saline (PBS) supplemented with 100 µl reaction mixture containing 2-(4-iodophenyl)-3-(4-nitrophenyl)-5-phenyl-tetrazolium chloride (INT), sodium lactate, NAD^+ and diaphorase. Time-dependent formation of the reaction product was quantified photometrically at 490 nm. The maximum amount of LDH release was determined after lysis of the cells using 0.1 percent Triton X-100 in culture medium and set to represent 100 percent cell death.

Annexin V/propidium iodide binding assay

The Annexin-V-Fluos Staining kit (Roche, Mannheim, Germany) was used to detect early and late apoptosis and necrosis. Nalm6 and BJAB cells and healthy human leucocytes were incubated with different concentrations of WQF 044 for 48 h at 37 °C. The preparation of the samples was made according to the instructions of the manufacturer. The data were analyzed by using the FACScan (Becton Dickinson, Heidelberg, Germany), equipped with the CELL Quest software. Early apoptosis was defined as Annexin V-positive and PI-negative and late apoptosis as Annexin V/PI-double-positive. Vital cells were Annexin V/PI-double-negative (Brauchle et al. 2014; Wlodkowic et al. 2011). Annexin V-negative and PI-positive marked necrotic cells that were damaged during the isolation procedure (van Engeland et al. 1998).

Measurement of DNA fragmentation

For detecting the percentage of apoptotic cells, different concentrations of WQF 044 were pipetted on the cells before incubating them for 72 h at 37 °C. Then, adherent cells were washed with 180 µl Phosphate-buffered saline (PBS) and treated with trypsin for 5 min at 37 °C. A centrifugation at 1500 rpm helped to collect all cells. Then, they were fixed in 200 µl PBS/2% (v/v) formaldehyde on ice for 30 min, continued by a centrifugation at 1500 rpm for 5 min by 4 °C. After incubating them with 180 µl ethanol/PBS (2:1, v/v) for 15 min, followed by a 5-min centrifugation at 1500 rpm, cells were resuspended in 50 µl PBS containing 40 µg/ml Rnase A that for 30 min at 37 °C. Cells were centrifuged at 1500 rpm for 5 min for a last time; then they were finally resuspended in 200 µl PBS containing 50 µg/ml propidium iodide. As described, the nuclear DNA fragmentation on the single cell level was measured by a modified cell cycle analysis (Essmann et al. 2000). By using a FACScan (Becton Dickinson, Heidelberg, Germany), equipped with the CELL Quest software, data were collected and analyzed. The results show the number of apoptotic cells reflected by the percentage of hypoploidy (subG1). In the end, the current apoptotic effects were calculated by subtracting the background apoptosis of the control cells from total apoptosis seen in the treated cells.

Immunoblotting

After 48 h of incubation with different concentrations of WQF 044, Nalm6 cells were washed twice with PBS and lysed in buffer containing 10 mM Tris–HCl, pH 7.5, 300 mM NaCl, 1% Triton X-100, 2 mM $MgCl_2$, 5 µM ethylenediamino tetra-acetic acid (EDTA), 1 µM pepstatin, 1 µM leupeptin, and 0.1 mM phenylmethyl-sulfonyl fluoride (PMSF). The same process was made with untreated RM82 and RM82SiHoVCR cells. By using the bicinchoninic acid assay from Pierce (Rockford, IL, USA), the protein concentration was determined and equal amounts of protein were separated by SDS–PAGE (Laemmli 1970; Smith 1985). The immunoblotting was performed as described (Wieder et al. 1994). The blocking of the membrane was made for 1 h in PBST (PBS, 0.05% Tween-20) containing BSA and incubated with different primary antibodies for 1 h. The anti-caspase-8, anti-caspase 9, anti-caspase-3, and anti-beta-actin from Sigma, Saint Louis, USA were used. After washing of the membrane with PBST, secondary antibody (anti-mouse IgG HRP from Bioscience, San Diego, USA and anti-rabbit IgG HRP from Promega, Minneapolis, USA) in

PBST was applied for 1 h. After washing, the protein bands were detected using the ECL enhanced chemiluminescence system (Amersham Buchler, Braunschweig, Germany). The western blot quantification was done using GeneTools (Syngene).

Measurement of the mitochondrial permeability transition

Nalm6 cells were treated with different concentrations of WQF 044 and incubated for 48 h at 37 °C. The cells were then centrifuged at 1500 rpm, 4 °C for 5 min. The JC-1 dye (5,5′,6,6′-tetrachloro-1,1′,3,3′-te-traethyl-benzimidazolyl-carbocyanin io-dide, Molecular Probes, Leiden, The Netherlands) was used on the cells to determine the mitochondrial permeability transition as described (Lambert et al. 1989; Reers et al. 1995). Most of the cells were resuspended in 500 µl phenol red free RPMI 1640 without supplements, and JC-1 was added to give a final concentration of 2,5 µg/µl. Control cells were left without JC-1. Thus, all cells were incubated for 30 min at 37 °C and moderately shaken. To collect the cells again, they were centrifuged at 1500 rpm for 5 min at 4 °C. 200 µl ice-cold PBS was used to wash cells. The flow cytometric determination of cells with decreased fluorescence was used to measure the mitochondrial permeability transition. The FACScan (Becton Dickinson, Heidelberg, Germany) was equipped with the CELL Quest software and analyzed the samples. Control cells with low $\Delta\Psi_m$ were subtracted from the values observed in the treated cells. Data are given in percentage of cells with low $\Delta\Psi_m$, which reflects the number of cells undergoing mitochondrial apoptosis.

Gene expression analysis

The differential expression of multiple genes involved in the different apoptosis pathways was analyzed by using the apoptosis specific RT2 profiler (polymerase chain reaction) PCR expression arrays (SuperArray PAHS-012Z; SABiosciences Corporation, Frederick, MD, USA), according to the manufacturer's instructions (Inohara et al. 1997). Nalm6 cells were incubated with 1 µM of WQF 044 for 16 h, RM82 and RM82SiHoVCR cells were left untreated. Then total RNA was extracted from the cells. RNAs were treated with Dnase I (2 U/µl) to eliminate possible genomic DNA contamination. The total RNA (700 ng/µl) was used as a template for the synthesis of a cDNA probe. It was then subjected to quantitative real-time PCR SuperArray analysis according to the manufacturer's instructions using a LightCycler480 (Roche Diagnostics). The hybridization signals were normalized by the means of nine housekeeping genes. The results were analyzed by using the SuperArray Analyzer Software. Data are given as x-fold expression of the respective genes as compared with control (untreated Nalm6 or RM82 cells) cells incubated in vehicle-containing medium for 16 h.

Isolation of healthy human leucocytes

10 ml RPMI 1640 medium was added to 50 ml blood of a healthy test person. Then, 4 ml of Ficoll (Saccharose-Epichlorhydrin-Copolymer) was pipetted in a 15-ml tube, followed by carefully adding 5 ml blood on the top. After 18 min of centrifugation at 657*g* (20 °C), the leucocytes were collected by slowly transferring them with a Pasteur pipette into a 45-ml tube. 20 ml of RPMI 1640 was added. This solution was centrifuged at 1500 rpm for 5 min. The cell count and viability were determined by CASY cell counter and analyzer system from Roche. Cells were seeded at a density of 3×10^5 cells/ml. The following steps are identical to those in the measurement of DNA fragmentation as described above.

Statistical analysis

Statistically significant values were compared using a one-tailed *t* test. *p* values were expressed with asterisk. $p < 0.05$ (*) was considered statistically significant, $p < 0.01$ (**) highly significant and $p < 0.001$ (***) extremely significant. If $p > 0.05$ is calculated, the result is not significant (n.s.).

Acknowledgements We thank the Dr. Kleist Stiftung Berlin, and the Fonds der Chemischen Industrie for their general support.

Author contributions All authors contributed to the study conception and design. Material preparation, data collection and analysis was performed by SMH. CF, MA, NW and NW supported the data collection for the testing of multidrug resistances of selected cell lines. The first draft of the manuscript was written by SMH and all authors commented on previous versions of the manuscript. All authors read and approved the final manuscript.

Funding Open Access funding enabled and organized by Projekt DEAL.

Declarations

Conflict of interest The authors declare that they have no conflict of interest.

Ethical approval This article does not contain any studies with human participants or animals performed by any of the authors.

References

Antonsson B, Martinou JC (2000) The Bcl-2 protein family. Exp Cell Res 256:50–57. https://doi.org/10.1006/excr.2000.4839

Baguley BC (2010) Multidrug resistance in cancer methods. Mol Biol 596:1–14. https://doi.org/10.1007/978-1-60761-416-6_1

Bao L et al (2019) The human transient receptor potential melastatin 2 ion channel modulates ROS through Nrf2. Sci Rep 9:14132. https://doi.org/10.1038/s41598-019-50661-8

Berkessel A, Brandenburg M, Leitterstorf E, Frey J, Lex J, Schafer M (2007) A practical and versatile access to dihydrosalen (Salalen) ligands: highly enantioselective titanium in situ catalysts for asymmetric epoxidation with aqueous hydrogen peroxide. Adv Synth Catal 349:2385–2391. https://doi.org/10.1002/adsc.200700221

Brauchle E, Thude S, Brucker SY, Schenke-Layland K (2014) Cell death stages in single apoptotic and necrotic cells monitored by raman microspectroscopy. Sci Rep 4:4698. https://doi.org/10.1038/srep04698

Bruijnincx PC, Sadler PJ (2008) New trends for metal complexes with anticancer activity. Curr Opin Chem Biol 12:197–206. https://doi.org/10.1016/j.cbpa.2007.11.013

Cohen GM (1997) Caspases: the executioners of apoptosis. Biochem J 326(1):1–16

Correa RS et al (2016) Ruthenium(II) complexes of 1,3-thiazolidine-2-thione: cytotoxicity against tumor cells and anti-trypanosoma cruzi activity enhanced upon combination with benznidazole. J Inorg Biochem 156:153–163. https://doi.org/10.1016/j.jinorgbio.2015.12.024

Cotterill SJ, Ahrens S, Paulussen M, Jurgens HF, Voute PA, Gadner H, Craft AW (2000) Prognostic factors in Ewing's tumor of bone: analysis of 975 patients from the European intergroup cooperative Ewing's sarcoma study group. J Clin Oncol 18:3108–3114. https://doi.org/10.1200/JCO.2000.18.17.3108

Dasari S, Tchounwou PB (2014) Cisplatin in cancer therapy: molecular mechanisms of action. Eur J Pharmacol 740:364–378. https://doi.org/10.1016/j.ejphar.2014.07.025

Dragoun M, Gunther T, Frias C, Berkessel A, Prokop A (2018) Metal-free salan-type compound induces apoptosis and overcomes multidrug resistance in leukemic and lymphoma cells in vitro. J Cancer Res Clin Oncol 144:685–695. https://doi.org/10.1007/s00432-018-2592-x

Dunleavy K et al (2013) Low-intensity therapy in adults with Burkitt's lymphoma. N Engl J Med 369:1915–1925. https://doi.org/10.1056/NEJMoa1308392

Edlich F (2018) BCL-2 proteins and apoptosis: recent insights and unknowns. Biochem Biophys Res Commun 500:26–34. https://doi.org/10.1016/j.bbrc.2017.06.190

Engels IH, Totzke G, Fischer U, Schulze-Osthoff K, Janicke RU (2005) Caspase-10 sensitizes breast carcinoma cells to TRAIL-induced but not tumor necrosis factor-induced apoptosis in a caspase-3-dependent manner. Mol Cell Biol 25:2808–2818. https://doi.org/10.1128/MCB.25.7.2808-2818.2005

Essmann F, Wieder T, Otto A, Muller EC, Dorken B, Daniel PT (2000) GDP dissociation inhibitor D4-GDI (Rho-GDI 2), but not the homologous rho-GDI 1, is cleaved by caspase-3 during drug-induced apoptosis. Biochem J 346(Pt 3):777–783

Fadok VA, Xue D, Henson P (2001) If phosphatidylserine is the death knell, a new phosphatidylserine-specific receptor is the bellringer. Cell Death Differ 8:582–587. https://doi.org/10.1038/sj.cdd.4400856

Gao J, Liu YG, Zhou Y, Zingaro RA (2007) Chiral salicyl diamines: potent anticancer molecules. ChemMedChem 2:1723–1729. https://doi.org/10.1002/cmdc.200700049

Garner TP, Lopez A, Reyna DE, Spitz AZ, Gavathiotis E (2017) Progress in targeting the BCL-2 family of proteins. Curr Opin Chem Biol 39:133–142. https://doi.org/10.1016/j.cbpa.2017.06.014

Ghanbari Z et al (2014) Structure-activity relationship for Fe(III)-salen-like complexes as potent anticancer agents. Sci World J 2014:745649. https://doi.org/10.1155/2014/745649

Gottesman MM, Pastan I (1988) The multidrug transporter, a double-edged sword. J Biol Chem 263:12163–12166

Gottesman MM, Fojo T, Bates SE (2002) Multidrug resistance in cancer: role of ATP-dependent transporters. Nat Rev Cancer 2:48–58. https://doi.org/10.1038/nrc706

Grutzke M, Zhao T, Immel TA, Huhn T (2015) Heptacoordinate heteroleptic salan (ONNO) and thiosalan (OSSO) titanium(IV) complexes: investigation of stability and cytotoxicity. Inorg Chem 54:6697–6706. https://doi.org/10.1021/acs.inorgchem.5b00690

Hengartner MO (2000) The biochemistry of apoptosis. Nature 407:770–776. https://doi.org/10.1038/35037710

Herr I, Debatin KM (2001) Cellular stress response and apoptosis in cancer therapy. Blood 98:2603–2614

Hopff SM, Onambele LA, Brandenburg M, Berkessel A, Prokop A (2020) Discovery of a cobalt (III) salen complex that induces apoptosis in Burkitt like lymphoma and leukemia cells, overcoming multidrug resistance in vitro. Bioorg Chem 104:104193. https://doi.org/10.1016/j.bioorg.2020.104193

Immel TA, Groth U, Huhn T, Ohlschlager P (2011) Titanium salan complexes displays strong antitumor properties in vitro and in vivo in mice. PLoS ONE 6:e17869. https://doi.org/10.1371/journal.pone.0017869

Immel TA, Grutzke M, Batroff E, Groth U, Huhn T (2012a) Cytotoxic dinuclear titanium-salan complexes: structural and biological characterization. J Inorg Biochem 106:68–75. https://doi.org/10.1016/j.jinorgbio.2011.08.029

Immel TA, Grutzke M, Spate AK, Groth U, Ohlschlager P, Huhn T (2012b) Synthesis and X-ray structure analysis of a heptacoordinate titanium(IV)-bis-chelate with enhanced in vivo antitumor efficacy. Chem Commun (camb) 48:5790–5792. https://doi.org/10.1039/c2cc31624b

Inohara N, Ding L, Chen S, Nunez G (1997) harakiri, a novel regulator of cell death, encodes a protein that activates apoptosis and interacts selectively with survival-promoting proteins Bcl-2 and Bcl-X(L). EMBO J 16:1686–1694. https://doi.org/10.1093/emboj/16.7.1686

Jesse P, Mottke G, Eberle J, Seifert G, Henze G, Prokop A (2009) Apoptosis-inducing activity of *Helleborus niger* in ALL and AML. Pediatr Blood Cancer 52:464–469. https://doi.org/10.1002/pbc.21905

Kater B, Hunold A, Schmalz HG, Kater L, Bonitzki B, Jesse P, Prokop A (2011) Iron containing anti-tumoral agents: unexpected apoptosis-inducing activity of a ferrocene amino acid derivative. J Cancer Res Clin Oncol 137:639–649. https://doi.org/10.1007/s00432-010-0924-6

Kater L et al (2012) The role of the intrinsic FAS pathway in titanocene Y apoptosis: the mechanism of overcoming multiple drug resistance in malignant leukemia cells. Toxicol in Vitro 26:119–124. https://doi.org/10.1016/j.tiv.2011.09.010

Kelland L (2007) The resurgence of platinum-based cancer chemotherapy. Nat Rev Cancer 7:573–584. https://doi.org/10.1038/nrc2167

Kilic A, Koyuncu I, Durgun M, Ozaslan I, Kaya IH, Gonel A (2018) Synthesis and characterization of the hemi-salen ligands and their triboron complexes: spectroscopy and examination of anticancer properties. Chem Biodivers. https://doi.org/10.1002/cbdv.201700428

Krammer PH (2000) CD95's deadly mission in the immune system. Nature 407:789–795. https://doi.org/10.1038/35037728

Krishna R, Mayer LD (2000) Multidrug resistance (MDR) in cancer. Mechanisms, reversal using modulators of MDR and the role of MDR modulators in influencing the pharmacokinetics of anticancer drugs. Eur J Pharm Sci 11:265–283

Kroemer G, Reed JC (2000) Mitochondrial control of cell death. Nat Med 6:513–519. https://doi.org/10.1038/74994

Kumar A, Sharma PR, Mondhe DM (2017) Potential anticancer role of colchicine-based derivatives: an overview. Anticancer Drugs 28:250–262. https://doi.org/10.1097/CAD.0000000000000464

Laemmli UK (1970) Cleavage of structural proteins during the assembly of the head of bacteriophage T4. Nature 227:680–685

Lambert IH, Hoffmann EK, Jorgensen F (1989) Membrane potential, anion and cation conductances in Ehrlich ascites tumor cells. J Membr Biol 111:113–131

Lavrik IN, Krammer PH (2012) Regulation of CD95/Fas signaling at the DISC cell. Death Differ 19:36–41. https://doi.org/10.1038/cdd.2011.155

Lee SY et al (2010) [NiII(3-OMe-salophene)]: a potent agent with antitumor activity. J Med Chem 53:6064–6070. https://doi.org/10.1021/jm100459k

Lee SY et al (2011) [Fe(III)(salophene)Cl], a potent iron salophene complex overcomes multiple drug resistance in lymphoma and leukemia cells. Leuk Res 35:387–393. https://doi.org/10.1016/j.leukres.2010.11.007

Li YJ et al (2017) Autophagy and multidrug resistance in cancer. Chin J Cancer 36:52. https://doi.org/10.1186/s40880-017-0219-2

Liang JX, Zhong HJ, Yang G, Vellaisamy K, Ma DL, Leung CH (2017) Recent development of transition metal complexes with in vivo antitumor activity. J Inorg Biochem 177:276–286. https://doi.org/10.1016/j.jinorgbio.2017.06.002

Lin JH, Yamazaki M (2003) Role of P-glycoprotein in pharmacokinetics: clinical implications. Clin Pharmacokinet 42:59–98. https://doi.org/10.2165/00003088-200342010-00003

Liu QA, Hengartner MO (1999) The molecular mechanism of programmed cell death in C elegans. Ann N Y Acad Sci 887:92–104

Marques MB et al (2019) Modeling drug–drug interactions of AZD1208 with vincristine and daunorubicin on ligand-extrusion binding TMD-domains of multidrug resistance P-glycoprotein (ABCB1). Toxicology 411:81–92. https://doi.org/10.1016/j.tox.2018.10.009

Meker S, Manna CM, Peri D, Tshuva EY (2011) Major impact of *N*-methylation on cytotoxicity and hydrolysis of salan Ti(IV) complexes: sterics and electronics are intertwined. Dalton Trans 40:9802–9809. https://doi.org/10.1039/c1dt11108f

Mir JM, Jain N, Jaget PS, Maurya RC (2017) Density functionalized [Ru(II)(NO)(Salen)(Cl)] complex: computational photodynamics and in vitro anticancer facets. Photodiagnosis Photodyn Ther 19:363–374. https://doi.org/10.1016/j.pdpdt.2017.07.006

Mukhametov A, Raevsky OA (2017) On the mechanism of substrate/non-substrate recognition by P-glycoprotein. J Mol Graph Model 71:227–232. https://doi.org/10.1016/j.jmgm.2016.12.008

Nagata S (2000) Apoptotic DNA fragmentation. Exp Cell Res 256:12–18. https://doi.org/10.1006/excr.2000.4834

Nair P, Lu M, Petersen S, Ashkenazi A (2014) Apoptosis initiation through the cell-extrinsic pathway. Methods Enzymol 544:99–128. https://doi.org/10.1016/B978-0-12-417158-9.00005-4

Nam E, Han J, Suh JM, Yi Y, Lim MH (2018) Link of impaired metal ion homeostasis to mitochondrial dysfunction in neurons. Curr Opin Chem Biol 43:8–14. https://doi.org/10.1016/j.cbpa.2017.09.009

Onambele LA et al (2010) Mitochondrial mode of action of a thymidine-based cisplatin analogue breaks resistance in cancer cells. Chemistry 16:14498–14505. https://doi.org/10.1002/chem.201000785

Orrenius S, Zhivotovsky B, Nicotera P (2003) Regulation of cell death: the calcium-apoptosis link. Nat Rev Mol Cell Biol 4:552–565. https://doi.org/10.1038/nrm1150

Ottaviano L et al (2010) Molecular characterization of commonly used cell lines for bone tumor research: a trans-European EuroBoNet effort. Genes Chromosom Cancer 49:40–51. https://doi.org/10.1002/gcc.20717

Painschab MS et al (2019) Prospective study of burkitt lymphoma treatment in adolescents and adults in malawi. Blood Adv 3:612–620. https://doi.org/10.1182/bloodadvances.2018029199

Peri D, Meker S, Manna CM, Tshuva EY (2011) Different ortho and para electronic effects on hydrolysis and cytotoxicity of diamino bis(phenolato) "salan" Ti(IV) complexes. Inorg Chem 50:1030–1038. https://doi.org/10.1021/ic101693v

Pieters R, Klumper E, Kaspers GJ, Veerman AJ (1997) Everything you always wanted to know about cellular drug resistance in childhood acute lymphoblastic leukemia. Crit Rev Oncol Hematol 25:11–26

Rabik CA, Dolan ME (2007) Molecular mechanisms of resistance and toxicity associated with platinating agents. Cancer Treat Rev 33:9–23. https://doi.org/10.1016/j.ctrv.2006.09.006

Reers M, Smiley ST, Mottola-Hartshorn C, Chen A, Lin M, Chen LB (1995) Mitochondrial membrane potential monitored by JC-1 dye. Methods Enzymol 260:406–417

Renault TT, Teijido O, Antonsson B, Dejean LM, Manon S (2013) Regulation of bax mitochondrial localization by Bcl-2 and Bcl-x(L): keep your friends close but your enemies closer. Int J Biochem Cell Biol 45:64–67. https://doi.org/10.1016/j.biocel.2012.09.022

Rubbiani R et al (2010) Benzimidazol-2-ylidene gold(I) complexes are thioredoxin reductase inhibitors with multiple antitumor properties. J Med Chem 53:8608–8618. https://doi.org/10.1021/jm100801e

Schlegel RA, Williamson P (2001) Phosphatidylserine, a death knell. Cell Death Differ 8:551–563. https://doi.org/10.1038/sj.cdd.4400817

Schmidt JH, Pietkiewicz S, Naumann M, Lavrik IN (2015) Quantification of CD95-induced apoptosis and NF-kappaB activation at the single cell level. J Immunol Methods 423:12–17. https://doi.org/10.1016/j.jim.2015.04.026

Smith PK et al (1985) Measurement of protein using bicinchoninic acid. Anal Biochem 150:76–85

Strasser A, Jost PJ, Nagata S (2009) The many roles of FAS receptor signaling in the immune system. Immunity 30:180–192. https://doi.org/10.1016/j.immuni.2009.01.001

Terenzi A et al (2016) Another step toward DNA selective targeting: Ni(II) and Cu(II) complexes of a Schiff base ligand able to bind gene promoter G-quadruplexes. Dalton Trans 45:7758–7767. https://doi.org/10.1039/c6dt00648e

Uderzo C, Conter V, Dini G, Locatelli F, Miniero R, Tamaro P (2001) Treatment of childhood acute lymphoblastic leukemia after the first relapse: curative strategies. Haematologica 86:1–7

Van Cruchten S, Van Den Broeck W (2002) Morphological and biochemical aspects of apoptosis, oncosis and necrosis. Anat Histol Embryol 31:214–223

van Engeland M, Nieland LJ, Ramaekers FC, Schutte B, Reutelingsperger CP (1998) Annexin V-affinity assay: a review on an apoptosis detection system based on phosphatidylserine exposure. Cytometry 31:1–9. https://doi.org/10.1002/(sici)1097-0320(19980101)31:1%3c1::aid-cyto1%3e3.0.co;2-r

van Maldegem AM et al (2015) Etoposide and carbo-or cisplatin combination therapy in refractory or relapsed Ewing sarcoma: a large retrospective study. Pediatr Blood Cancer 62:40–44. https://doi.org/10.1002/pbc.25230

van Valen F, Winkelmann W, Jurgens H (1992) Expression of functional Y1 receptors for neuropeptide Y in human Ewing's sarcoma cell lines. J Cancer Res Clin Oncol 118:529–536. https://doi.org/10.1007/bf01225268

Van Valen F et al. (2000) Apoptotic responsiveness of the Ewing's sarcoma family of tumours to tumour necrosis factor-related apoptosis-inducing ligand (TRAIL). Int J Cancer 88:252–259. doi: https://doi.org/10.1002/1097-0215(20001015)88:2<252::aid-ijc17>3.0.co;2-u

Voisard R, Dartsch PC, Seitzer U, Roth D, Kochs M, Hombach V (1991) Cell culture as a prescreening system for drug prevention of restenosis? Vasa 33:140–141

Wang Y, Cui J, Dai Y, Wu Y, Huang W, Qian H, Ge L (2017) Reversal of P-glycoprotein-mediated multidrug resistance and pharmacokinetics study in rats by WYX-5. Can J Physiol Pharmacol 95:580–585. https://doi.org/10.1139/cjpp-2016-0518

Wieder T, Geilen CC, Wieprecht M, Becker A, Orfanos CE (1994) Identification of a putative membrane-interacting domain of CTP:phosphocholine cytidylyltransferase from rat liver. FEBS Lett 345:207–210

Wieder T, Orfanos CE, Geilen CC (1998) Induction of ceramide-mediated apoptosis by the anticancer phospholipid analog, hexadecylphosphocholine. J Biol Chem 273:11025–11031

Wieder T et al (2001) Activation of caspase-8 in drug-induced apoptosis of B-lymphoid cells is independent of CD95/Fas receptor-ligand interaction and occurs downstream of caspase-3. Blood 97:1378–1387

Wild A et al (2012) Synthesis of a glycopolymeric Pt(II) carrier and its induction of apoptosis in resistant cancer cells. Chem Commun (camb). https://doi.org/10.1039/c2cc31275a

Wlodkowic D, Telford W, Skommer J, Darzynkiewicz Z (2011) Apoptosis and beyond: cytometry in studies of programmed cell death. Methods Cell Biol 103:55–98. https://doi.org/10.1016/B978-0-12-385493-3.00004-8

Won JH et al (2018) 23-Hydroxyursolic acid isolated from the stem bark of cussonia bancoensis induces apoptosis through fas/caspase-8-dependent pathway in HL-60 human promyelocytic leukemia cells. Molecules. https://doi.org/10.3390/molecules23123306

Yang Y, Karakhanova S, Hartwig W, D'Haese JG, Philippov PP, Werner J, Bazhin AV (2016) Mitochondria and mitochondrial ROS in cancer: novel targets for anticancer therapy. J Cell Physiol 231:2570–2581. https://doi.org/10.1002/jcp.25349

Bioorganic Chemistry 104 (2020) 104193

Contents lists available at ScienceDirect

Bioorganic Chemistry

journal homepage: www.elsevier.com/locate/bioorg

Discovery of a cobalt (III) salen complex that induces apoptosis in Burkitt like lymphoma and leukemia cells, overcoming multidrug resistance in vitro

Sina M. Hopff[a,*], Liliane A. Onambele[a], Marc Brandenburg[b], Albrecht Berkessel[b], Aram Prokop[a,c]

[a] Department of Pediatric Hematology/Oncology, Children's Hospital Cologne, Amsterdamer Straße 59, 50735 Cologne, Germany
[b] Department of Chemistry, Organic Chemistry, University of Cologne, Greinstraße 4, 50939 Cologne, Germany
[c] Department of Pediatric Hematology/Oncology, Helios Clinic Schwerin, Wismarsche Straße 393-397, 19055 Schwerin, Germany

ARTICLE INFO

Keywords:
Acute lymphoblastic leukemia
Burkitt like lymphoma
Cobalt-salen complex
Multidrug resistance
P-glycoprotein
Caspases

ABSTRACT

A very small number of cobalt complexes is examined in oncology research. In this work, we investigate the cobalt (III) salen complex **MBR-60** that turns out to be a promising anticancer drug. It induces apoptosis in Nalm6 leukemia and BJAB lymphoma cells and overcomes multidrug resistances by blocking the drug efflux pump P-glycoprotein. It further develops the apoptotic effects over the intrinsic pathway. An activation of caspase-3, caspase-8 and caspase-9 can be detected by western blot analysis. The independence of CD95 is shown by similar apoptotic inductions in BJAB and BJAB FADDdn cells. **MBR-60** displays synergistic effects with daunorubicin and vincristine and has a selectivity to tumor cells. In comparison to the apoptotic effects of **MBR-60** in BJAB lymphoma cells, the cobalt-free ligand **5** does not influence these cells. The research highlights that a cobalt complex has a therapeutic potential for cancer treating with a focus on drug-resistant tumors.

1. Introduction

Salen ligands (**3**) are typically generated in a one-step procedure by the condensation of two equivalents of a salicylic aldehyde ("sal", **1**) with ethylene diamine ("en", **2**) or a related diamine. Due to the simplicity of their preparation, they represent one of the most widely used ligand motifs in coordination chemistry. Cobalt (Co) salens, e.g. "salcomine" (**4**), the Co(II) complex of the parent salen ligand, have been known since more than a century, and they have found widespread application as reversible oxygen binders and oxidation catalysts. More recently, chiral Co-salens - in most cases derived from *trans*-1,2-diamino-cyclohexane - have found use as important catalysts for highly enantioselective transformations, e.g. for the hydrolytic kinetic resolution of racemic terminal epoxides [1,2], or for the reaction of epoxide with carbon dioxide, affording cyclic or polymeric carbonates [3,4]. In this area, in particular Co(III)-complexes based on *tert.*-butylated and *trans*-DACH derived salen ligand **5** have found widespread use [1–4]. The catalytically active Co(III)-complexes are typically prepared from the Co(II)-complex of the commercially available ligand **5** by air oxidation, prior to application, in the presence of the corresponding co-ligand. For the preparation of the Co(III)-complex **MBR-60** investigated here, the air oxidation of the Co(II)-complex of **5** was carried out in the presence of 4-*tert.*-butylbenzoic acid. In aqueous environment, the axial co-ligands of Co(III)-salen complexes such as **MBR-60** (in this case: 4-*tert.*-butyl benzoate) are exchanged for water, i.e. the hydroxo complex results (**MBR-60**, R = OH), independent of the precursor complex. The resulting Co(III)salen-OH complex is indefinitely stable towards demetallation under neutral conditions [5].

With regard to the biological activity, some Co-salen complexes have been found, inter alia, to possess structure-dependent anti-cancer activity [6–9]. However, and to our surprise, the catalytically highly successful *tert.*-butylated and *trans*-DACH derived Co-salen complexes mentioned before, appear not to have been examined for their anti-cancer activity yet. With this in mind, we set out to explore the potential of the Co-salen **MBR-60** with regard to the cancer activity in different tumor cell lines and observed apoptotic effects in Burkitt like lymphoma and leukemia cell lines (see Table 1). We found out that the substance overcomes multidrug resistances in leukemia cells, acts over the intrinsic pathway and shows an important selectivity between healthy human leucocytes and tumor cells.

2. Results

2.1. MBR-60 has apoptotic and anti-proliferative effects on BJAB cells

To get a first idea of how the substance **MBR-60** effects tumor cells, the DNA fragmentation in Burkitt like lymphoma cells (BJAB) was measured after 96 h of incubation. As comparison, the metal-free ligand

* Corresponding author.
E-mail address: sinamariehopff@t-online.de (S.M. Hopff).

https://doi.org/10.1016/j.bioorg.2020.104193
Received 26 February 2020; Received in revised form 19 June 2020; Accepted 2 August 2020
Available online 01 September 2020
0045-2068/

Table 1
AC_{50} values of the used cell lines. They describe the concentration of **MBR-60** able to induce apoptosis in 50 percent of the cells after 96 h of incubation.

Cell line	AC_{50} of **MBR-60**
BJAB	< 50 μM
BJAB FADDdn	< 50 μM
7CCA	> 50 μM
Nalm6	< 70 μM
NDau	< 70 μM

5 (Fig. 1) of **MBR-60** was pipetted to the cells. He showed no apoptotic activity whereas the Co-complex reaches high levels of apoptosis at 50 μM of the substance (Fig. 2**a**).

The cell count of BJAB cells was determined by CASY cell counter and analyzer system. Previously, the cells were treated with four different concentrations of **MBR-60** and were incubated for 24 h. Fig. 2**b** shows that the cell proliferation was inhibited by **MBR-60** in a dose-dependent manner. At a **MBR-60** concentration of 50 μM, the cell growth was reduced by 80 percent.

Furthermore, there are two cases of a decrease in cell counts: necrosis and apoptosis [10]. We proved that the inhibition of proliferation in the BJAB cells was due to apoptosis and not to necrosis by using the enzyme lactate dehydrogenase (LDH). This enzyme is released by plasma membrane lysis and characterizes cell necrosis caused by a loss of the membrane integrity. Though, apoptotic cells maintain their membrane integrity and LDH is not released within the first hours [11,12]. Therefore, BJAB cells were incubated with different concentrations of **MBR-60** for 1 h. Fig. 2**c** illustrates that **MBR-60** has no significant unspecific cytotoxic effects on BJAB cells because the viability of the cells stays at 100 percent at all concentrations.

2.2. MBR-60 is independent of CD95, but activates caspase-8

The induction of apoptosis in BJAB cells was proved by measuring the DNA fragmentation via FACS scan analysis. The cells were treated with different concentrations of **MBR-60**. Fig. 3 shows that the apoptotic effects start at a concentration of 30 μM and reach high levels of apoptosis at 50 μM of **MBR-60**.

Next to the regular BJAB cells, BJAB FADDdn cells were used to declare that **MBR-60** acts independently of CD95. The BJAB FADDdn cells overexpress a dominant-negative FADD (Fas-associated death domain) mutant which is part of the extrinsic cell signaling pathway during apoptosis such as Fas (CD95) [13]. FADD activates the protease procaspase-8 followed by an apoptotic protease cascade [14].

In Fig. 3 it is clearly shown that BJAB and BJAB FADDdn cells have similar levels of apoptosis after treating them with 30 μM and 50 μM of **MBR-60**. In the **MBR-60** treated BJAB FADDdn cells the amount of cell death is not stronger inhibited than this in the BJAB cells. A main role of the extrinsic pathway in the induction of apoptosis can be excluded.

A previous study has demonstrated that the activation of caspase-8 is independent of the CD95 ligand and the CD95 death-inducing signaling complex in BJAB cells [15]. In addition, they described that caspase-3, a protease of the intrinsic pathway, can cause an activation of caspase-8. Consequently, a connection between the intrinsic and extrinsic pathway is possible. This explains the processing of caspase-8 in BJAB cells under the influence of **MBR-60** in the western blot analysis (Fig. 7). BJAB cells were treated with 40 μM and 50 μM of **MBR-60** and were incubated for 36 h.

2.3. MBR-60 overcomes daunorubicin resistance

We found out that the daunorubicin resistant Nalm6 cells (NDau) have a significant overexpression of the drug efflux pump P-glycoprotein. This protein is also called MDR1 transporter as it is a multidrug resistant (MDR) protein that causes resistances against different cytostatic agents such as the anthracyclines and vinca-alkaloids [16,17]. The MDR1 decreases the intracellular drug concentration by carrying them out of the cells [18,19]. The blocking of this transporter results in a higher drug concentration in the cells so that the substance can initiate the apoptosis. Experiments with fludarabine, paclitaxel, vincristine, vindesine, vinorelbine, vinblastine, idarubicin, doxorubicin, epirubicin and etoposide revealed that NDau cells are resistant against these cytostatic drugs underlining their multidrug resistant character. Drug resistance is an important disadvantage for many existing anticancer drugs [20].

Now, Nalm6 and NDau cells were treated with 10 μM, 50 μM and 70 μM of **MBR-60** (Fig. 4). After 96 h of incubation the results of the FACS scan analysis show similar and at 70 μM of **MBR-60** even higher apoptotic effects in NDau cells. This demonstrates that **MBR-60** overcomes the multidrug resistance in NDau cells.

2.4. MBR-60 has an important influence on the mitochondrial pathway

The apoptosis can be triggered by extrinsic or intrinsic pathway of apoptosis [21]. The intrinsic pathway of apoptosis is based on a change in the mitochondrial membrane potential. Caspase-3 induces cell death when it is activated and can be described as the key executioner of apoptosis. The protease caspase-9 initiates the mitochondrial pathway of apoptosis [22,23]. The doxorubicin-resistant Burkitt lymphoma cell line (7CCA) helped finding out about a main role of caspase-3 in the induction of apoptosis via **MBR-60**. The cell line is characterized by an

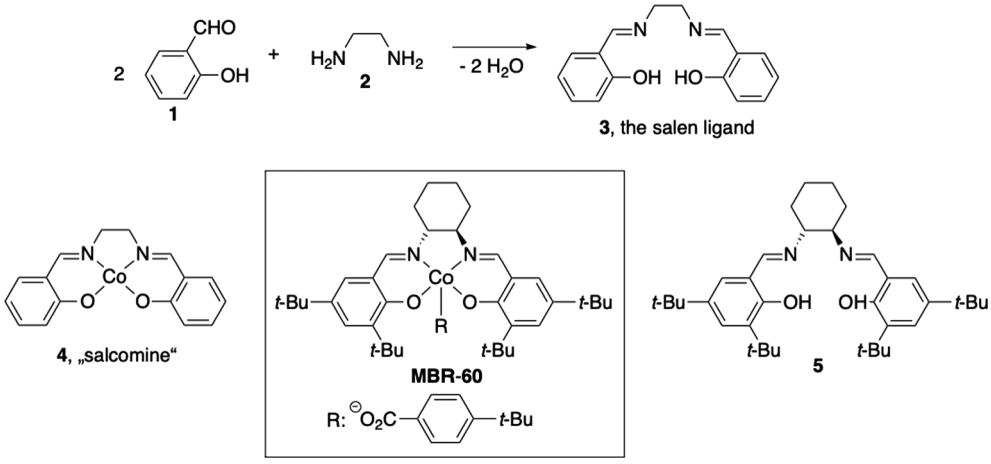

Fig. 1. Generating the Co-salen complex **MBR-60**.

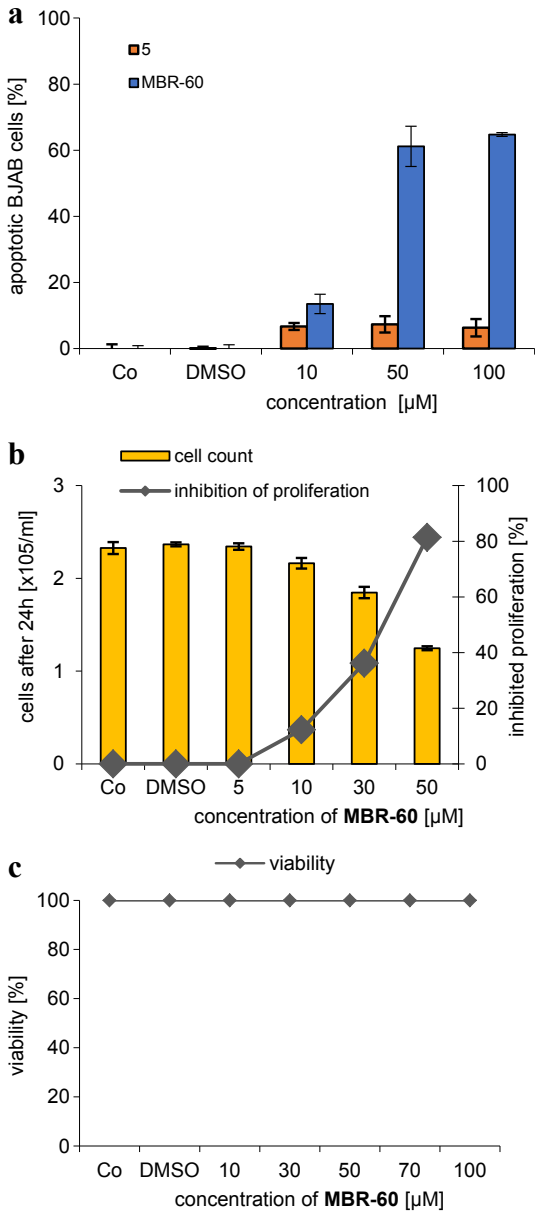

Fig. 2. DNA-fragmentation, inhibition of proliferation and cell viability. Control cells (Co) were left untreated. **a** 10 µM, 50 µM and 100 µM of **5** and **MBR-60** were pipetted on BJAB cells. After 96 h of incubation, the induction of apoptosis was measured by flow cytometric analysis of nuclear DNA fragmentation. Results were expressed at means ± SD (n = 3). **b** BJAB cells were treated with 5 µM, 10 µM, 30 µM and 50 µM of **MBR-60** and incubated for 24 h. Proliferation was measured by using the CASY cell count and analyzer system. Values are given as percentage of inhibition of cell proliferation. Three batches per concentration were analyzed. **c** BJAB cells were treated with 5 µM up to 100 µM of **MBR-60** for 1 h. The LDH release assay was used to determine the viability and the values are given as percentage of the control (n = 3).

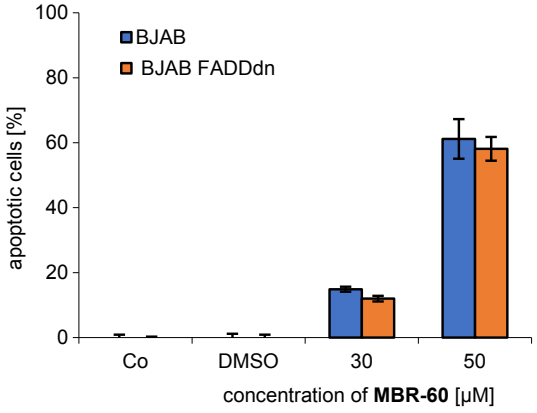

Fig. 3. BJAB and BJAB FADDdn cells were treated with concentrations of 30 µM and 50 µM of **MBR-60**. Control cells (Co) were left untreated. After 96 h of incubation the induction of apoptosis was measured by flow cytometric analysis of nuclear DNA fragmentation. Three batches per concentration were analyzed. Results were expressed at means ± SD.

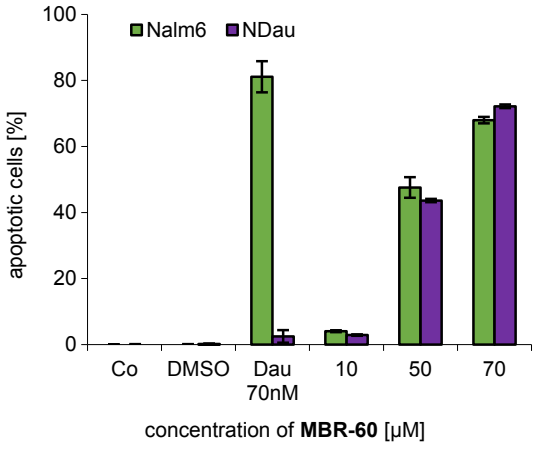

Fig. 4. The overcoming of NDau cells is proved by treating them with different concentrations of **MBR-60**. As a comparison, Nalm6 cells were treated with the substance. A control with 70 nM of daunorubicin (Dau) proves the resistance of NDau against this cytostatic drug. After 96 h of incubation, the DNA fragmentation was measured by flow cytometric of cellular DNA content, using three batches per concentration. The first column describes the untreated control cells (Co). The values are shown as percentages of cells with hypodiploid DNA ± SD.

under-expression of caspase-3. BJAB and 7CCA cells were treated with different concentrations of **MBR-60** and incubated for 96 h. Then, we measured the DNA fragmentation and found out that at a concentration of 30 µM and 50 µM the apoptotic effect in BJAB cells is significantly higher than this in 7CCA cells (Fig. 5). Therefore, **MBR-60** develops better results in defending tumor cells when caspase-3 is available because **MBR-60** can activate this protease to initiate the apoptosis.

To underline the initiation of cell death through the mitochondrial pathway, a western blot analysis was done. After incubating BJAB cells with 40 µM and 50 µM of **MBR-60** for 36 h the consumption of different caspases can be observed (Fig. 7): the processed procaspase-9 (49 kDa) shows smaller bands than in the control group what means that these proteases are cleaved in order to activate them. The processing of caspase-3 (32 kDa) and the appearance of their 17 kDa active subunit underlines the involvement of caspase-3 in the mechanism of **MBR −60**.

The inclusion of **MBR-60** in the intrinsic pathway is further illustrated by flow cytometric with a JC-1 stain. The loss of mitochondrial membrane potential is measured in **MBR-60** effected Nalm6 cells after 48 h of incubation. This results in a significant breakdown of the potential in the treated cells. At 70 µM concentration of **MBR-60** a loss of more than 70 percent of the mitochondrial membrane potential can be detected (Fig. 6). This process leads to an activation of procaspase-9 in the cascade of cell death via the mitochondrial pathway. These results match with the western blot analysis verifying the use of procaspase-9 (Fig. 7).

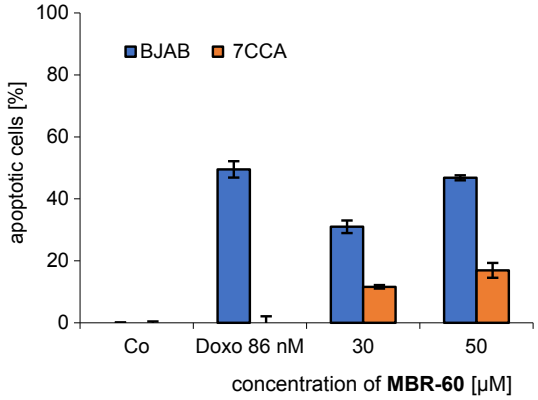

Fig. 5. Treating BJAB and 7CCA cells with 30 µM and 50 µM of **MBR-60** and incubating them for 96 h. Control cells are untreated (Co). 86 nM of doxorubicin (Doxo) was added in second control to demonstrate the resistance of 7CCA. Using three batches per concentration, the induction of apoptosis was measured by flow cytometric of cellular content. Values are given as percentages of cells with hypodiploid DNA ± SD.

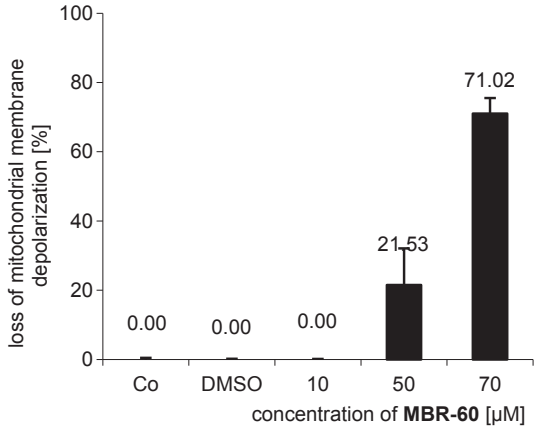

Fig. 6. Mitochondrial permeability transition was measured by flow cytometric analysis for Nalm6 cells after 48 h incubation with 10 µM, 50 µM and 70 µM of **MBR-60** and without **MBR-60** (Co). Values of the mitochondrial permeability transition are given as percentage of cells with low $\Delta\Psi_m$ ± SD. Three batches per concentration were used.

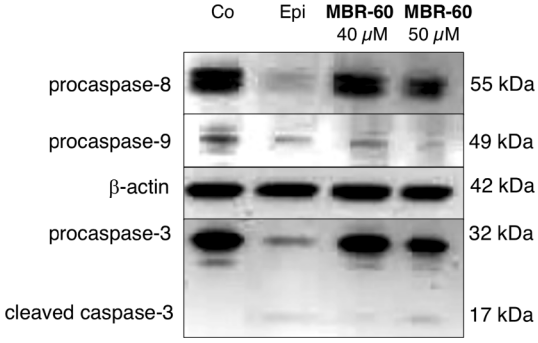

Fig. 7. MBR-60 induces procaspase-8, procaspase-9 and procaspase-3 activation. BJAB cells were treated with 2,2 µM epirubicine (*Epi*) as a positive control and with 40 µM and 50 µM of **MBR-60**. Control cell line (Co) was left untreated. All cells were incubated for 36 h. Separation of 20 µg of cytosolic proteins was made by SDS-PAGE, followed by subjecting them to the western blot analysis. Immunblotting was done with anti procaspase-8, anti procaspase-9 and anti procaspase-3 antibodies. To prove equal loading and blotting, the 43 kDa β-actin band was detected.

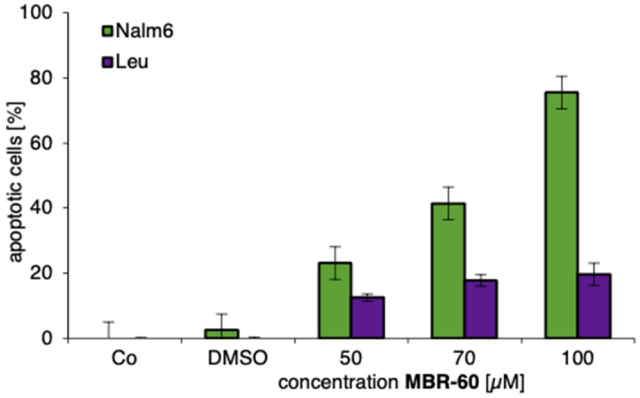

Fig. 8. Selectivity of **MBR-60**. Nalm6 cells and healthy human leucocytes (Leu) were treated with 50 µM, 70 µM and 100 µM of **MBR-60**. As a control, some cells were left untreated (Co). After 96 h of incubation, induction of apoptosis was measured by flow cytometric of cellular content. Three batches per concentration were used and values are given as percentages of cells with hypodiploid DNA ± SD.

2.5. MBR-60 significantly causes smaller apoptotic effects in healthy human leucocytes than in leukemia cells

To compare the effect of **MBR-60** in healthy human leucocytes with the apoptotic effect in Nalm6 cells, a selectivity test was done. The cells were treated with different concentrations of **MBR-60** and incubated for 96 h at 37 °C. Fig. 8 clearly illustrates a certain differentiation of the substance between tumor cells and healthy leucocytes. In high concentrations (100 µM), more than 75 percent of the Nalm6 cells are apoptotic whereas in the healthy leucocytes less than 20 percent of apoptotic cells can be observed.

2.6. Synergistic effects with daunorubicin and vincristine in leukemia cells

Next to the apoptotic effects of **MBR-60** in the Nalm6 cell line, a synergistic effect can be observed by treating the cells with **MBR-60** plus daunorubicin or vincristine (Figs. 9, 10). Very low concentrations of **MBR-60** were used that do not affect the cells in single use. By adding daunorubicin in low concentration, 378 percent more cells were apoptotic. The experiment was repeated with vincristine and resulted in over more than 160 percent of apoptotic cells compared to the addition of the single use apoptosis of both substances.

3. Discussion

The in vitro cytotoxicity of the substance **MBR-60** in Burkitt like lymphoma cells and leukemia cells suggests that the Co-complex is a potential anticancer drug. The different cell lines reflect a wide range of tumors in which **MBR-60** can develop its effect. The compound induces apoptosis in up to 68 percent of Nalm6 cells with a half maximal concentration (AC_{50}) of < 70 µM (Fig. 4, Table 1). The values are even higher in BJAB cells with almost 60 percent of apoptotic cells at 50 µM of **MBR-60** after 96 h of incubation (Figs. 2**a,** 3).

The interest in organometallic complexes is very high because during the last years, important biological effects have been observed [24–26]. The antitumor agent cisplatin was pioneering in this field, but most of the leukemia and lymphoma cells are cisplatin-resistant whereas our compound shows high apoptotic effects in these leukemia and tumor cells [27]. In our lab, we tested other substances with organometallic compounds like the series of new organotin (IV) carboxylate complexes. These substances showed anticancer potential against breast carcinoma cells (MCF7), colon carcinoma cells (HT-29) and Nalm6 cells. In particular, they also overcame the daunorubicin resistance in NDau cells [28]. Treating Nalm6 and NDau cells with

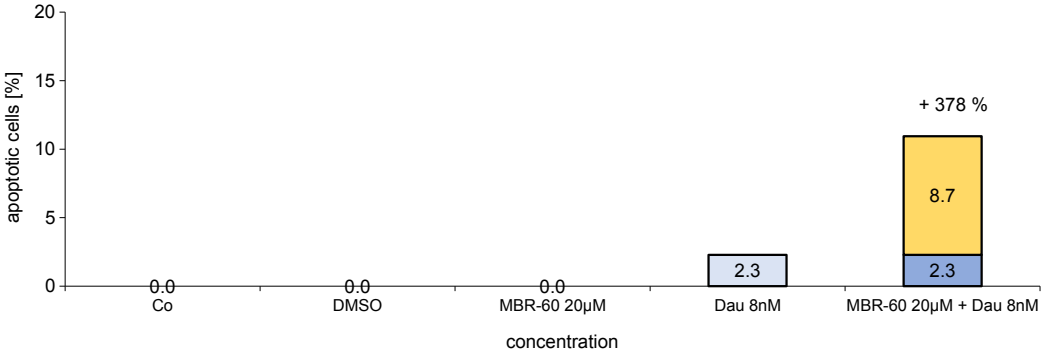

Fig. 9. Testing the synergistic effect of **MBR-60** with daunorubicin (Dau): Nalm6 cells were treated with 20 µM of **MBR-60** and 8 nM of daunorubicin. As an addition, both substances were added to the cells together. Results demonstrate the effect after 96 h of incubation. Control cells were left untreated (Co). After measuring the DNA-fragmentation, three batches per concentration were used and values are given as percentages of cells with hypodiploid DNA ± SD. Dividing the additional apoptotic effect (yellow bar) by the addition of the apoptotic effects of the single treatments with **MBR-60** and daunorubicin (dark blue bar) equals the percentage of the synergistic effect. (For interpretation of the references to colour in this figure legend, the reader is referred to the web version of this article.)

benzimidazolylidene-rhodium (1,5-cyclooctadiene) derivatives [29] showed the same phenomenon.

Schmidt et al. (2017) found out that a gold(I) NHC complex is not dependent on the P-glycoprotein so that it induced more apoptosis in NDau than it did in Nalm6 cells [30]. The tetrazole-containing gold(I) complexes and Titanocene Y revealed to similar results in Nalm6 and vincristine-resistant Nalm6 (NVCR) cells [31,32]. The NVCR cells are also characterized by an over-expression of P-glycoprotein. Other dinuclear gold(I)-carbene complexes are proven to be potential antimitochondrial and anticancer agents [33].

MBR-60 is proved to be a potential anti-cancer agent with Co in its center. The discovery of the toxicity of Co-complexes started in 1952 [34]. The use of [Co2(CO)6]–acetylene complexes as potential anticancer agents was published in different studies [35–38]. Singh et. al examined two phenolate based metallomacrocyclic xanthate complexes of Co^{II} and Cu^{I} with apoptotic activity in hepatoma and neuroblastoma cells [39]. In another study, chlorinated cobalt alkyline complexes were tested on different tumor cell lines [40]. Apoptotic effects in MCF7, HT-29 and MDA-MB-231 (hormone-independent breast cancer) cells were described in low micromolar concentrations of the substances. Ali et. al (2016) synthesized Co-salen complexes and tested them on solid tumor cells [6]. The investigation of Co-complexes based on salen ligands is rare. Our investigations revealed apoptotic effects not only on solid tumor cells, but also on acute lymphoblastic leukemia cells. This describes a new discovery in research of metal complexes.

Furthermore, the formation of several resistances against common cytostatic drugs is a leading obstacle in chemotherapy [41]. Therefore, metal complexes like **MBR-60** that overcome resistances are very important for future treatment of drug resistant cancers.

MBR-60 is more effective in NDau cells than in the Nalm6 cells with more than 70 percent of apoptosis in 70 µM of the substance compared to 68 percent of apoptosis in Nalm6 cells at the same concentration (Fig. 4). Knowing the resistance mechanisms of the NDau cells helps to understand how **MBR-60** acts. The overexpression of P-glycoprotein in the cells and the significant effects of **MBR-60** underlines the importance as a potential drug against multidrug resistance in leukemia. The influence on MDR1 also proves that **MBR-60** attacks the tumor cells over the intrinsic pathway. Further experiments with the BJAB cells, the western blot analysis and the measurement of the mitochondrial membrane potential highline the inclusion of the mitochondrial pathway. Higher apoptotic effects in BJAB cells compared to those in 7CCA cells revealed that **MBR-60** is dependent of caspase-3 (Fig. 5). This is also shown in the western blot analysis. The processing of caspase-3 and procaspase-9 is observed (Fig. 7). Furthermore, the influence of **MBR-60** on the mitochondrial membrane potential in Nalm6 cells is demonstrated in Fig. 6 with a huge loss of the membrane depolarization at a **MBR-60** concentration of 70 µM.

Moreover, the similar AC_{50} values (< 50 µM) of BJAB FADDdn cells and BJAB cells are a sign that **MBR-60** is independent of the extrinsic pathway (Fig. 3, Table 1). The processing of caspase-8 in the western blot analysis supports the fact that this protease is activated by caspase-3 (Fig. 7). These results confirm the statement of Wieder et. al (2001)

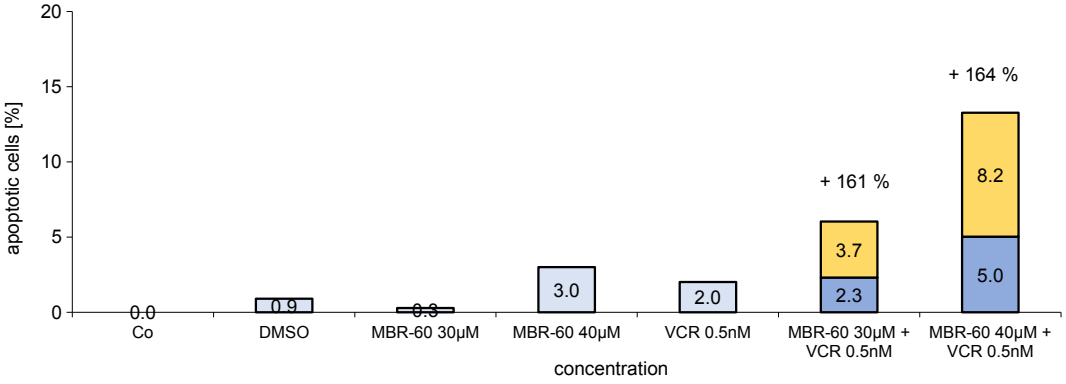

Fig. 10. Testing the synergistic effect of **MBR-60** with vincristine (VCR): Nalm6 cells were treated with 30 µM and 40 µM of **MBR-60** and 0.5 nM of vincristine. Then, 30 µM of **MBR-60** and 0.5 nM of vincristine were added, secondly 40 µM of **MBR-60** and 0.5 nM of vincristine were given to the cells. Results demonstrate the effect after 96 h of incubation. Control cells were left untreated (Co). After measuring the DNA-fragmentation, three batches per concentration were used and values are given as percentages of cells with hypodiploid DNA ± SD. Dividing the additional apoptotic effect (yellow bar) by the addition of the apoptotic effects of the single treatments with **MBR-60** and vincristine (dark blue bar) equals the percentage of the synergistic effect.

that caspase-8 is not activated by CD95/Fas receptor ligand in BJAB cells [15].

To underline the importance of the Co-molecule in **MBR-60**, we tested the metal-free ligand **5** and expected no apoptotic effects. The results of the DNA-fragmentation of the ligand in BJAB cells confirm our expectations: up to 100 μM of **5** no apoptotic effects were detected in BJAB cells (Fig. 2**a**).

Another very interesting discovery was that **MBR-60** sensitizes Nalm6 cells and causes significant higher apoptotic effects in combination with common cytostatic agents. Very low concentrations of **MBR-60**, daunorubicin (Fig. 9) and vincristine (Fig. 10) were necessary to get great apoptotic effects. This makes **MBR-60** even more interesting as a potential drug against leukemia. Furthermore, the significant selectivity of **MBR-60** between healthy human leucocytes and tumor cells is a very important aspect for the future of **MBR-60**. Fig. 8 illustrates the decisive difference between the apoptotic effects in healthy leucocytes (20 percent apoptosis) and Nalm6 cells (more than 40 percent apoptosis) in a high **MBR-60** concentration of 70 μM.

4. Conclusion

Overall, **MBR-60** is a very interesting Co-salen complex for future chemotherapy, especially in drug resistant tumors. Our investigations revealed high apoptotic effects in acute lymphoblastic leukemia and Burkitt like lymphoma cells. The overcoming of daunorubicin-resistance in NDau cells and the understanding of the mode of action of **MBR-60** render the substance very promising for future use in cancer therapy. We observed an involvement in the intrinsic pathway of apoptosis. This is shown by a dependence on caspase-3, an independence on CD95, and the loss of mitochondrial membrane depolarization in Nalm6 cells after treating them with **MBR-60.** The impressive synergistic effects of **MBR-60** with daunorubicin and vincristine are very remarkable. With these combinations, lower concentrations of **MBR-60** are necessary to be effective against leukemia. Furthermore, the healthy leucocytes were hardly affected by **MBR-60**. The results are relevant in the exploration of metal complexes, especially due to the fact that no biological activity of Co-salen complexes in leukemia cells has been reported as yet. The data are very promising for treatment of leukemia and lymphoma especially due to the fact that most of these cells are platin resistant.

5. Materials and methods

5.1. Materials

The used RNase A was from Qiagen (Hilden, Germany) and the Propidium iodide (50 μg/ml) was from Serva (Heidelberg, Germany). The cytostatic agents daunorubicin, doxorubicin and vincristine were provided by the Children's Hospital of the City Cologne, Amsterdamer Straße. Before starting the experiments, the agents were freshly dissolved as stock solutions in DMSO. The salen-ligand **5** is commercially available and was obtained from Sigma-Aldrich. This ligand was converted to the Co(III)-salen complex **MBR-60** by a typical literature procedure [2]. The resulting dark brown solid was characterized by HR-MS [cald. for $C_{36}H_{52}CoN_2O_2$ (**MBR-60**–4-*t*Bu-benzoate) = 603.336; found: 603.337]. For the preparation of 40 mM stock solutions, both the ligand **5** and the Co(III)-complex **MBR-60** were dissolved in DMSO. Besides the regular control cells in the experiments, some cells were incubated with an equal amount of DMSO only, as DMSO control, resulting in similar effects than in the untreated control.

5.2. Cell lines and cell cultures

The cell line Nalm6 (human b cell precursor leukemia cells) is provided by AG Henze, Charité, Berlin. In addition to this a daunorubicin-resistant Nalm6 cell line was generated in our lab by treating Nalm6 cells with increasing concentrations until a cell toleration of high concentrations was given without the loss of cell vitality.

BJAB mock (Burkitt like lymphoma cells) and BJAB FADDdn cells were kindly donated by AG Daniel, Charité Berlin. The BJAB FADDdn cells are transfected with pcDNA3-FADD−/−. They are expressing a dominant negative FADD mutant that is lacking the death domain. The BJAB mock cells have a pcDNA3-Primer without the FADD dn-Gen.

The doxorubicin-resistant 7CCA cells were established in our lab by treating BJAB cells with increasing concentrations of doxorubicin. The cells tolerate 86 nM of the cytostatic agent without a loss of vitality. At the same concentration BJAB cells show 50 percent of apoptosis.

The cell lines are incubated in 250 ml cell culture bottles at 37 °C. The RPMI 1640 medium (GIBCO, Invitrogen, Karlsruhe, Germany) was used. Heat inactivated fetal calf serum (FCS, 10%, v/v), L-glutamine (0.56 g/l), penicillin (100,000 i.u.) and streptomycin (0.1 g/l) were added. All cells were passaged 2–3 times per week and diluted to a concentration of $1x10^5$ cells/ml. All cells were adjusted to $3x10^5$ cells/ml 24 h before the assay setup to guarantee standard conditions. Before treating the cells with **MBR-60** for proliferation and apoptosis assays, they were diluted to $1x10^5$ cells/ml. All experiments were repeated and showed similar results.

5.3. Determination of cell concentration and cell viability

The cell count and viability was determined by CASY cell counter and analyzer system from Roche. Settings were specifically defined for the requirements of the cells used. With this system, in one measurement the cell concentration is simultaneously analyzed in three different size ranges: the cell debris, dead cells and viable cells [42]. The cells were seeded at a density of 1×10^5 cells/ml in 6-well-plates and they were treated with different concentrations of **MBR-60**. As a control, some cells were incubated untreated and with DMSO. After 24 h of incubation at 37 °C, the cells were resuspended and 100 μl of each well was diluted in 10 ml of CASYton (ready-to-use isotonic saline solution) for an immediate automated count of the cells. The control group of the cells was defined as 100 percent growth. A cell concentration, that was not higher than at the beginning of the experiment, showed the maximal inhibition of proliferation.

5.4. LDH release assay for measuring the cell death

The cytotoxicity of **MBR-60** in BJAB cells was measured by LDH release after a one hour-incubation with different concentrations of the substance. The release of LDH was measured in the cell culture supernants by using the Cytotoxicity Detection Kit from Roche Diagnostics® (Mannheim, Germany). After centrifugation at 1500 rpm for 5 min, 20 μl of cell-free supernatants were diluted with 80 μl phosphate-buffered saline (PBS). Then 100 μl reaction mixture from the Detection Kit was added. The quantification of time-dependent formation of the reaction product occured photometrically at 490 nm. 0.1% Triton X-100 in culture medium was used to measure the maximum amount of LDH release in the lysed cells what represents 100 percent cell death.

5.5. Measurement of induction of apoptosis

The DNA fragmentation was measured by a modified cell cycle analysis, which detects DNA fragmentation on the single cell level as described [43]. After seeding the cells to a density of 1×10^5 cells/ml, they were treated with different concentrations of **MBR-60** or **5**. BJAB mock, BJAB FADDdn, 7CCA, Nalm6 and NDau cells were incubated by 37 °C for 96 h. After incubation, the cells were collected by centrifugation at 1500 rpm for 5 min. Cells were fixed in 200 μl PBS/2% (v/v) formaldehyde on ice for 30 min. After fixation, cells were centrifuged again at 1500 rpm for 5 min by 4 °C, then incubated with 180 μl ethanol/PBS (2:1, v/v) for 15 min, pelleted by centrifugation and resuspended in 50 μl PBS containing 40 μg/ml RNase A. RNA was

digested for 30 min at 37 °C and cells were centrifuged again at 1500 rpm for 5 min, then finally resuspended in 200 µl PBS containing 50 µg/ml propidium iodide. Nuclear DNA fragmentation was quantified by flow cytometric determination of hypodiploid DNA (Fluorescence-activated cell sort, FACS). By using a FACScan (Becton Dickinson, Heidelberg, Germany), equipped with the CELLQuest software, data were collected and analyzed. The number of apoptotic cells was reflected by the percentage of hypoploidy (subG1). Apoptosis, specifically induced by the compounds was calculated by subtracting background apoptosis, observed in control cells, from total apoptosis seen in the treated cells.

5.6. Immunoblotting

After 36 h of incubation with 40 µM and 50 µM of **MBR-60**, BJAB cells were washed twice with PBS and lysed in buffer containing 10 mM Tris–HCl, pH 7.5, 300 mM NaCl, 1% Triton X-100, 2 mM $MgCl_2$, 5 µM ethylenediamino tetra-acetic acid (EDTA), 1 µM pepstatin, 1 µM leupeptin, and 0,1 mM phenylmethylsulfonyl fluoride (PMSF). By using the bicinchoninic acid assay form Pierce (Rockford, IL, USA) [44], the protein concentration was determined and equal amounts of protein were separated by SDS–PAGE [45]. The immunoblotting was performed as described [46]. The blocking of the membrane was made for 1 h in PBST (PBS, 0.05% Tween-20) containing BSA and incubated with different primary antibodies for 1 h. The anti-caspase 3, anti-caspase 8, anti-caspase 9 and anti-beta-Aktin from Sigma, Saint Louis, USA were used. After the membrane was washed in PBST, the secondary antibody (anti-mouse IgG HRP from Bioscience, San Diego, USA and anti-rabbit IgG HRP from Promega, Minneapolis, USA) in PBST was applied for 1 h. After washing, the ECL enhanced chemiluminescence system (Amersham Buchler, Braunschweig, Germany) was used to detect the protein bands.

5.7. Measurement of the mitochondrial permeability transition

After 48 h of incubation with **MBR-60**, Nalm6 cells were centrifuged at 300*g*, 4 °C for 5 min. The cells were stained with 5,5‘,6,6‘-tetrachloro-1,1‘,3,3‘-tetraethyl-benzimidazolylcarbocyanin iodide (JC-1; Molecular Probes, Leiden, The Netherlands) as described [21,47] to measure the mitochondrial permeability transition. The cells were resuspended in 500 µl phenol red free RPMI 1640 without supplements, then JC-1 was added to give a final concentration of 2.5 µg/µl. After 30 min of incubation at 37 °C and regular shaking, the cells were collected by centrifugation at 300*g*, 4 °C for 5 min. Control cells were incubated in the absence of JC-1 dye. All cells were washed with ice-cold PBS, and resuspended in 200 µl PBS at 4 °C. The mitochondrial permeability transition was quantified by flow cytometric determination of cells with decreased fluorescence. A FACScan (Becton Dickinson) equipped with the CELLQuest software was used for analysis. Data are given in percentage cells with low $\Delta\Psi_m$, which reflects the number of cells undergoing mitochondrial apoptosis.

5.8. Isolation of healthy human leucocytes

50 ml fresh blood was taken, 10 ml RPMI 1640 medium (FCS, 20%, v/v) was added. Next 4 ml of Ficoll (Saccharose-Epichlorhydrin-Copolymer) was pipetted in a 15 ml tube, then 5 ml blood was carefully added on the top. After 18 min of centrifugation at 657g, 20 °C, leucocytes were collected by slowly transferring them with a Pasteur pipette into a 45 ml tube. 20 ml of RPMI 1640 (FCS, 20%, v/v) was added, then dilution was centrifuged at 1500 rpm for 5 min. The cell count and viability was determined by CASY cell counter and analyzer system from Roche. Cells were seeded at a density of $3x10^5$ cells/ml. The following treatment is equal to the steps in measurement of DNA fragmentation as described above.

5.9. Synthesis of the Co(III)-salen 4-tert.-butylbenzoate complex MBR-60

For the synthesis of the benzoate Co(III) salen complex **MBR-60**, the corresponding and commercially available Co(II) salen complex derived from (*R*,*R*)-1,2-diaminocyclohexane was employed. A solution of this complex (100 mg, 166 µmol) in 2 ml abs. dichloromethane was prepared, and molecular sieves were added. 4-*tert*.-Butylbenzoic acid (29.6 mg, 166 µmol) was dissolved in a mixture of 2 ml abs. dichloromethane and 2 ml acetone. The solution of the acid was added to the solution of the Co(II) complex, and the mixture was stirred under O_2-atmosphere for 2 h. Filtration through Celite and removal of the solvent *in vacuo* afforded 120 mg (154 µmol, 93 percent) of a dark brown solid of m.p. > 250 °C.

M.W.: 780,96 g/mol.

Declaration of Competing Interest

The authors declare that they have no known competing financial interests or personal relationships that could have appeared to influence the work reported in this paper.

Acknowledgements

We thank Corazon Frias for her support in our lab and Peter Daniel (Charité, Berlin) for providing BJAB FADDdn cells. Financial support from the Dr. Kleist Foundation (Berlin) and generous support by the Fonds der Chemischen Industrie (Doctoral Fellowship to M.B.) is gratefully acknowledged.

Appendix A. Supplementary material

Supplementary data to this article can be found online at https://doi.org/10.1016/j.bioorg.2020.104193.

References

[1] E.N. Jacobsen, Asymmetric catalysis of epoxide ring-opening reactions, Acc. Chem. Res. 33 (2000) 421–431.
[2] S.E. Schaus, B.D. Brandes, J.F. Larrow, M. Tokunaga, K.B. Hansen, A.E. Gould, M.E. Furrow, E.N. Jacobsen, Highly selective hydrolytic kinetic resolution of terminal epoxides catalyzed by chiral (salen)Co(III) complexes. Practical synthesis of enantioenriched terminal epoxides and 1,2-diols, J. Am. Chem. Soc. 124 (2002) 1307–1315.
[3] A. Berkessel, M. Brandenburg, Catalytic asymmetric addition of carbon dioxide to propylene oxide with unprecedented enantioselectivity, Org. Lett. 8 (2006) 4401–4404.
[4] M. Hatazawa, K. Nakabayashi, S. Ohkoshi, K. Nozaki, In Situ Generation of Co(III) -Salen Complexes for Copolymerization of Propylene Oxide and CO2, Chemistry 22 (2016) 13677–13681.
[5] L.P. Nielsen, C.P. Stevenson, D.G. Blackmond, E.N. Jacobsen, Mechanistic investigation leads to a synthetic improvement in the hydrolytic kinetic resolution of terminal epoxides, J. Am. Chem. Soc. 126 (2004) 1360–1362.
[6] A. Ali, M. Kamra, A. Bhan, S.S. Mandal, S. Bhattacharya, New Fe(iii) and Co(ii) salen complexes with pendant distamycins: selective targeting of cancer cells by DNA damage and mitochondrial pathways, Dalton Trans. 45 (2016) 9345–9353.
[7] R. Gust, I. Ott, D. Posselt, K. Sommer, Development of cobalt(3,4-diarylsalen) complexes as tumor therapeutics, J. Med. Chem. 47 (2004) 5837–5846.
[8] S.S. Mandal, U. Varshney, S. Bhattacharya, Role of the central metal ion and ligand charge in the DNA binding and modification by metallosalen complexes, Bioconjug. Chem. 8 (1997) 798–812.
[9] I. Ott, R. Gust, Non platinum metal complexes as anti-cancer drugs, Arch. Pharm. (Weinheim) 340 (2007) 117–126.
[10] G. Majno, I. Joris, Apoptosis, oncosis, and necrosis. An overview of cell death, Am. J. Pathol. 146 (1995) 3–15.
[11] S. Van Cruchten, W. Van Den Broeck, Morphological and biochemical aspects of apoptosis, oncosis and necrosis, Anat. Histol. Embryol. 31 (2002) 214–223.
[12] G. Majno, M. La Gattuta, T.E. Thompson, Cellular death and necrosis: chemical, physical and morphologic changes in rat liver, Virchows Arch. Pathol. Anat. Physiol. Klin. Med. 333 (1960) 421–465.
[13] S. Nagata, Apoptosis by death factor, Cell 88 (1997) 355–365.
[14] R. van Horssen, T.L. Ten Hagen, A.M. Eggermont, TNF-alpha in cancer treatment: molecular insights, antitumor effects, and clinical utility, Oncologist 11 (2006) 397–408.
[15] T. Wieder, F. Essmann, A. Prokop, K. Schmelz, K. Schulze-Osthoff, R. Beyaert,

B. Dorken, P.T. Daniel, Activation of caspase-8 in drug-induced apoptosis of B-lymphoid cells is independent of CD95/Fas receptor-ligand interaction and occurs downstream of caspase-3, Blood 97 (2001) 1378–1387.
[16] R. Krishna, L.D. Mayer, Multidrug resistance (MDR) in cancer. Mechanisms, reversal using modulators of MDR and the role of MDR modulators in influencing the pharmacokinetics of anticancer drugs, Eur. J. Pharm. Sci. 11 (2000) 265–283.
[17] R. Pieters, E. Klumper, G.J. Kaspers, A.J. Veerman, Everything you always wanted to know about cellular drug resistance in childhood acute lymphoblastic leukemia, Crit. Rev. Oncol. Hematol. 25 (1997) 11–26.
[18] M.M. Gottesman, I. Pastan, The multidrug transporter, a double-edged sword, J. Biol. Chem. 263 (1988) 12163–12166.
[19] S.F. Zhou, L.L. Wang, Y.M. Di, C.C. Xue, W. Duan, C.G. Li, Y. Li, Substrates and inhibitors of human multidrug resistance associated proteins and the implications in drug development, Curr. Med. Chem. 15 (2008) 1981–2039.
[20] Y.A. Luqmani, Mechanisms of drug resistance in cancer chemotherapy, Med. Princ. Pract. 14 (Suppl 1) (2005) 35–48.
[21] I.H. Lambert, E.K. Hoffmann, F. Jorgensen, Membrane potential, anion and cation conductances in Ehrlich ascites tumor cells, J. Membr. Biol. 111 (1989) 113–131.
[22] G.M. Cohen, Caspases: the executioners of apoptosis, Biochem. J. 326 (Pt 1) (1997) 1–16.
[23] A.G. Porter, R.U. Janicke, Emerging roles of caspase-3 in apoptosis, Cell Death Differ. 6 (1999) 99–104.
[24] G. Gasser, I. Ott, N. Metzler-Nolte, Organometallic anticancer compounds, J. Med. Chem. 54 (2011) 3–25.
[25] A.L. Noffke, A. Habtemariam, A.M. Pizarro, P.J. Sadler, Designing organometallic compounds for catalysis and therapy, Chem. Commun. (Camb) 48 (2012) 5219–5246.
[26] M. Patra, G. Gasser, Organometallic compounds: an opportunity for chemical biology? ChemBioChem 13 (2012) 1232–1252.
[27] B. Rosenberg, L. VanCamp, J.E. Trosko, V.H. Mansour, Platinum compounds: a new class of potent antitumour agents, Nature 222 (1969) 385–386.
[28] K. Navakoski de Oliveira, V. Andermark, L.A. Onambele, G. Dahl, A. Prokop, I. Ott, Organotin complexes containing carboxylate ligands with maleimide and naphthalimide derived partial structures: TrxR inhibition, cytotoxicity and activity in resistant cancer cells, Eur. J. Med. Chem. 87 (2014) 794–800.
[29] L. Oehninger, L.N. Kuster, C. Schmidt, A. Munoz-Castro, A. Prokop, I. Ott, A chemical-biological evaluation of rhodium(I) N-heterocyclic carbene complexes as prospective anticancer drugs, Chemistry 19 (2013) 17871–17880.
[30] C. Schmidt, B. Karge, R. Misgeld, A. Prokop, R. Franke, M. Bronstrup, I. Ott, Gold(I) NHC Complexes: Antiproliferative Activity, Cellular Uptake, Inhibition of Mammalian and Bacterial Thioredoxin Reductases, and Gram-Positive Directed Antibacterial Effects, Chemistry 23 (2017) 1869–1880.
[31] L. Kater, J. Claffey, M. Hogan, P. Jesse, B. Kater, S. Strauss, M. Tacke, A. Prokop, The role of the intrinsic FAS pathway in Titanocene Y apoptosis: The mechanism of overcoming multiple drug resistance in malignant leukemia cells, Toxicol. In Vitro 26 (2012) 119–124.
[32] T.V. Serebryanskaya, A.S. Lyakhov, L.S. Ivashkevich, J. Schur, C. Frias, A. Prokop, I. Ott, Gold(I) thiotetrazolates as thioredoxin reductase inhibitors and antiproliferative agents, Dalton Trans. 44 (2015) 1161–1169.
[33] P.J. Barnard, M.V. Baker, S.J. Berners-Price, D.A. Day, Mitochondrial permeability transition induced by dinuclear gold(I)-carbene complexes: potential new antimitochondrial antitumour agents, J. Inorg. Biochem. 98 (2004) 1642–1647.
[34] F.P. Dwyer, E.C. Gyarfas, W.P. Rogers, J.H. Koch, Biological activity of complex ions, Nature 170 (1952) 190–191.
[35] M. Jung, D.E. Kerr, P.D. Senter, Bioorganometallic chemistry–synthesis and antitumor activity of cobalt carbonyl complexes, Arch. Pharm. (Weinheim) 330 (1997) 173–176.
[36] I. Ott, B. Kircher, R. Gust, Investigations on the effects of cobalt-alkyne complexes on leukemia and lymphoma cells: cytotoxicity and cellular uptake, J. Inorg. Biochem. 98 (2004) 485–489.
[37] K. Schmidt, M. Jung, R. Keilitz, B. Schnurr, R. Gust, Acetylenehexacarbonyldicobalt complexes, a novel class of antitumor drugs, Inorg. Chim. Acta 306 (2000) 6–16.
[38] C.R. Munteanu, K. Suntharalingam, Advances in cobalt complexes as anticancer agents, Dalton Trans. 44 (2015) 13796–13808.
[39] V.K. Singh, R. Kadu, H. Roy, P. Raghavaiah, S.M. Mobin, Phenolate based metallomacrocyclic xanthate complexes of Co(II)/Cu(II) and their exclusive deployment in [2: 2] binuclear N,O-Schiff base macrocycle formation and in vitro anticancer studies, Dalton Trans. 45 (2016) 1443–1454.
[40] V. Obermoser, D. Baecker, C. Schuster, V. Braun, B. Kircher, R. Gust, Chlorinated cobalt alkyne complexes derived from acetylsalicylic acid as new specific antitumor agents, Dalton Trans. 47 (2018) 4341–4351.
[41] C.A. Rabik, M.E. Dolan, Molecular mechanisms of resistance and toxicity associated with platinating agents, Cancer Treat Rev. 33 (2007) 9–23.
[42] R. Voisard, P.C. Dartsch, U. Seitzer, D. Roth, M. Kochs, V. Hombach, Cell culture as a prescreening system for drug prevention of restenosis? Vasa Suppl. 33 (1991) 140–141.
[43] F. Essmann, T. Wieder, A. Otto, E.C. Muller, B. Dorken, P.T. Daniel, GDP dissociation inhibitor D4-GDI (Rho-GDI 2), but not the homologous rho-GDI 1, is cleaved by caspase-3 during drug-induced apoptosis, Biochem. J. 346 (Pt 3) (2000) 777–783.
[44] P.K. Smith, R.I. Krohn, G.T. Hermanson, A.K. Mallia, F.H. Gartner, M.D. Provenzano, E.K. Fujimoto, N.M. Goeke, B.J. Olson, D.C. Klenk, Measurement of protein using bicinchoninic acid, Anal. Biochem. 150 (1985) 76–85.
[45] U.K. Laemmli, Cleavage of structural proteins during the assembly of the head of bacteriophage T4, Nature 227 (1970) 680–685.
[46] T. Wieder, C.C. Geilen, M. Wieprecht, A. Becker, C.E. Orfanos, Identification of a putative membrane-interacting domain of CTP:phosphocholine cytidylyltransferase from rat liver, FEBS Lett. 345 (1994) 207–210.
[47] M. Reers, S.T. Smiley, C. Mottola-Hartshorn, A. Chen, M. Lin, L.B. Chen, Mitochondrial membrane potential monitored by JC-1 dye, Methods Enzymol. 260 (1995) 406–417.

Biometals (2021) 34:211–220
https://doi.org/10.1007/s10534-020-00273-x

Sensitizing multidrug-resistant leukemia cells to common cytostatics by an aluminium-salen complex that has high-apoptotic effects in leukemia, lymphoma and mamma carcinoma cells

Sina M. Hopff · Liliane A. Onambele · Marc Brandenburg · Albrecht Berkessel · Aram Prokop

Received: 23 January 2020 / Accepted: 18 November 2020 / Published online: 9 February 2021

Abstract We investigated the aluminium-salen complex **MBR-8** as a potential anti-cancer agent. To see apoptotic effects induced by **MBR-8,** alone and in combination with common cytostatic drugs, DNA-fragmentations were studied using the flow cytometric analysis. Western blot analysis and measurement of the mitochondrial membrane potential with a JC-1 dye were employed to identify the pathway of apoptosis. An impressive overcoming of multidrug-resistance in leukemia (Nalm6) cells was observed. Additionally, solid tumor cells including Burkitt-like lymphoma (BJAB) and mamma carcinoma cells (MCF-7) are affected by **MBR-8** in the same way. Western blot analysis revealed activation of caspase-3. **MBR-8** showed very pronounced selectivity with regard to tumor cells and high synergistic effects in Nalm6 and daunorubicin-resistant Nalm6 cells when administered in combination with vincristine, daunorubicin and doxorubicin. The aluminium-salen complex **MBR-8** showed very promising anti-cancer properties which warrant further development towards a cytostatic agent for future chemotherapy. Studies on aluminium compounds for cancer therapy are rare, and our report adds to this important body of knowledge.

Keywords Acute lymphatic leukemia · Burkitt like lymphoma · Mamma carcinoma · Aluminium-salen tosylate complex · MBR-8

S. M. Hopff (✉) · L. A. Onambele · A. Prokop
Department of Pediatric Hematology/Oncology, Children's Hospital Cologne, Amsterdamer Straße 59, 50735 Cologne, Germany
e-mail: sinamariehopff@t-online.de

M. Brandenburg · A. Berkessel
Department of Chemistry, Organic Chemistry, University of Cologne, Greinstraße 4, 50939 Cologne, Germany

A. Prokop
Department of Pediatric Hematology/Oncology, Helios Clinic Schwerin, Wismarsche Straße 393-397, 19055 Schwerin, Germany

Introduction

Salen ligands (**3**) are typically generated in a one-step procedure by the condensation of two equivalents of a salicylic aldehyde ("sal", **1**) with ethylene diamine ("en", **2**) or a related diamine. Due to the simplicity of their preparation, they represent one of the most widely used ligand motifs in coordination chemistry. Recently, chiral Al-salens—derived from *trans*-1,2-diamino-cyclohexane (such as **MBR-8**) - have found use as catalysts for highly enantioselective transformations, *e.g.* for the asymmetric Michael addition of cyanide to α,β-unsaturated imides (Sammis and Jacobsen 2003), or for the stereospecific conversion of epoxides with CO_2 to cyclic carbonates (Berkessel and Brandenburg 2006). In contrast to applications in asymmetric catalysis, there appear to be no reports on

the biological activity of Al-salens in the literature. With this in mind, we decided to explore the potential of the chiral Al-salen complex **MBR-8** for the selective targeting of leukemia and solid tumor cells. We furthermore tested the ligand **4** alone, to make sure that the biological activity resides in the intact aluminium-complex, and not in the metal-free ligand (Fig. 1). The synthesis and characterization of the Al-salen **MBR-8** have been described by us earlier (Berkessel and Brandenburg 2006). According to HR-MS and NMR spectroscopy (^{1}H, ^{13}C), the Al-complex **MBR-8** thus obtained is > 98 % pure.

Results

LDH release and anti-proliferative effects of MBR-8

Our first investigations addressed the question how **MBR-8** causes cell death. There are two causes for a decrease in cell counts: necrosis or apoptosis (Majno and Joris 1995). To show that the decrease in proliferation of Burkitt like lymphoma (BJAB) cells was due to apoptosis and not to necrosis, the enzyme lactate dehydrogenase (LDH) was used. This enzyme is released by plasma membrane lysis and characterizes cell necrosis due to a loss of the membrane integrity whereas apoptotic cells maintain their membrane integrity (Van Cruchten and Van Den Broeck 2002). Therefore, BJAB cells were incubated with different concentrations of **MBR-8** for 1 h. Fig. 2a clearly indicates that significant cytotoxic effects of **MBR-8** can be excluded.

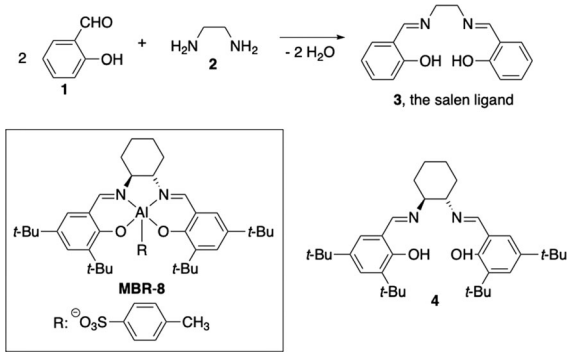

Fig. 1 General synthesis of the salen-ligands **3**, structure of the Al-salen complex **MBR-8** and of its ligand **4**

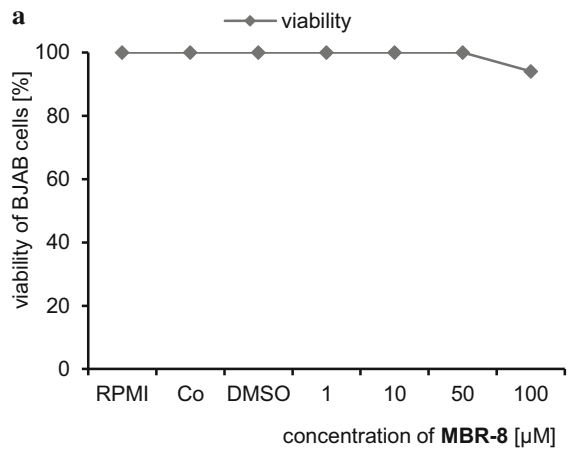

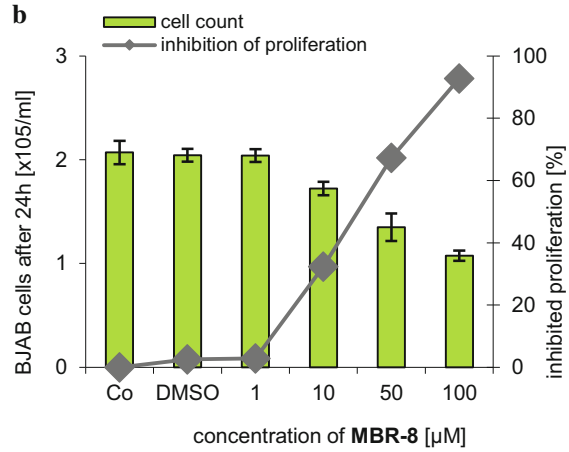

Fig. 2 Inhibition of proliferation and cell viability. **a** BJAB cells were treated with 1 µM, 10 µM, 50 µM and 100 µM of **MBR-8**. LDH release assay was used to determine the viability. Values are given as percentage of the control (Co). **b** 1 µM, 10 µM, 50 µM and 100 µM of **MBR-8** were pipetted on BJAB cells. Control cells (Co) were left untreated. After 24 h of incubation, cell proliferation was measured by using the CASY count system. Values are given as percentage of inhibition of cell proliferation

The proliferation of BJAB cells in the presence of **MBR-8** gives a first hint of the effectiveness of the substance in tumor cells. It can be noted that the number of cells starts to decrease at a concentration of 10 µM (Fig. 2b). At 100 µM of **MBR-8** and after 24 h of incubation, almost 100% of the proliferation is inhibited.

MBR-8 shows apoptotic effects in Burkitt like lymphoma cells

The next step in the exploration of **MBR-8** addressed DNA-fragmentation in BJAB cells, to further establish its apoptotic effects. Thus, BJAB cells were exposed to different concentrations of **MBR-8** in a micromolar range. After 96 h of incubation an effect of more than 50 percent can be observed at a **MBR-8** concentration of 30 µM (Fig. 3). The number of apoptotic cells increases with the following concentrations and reaches over 80 percent of apoptotic cells at a **MBR-8** concentration of 50 µM. We repeated the experiment with the ligand **4** to prove that the intact aluminium-complex is necessary for the apoptotic effects. As expected, **4** does not affect the BJAB cells in a significant way (Fig. 3).

MBR-8 effectively eliminates daunorubicin-resistant leukemia cells

Another cell line that was confronted with the substance is a human b cell precursor leukemia cell line (Nalm6). At the same time, the daunorubicin-resistant Nalm6 cells (NDau) were tested with the substance. First of all, **MBR-8** causes apoptosis in the Nalm6 cell line from a concentration of 30 µM on (Fig. 4). More than 60 percent of the cells are apoptotic

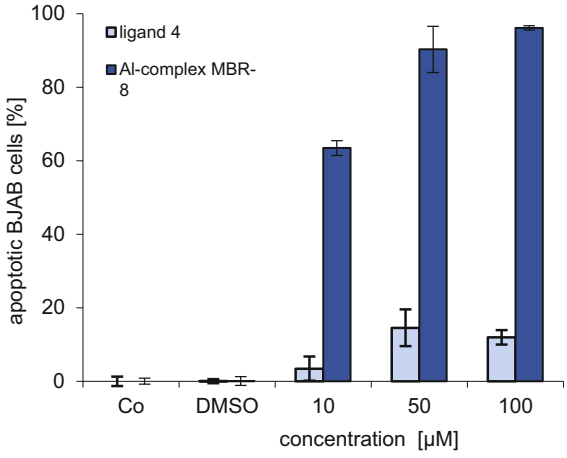

Fig. 3 BJAB cells were treated with 10 µM , 50 µM and 100 µM of **4** and **MBR-8** and incubated for 96 h. Control cells (Co) were left untreated. The induction of apoptosis was measured by flow cytometric analysis of nuclear DNA fragmentation. Values are given in percentage of apoptotic cells and were expressed at means ± SD. Three batches per concentration were analyzed

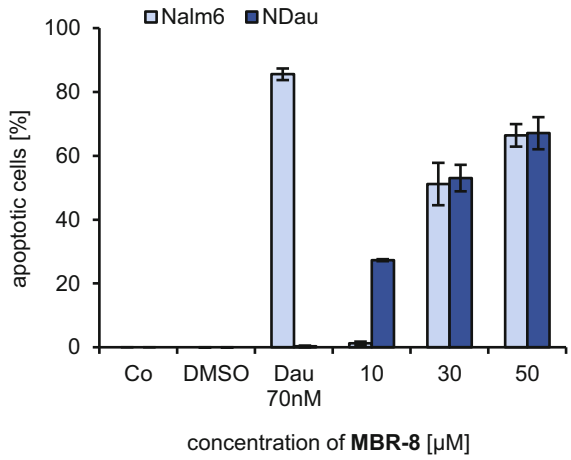

Fig. 4 To prove the overcoming of daunorubicin-resistance, Nalm6 and NDau cells were treated with 10 µM, 30 µM and 50 µM of **MBR-8**. Control cells (Co) were left untreated. 70 nM daunorubicin (Dau) were pipetted in both cell lines to prove the resistance. After 96 h of incubation, DNA fragmentation was measured by flow cytometric of cellular DNA content, using three batches per concentration. Values are given in percentage of apoptotic cells and were expressed at means ± SD

at 50 µM of **MBR-8** concentration. Furthermore, **MBR-8** surpasses these effects in the NDau cells. Here, a significant effect can already be observed at 10 µM. With increasing concentrations, the number of apoptotic cells is as high as in the Nalm6 cells.

MBR-8 induced apoptosis is caspase-3-dependent

To learn more about the apoptotic pathways involved in **MBR-8** action, a special cellular model system was used. MCF-7/mock cells are regular human breast adenocarcinoma cells that are caspase-3 defective (Engels et al. 2005). Therefore, caspase-3 is later incorporated in the MCF-7/casp-3 cell line. A DNA-fragmentation with **MBR-8** in both cell lines reveals that the substance induces more apoptosis in lower concentrations in the MCF-7/casp-3 cells than in the MCF-7/mock cells (Fig. 5). At 70 µM of **MBR-8** more than 40 percent of the cells are apoptotic. In comparison with this, the MCF-7/mock cells only reach around 30 percent of apoptosis at this concentration. This gives a first hint on a caspase-3-dependent induction of apoptosis.

A western blot analysis underlined the involvement of caspase-3 in the molecular mechanisms of **MBR-8**. Fig. 6 illustrates the smaller caspase-3-bands and the

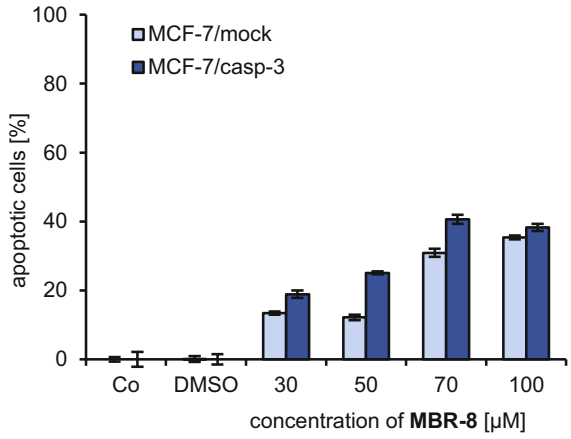

Fig. 5 Caspase-3-dependence was shown by treating MCF-7/mock and MCF-7/casp-3 cells with 30 µM, 50 µM, 70 µM and 100 µM of **MBR-8**. Co stands for "control", i.e. untreated cells. After 96 h of incubation, DNA fragmentation was measured by flow cytometry of cellular DNA content, using three batches per concentration. Values are given in percentage of apoptotic cells and were expressed at means ± SD

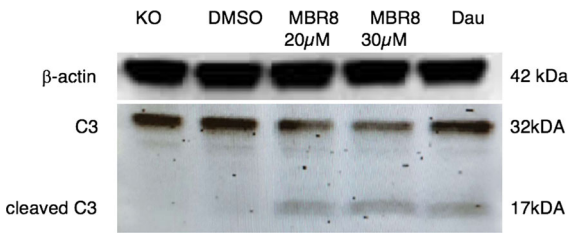

Fig. 6 **MBR-8** induces caspase-3 (C3) activation in BJAB cells. Daunorubicin (Dau) was used as positive control. BJAB cells were treated with 20 µM and 30 µM of **MBR-8**. Control cells (KO) were left untreated. All cells were incubated for 48 h. The separation of 20 µg cytosolic proteins was done by SDS-PAGE, followed by subjecting them to the Western blot analysis. Immunblotting was then done with an anti-C3 antibody. 43 kDa β-actin was detected to prove equal loading

cleaved caspase-3-bands in **MBR-8** treated Nalm6 cells as a sign of consumption of caspase-3.

A loss of mitochondrial membrane potential is caused by MBR-8

To prove that **MBR-8** triggers the mitochondrial pathway of apoptosis, a JC1-measurement was done. The results in Fig. 7 show that **MBR-8** reduces the mitochondrial membrane potential after staining Nalm6 cells with the dye JC-1. The mitochondrial permeability was quantified by flow cytometric determination of Nalm6 cells with decreased fluorescence.

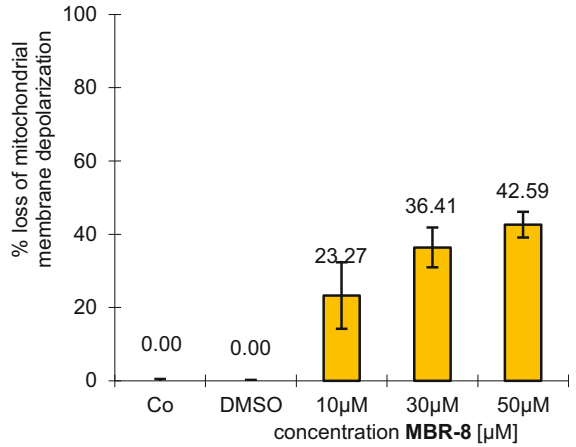

Fig. 7 Mitochondrial permeability transition was measured by flow cytometric analysis for Nalm6 cells after 48 h incubation without (Co) and with 10 µM, 30 µM and 50 µM **MBR-8**. Values of the mitochondrial permeability transition are given as percentage of cells with low $\Delta\Psi_m$ ± SD. Three batches per concentration were used

At a **MBR-8** concentration of 10 µM more than 20 percent of the membrane potential is lost. The values increase with concentrations of 30 µM and 50 µM of **MBR-8**.

MBR-8 shows high selectivity for tumor cells

We tested the substance **MBR-8** in healthy human leucocytes to see if it shows a pronounced selectivity for tumor cells. The results in Fig. 8 confirm this assumption. At the decisive concentrations of **MBR-8** (30 µM and 50 µM), less than five percent of the leucocytes were apoptotic.

MBR-8 strongly sensitizes leukemia cells and its resistant NDau cell line

In further experiments, we tested whether **MBR-8** has synergistic effects with common cytostatic agents. Firstly, we used the Nalm6 cell line and pipetted 1 µM of **MBR-8** in combination with 6 and 8 nM of daunorubicin. We observed enormous apoptotic effects of over 2000 percent compared to the sum of the single treatments (Fig. 9a). Similar synergistic effects can be noted in Nalm6 cells that were treated with **MBR-8** and vincristine or doxorubicin. Here, we needed 3 µM **MBR-8** and used two different concentrations of vincristine and doxorubicin to illustrate the

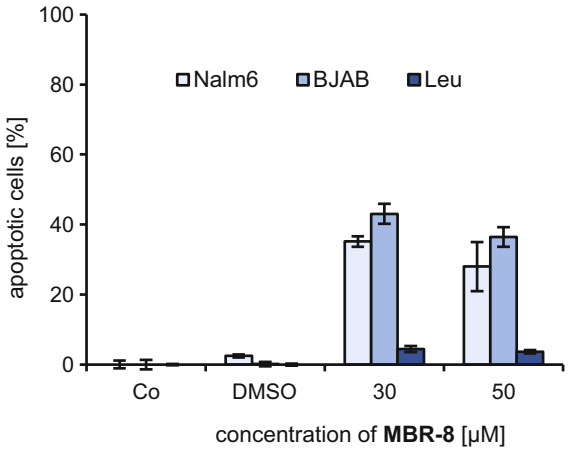

Fig. 8 Selectivity of **MBR-8**. Nalm6, BJAB and leucocytes were treated with 30 µM and 50 µM of the substance. Control cells (Co) were left untreated. All cells were incubated for 96 h, then induction of apoptosis was measured by flow cytometric of cellular content. Three batches per concentration were used. Values are given as percentage of cells with hypodiploid DNA ± SD

effects (Fig. 9b, c). As it turned out, **MBR-8** sensitizes leukemia cells such that only very low concentrations of **MBR-8** combined with low concentrations of the common cytostatic drugs are needed.

Due to the high interest in new substances that defeat resistant tumor cell lines, we repeated the experiment in NDau cells. Again, synergistic effects of **MBR-8** plus daunorubicin were as high as in the Nalm6 cells (Fig. 9d). Higher concentrations of daunorubicin were used in the experiment with NDau where a high apoptotic effect in regular Nalm6 is known (Dragoun et al. 2018).

Discussion

The paramount importance of metal complexes as anti-cancer agents is probably best exemplified by well-known cisplatin (Jung and Lippard 2007). In the current project, we examined the aluminium-salen tosylate complex **MBR-8**. Only few other aluminium-complexes have been explored as potential cytostatic drugs. An aluminium(III) phthalocyanine chloride tetrasulphonate has been used in experiments of photodynamic therapy and showed induction of apoptosis and necrosis in melanoma cells (Ndhundhuma and Abrahamse 2017). Furthermore, a luminescent aluminium salen complex was described as a potential molecule for monitoring dynamic vesicle trafficking from the Golgi apparatus to lysosomes in living human cervix epitheloid carcinoma cells (HeLa) (Tang et al. 2018). Antiapoptotic effects of aluminium-complexes have not yet been reported. Other complexes involving third main group elements have been investigated. A binuclear boron-fluoride complex showed apoptotic effects in MCF-7 cells, along with effects in other cancer cells (Tuluce et al. 2017). In addition, boron dipyrromethene derivatives, so called BODIPY complexes, are used as trackable therapeutic agents to learn about the working mechanism of metal-based drugs (Tasan et al. 2013; Doulain et al. 2015; Gupta et al. 2016; Trommenschlager et al. 2017). Experiments with complexes of BODIPY and gold revealed anti-apoptotic effects in breast (MDA-MB-231), prostate (PC3) and colon (SW480) cancer cells (Trommenschlager et al. 2017). Gallium is another metal-ion of the third main group in the periodic table. It has been shown that various gallium-complexes defeat tumor cells. Two gallium phosphinoarylbisthiolato complexes overcame the platinum-resistance in A2780cis ovary carcinoma cells (Fischer-Fodor et al. 2014).

The exploration of antiapoptotic-effects of the aluminium-complex **MBR-8** turned out to be equally rewarding. Besides the fact that **MBR-8** triggers apoptosis in Burkitt like lymphoma cells (Fig. 3), it overcomes daunorubicin resistance in leukemia cells (Fig. 4). It is known that the NDau cells are characterized by a significant overexpression of the drug efflux pump P-glycoprotein (P-gp). This transporter can efflux several molecules, including anticancer drugs, out of the cells (Zhou 2008; Ledwitch et al. 2016). We furthermore found co-resistances of the cells against fludarabine and paclitaxel which means that the cells are multidrug resistant (MDR) (Kater et al. 2012). A P-gp inhibition and overcoming of MDR is proven by the fact that the apoptosis is higher in the P-gp overexpressed NDau cells than in the Nalm6 cells (Fig. 4).

A significant cause of failure in chemo-therapy treatment is chemoresistance (Klumper et al. 1995; Poulard et al. 2018). Therefore, the identification of substances that overcome resistances and sensitize common chemotherapeutics is of high interest. The Nalm6 cells have already been used for several explorations of new substances. For example, it is

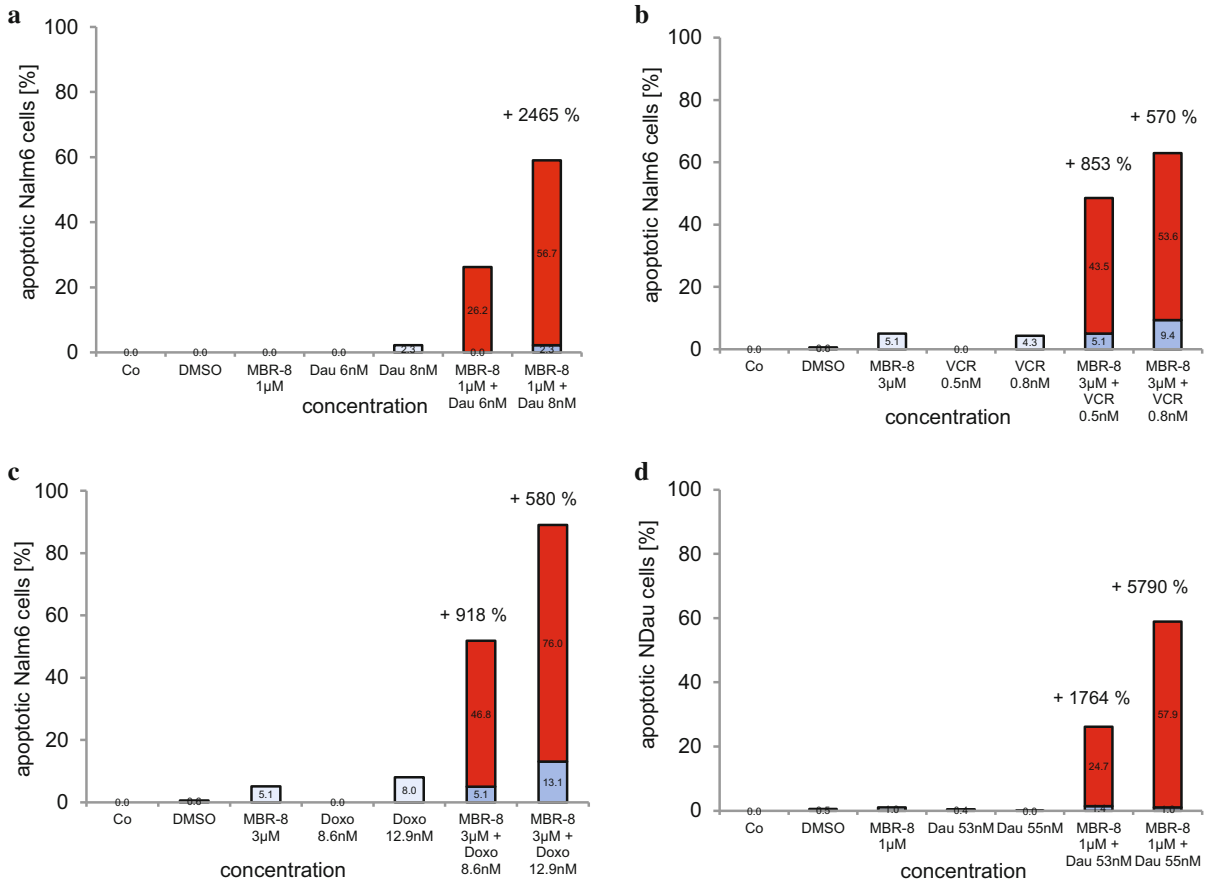

Fig. 9 Synergistic effects of **MBR-8** and common cytostatic agents in leukemia cells. Cells were treated with different substances. Control cells (Co) were left untreated. Incubation time was 96 h. Three batches per concentration are used and values are given in percentage of apoptotic cells. **a** Nalm6 cells were treated with 1 µM **MBR-8** and 6nM/8 nM of daunorubicin (Dau), alone and in combination. **b** Nalm6 cells were treated with 3 µM **MBR-8** and 0,5 nM/0,8 nM of vincristine (VCR), alone and in combination. **c** Nalm6 cells were treated with 3 µM **MBR-8** and 8,6 nM/12,9 nM of doxorubicin (Doxo), alone and in combination. **d** 1 µM **MBR-8** and 53 nM/55 nM daunorubicin were pipetted alone and in combination on NDau cells

known that the substance JIB-04, a selective JmjC family lysine demethylase inhibitor, selectively enhances glucocorticoid (GC)-induced cell death in Nalm6 cells (Poulard et al. 2018). Another proven GC sensitizer is a c-Myc inhibitor that induces enhanced apoptosis in Nalm6 cells in combination with the GC dexamethasone (Lv et al. 2018). Next to GCs, other leukemia cells are sensitized for several chemotherapeutics with other substances (Duraj et al. 2006; Xu et al. 2017; Ghelli Luserna Di Rora et al. 2018).

Interestingly, we found that **MBR-8** efficiently sensitizes leukemia cells. Combining low concentrations of daunorubicin and **MBR-8** results in high apoptotic effects in Nalm6 cells (Fig. 9a) and even in the daunorubicin resistant cell line (Fig. 9d). Repeating the experiment in Nalm6 cells with different concentrations of vincristine and doxorubicin also resulted in remarkable apoptotic effects (Fig. 9b, c). The results are very impressive and make **MBR-8** a very promising substance for fighting tumor resistances by using poly-chemotherapy.

Due to the fact, that **MBR-8** facilitates the induction of apoptosis in Nalm6 and P-gp overexpressed NDau cells, an influence of the substance on P-gp does not seem to be the main characteristic in the molecular mechanism, but nevertheless seems to play a role (Fig. 9d). At this point, further experiments would be necessary to find out more about the mechanisms.

Another piece of evidence is the loss of mitochondrial membrane potential upon application of the JC-1

dye (Fig. 7). In addition, the assumption of mitochondrial pathway reactions is supported by the fact that **MBR-8** causes stronger apoptotic effects in the MCF-7/casp-3 cells with included caspase-3 compared to the MCF-7/mock cells without the protease (Fig. 5). The detection of 17 kDa cleaved-caspase-3 bands in the western blot analysis (Fig. 6) confirms the involvement of caspase-3 in the apoptosis induction of **MBR-8**.

Especially the high sensitizing activity of **MBR-8** speaks for a potential future use in combination chemotherapy. The effects in three different tumor cell lines comprising leukemia and solid tumors make **MBR-8** even more attractive. Last but not least, the negligible effect of **MBR-8** in healthy human leucocytes (Fig. 8) underlines its therapeutic potential.

Experimental

Materials

RNase A was from Qiagen (Hilden, Germany). Propidium iodide (50 µg/ml) was from Serva (Heidelberg, Germany). Doxorubicin (Dox), vincristine (VCR) and daunorubicin (Dau) were provided by the Children's Hospital of the City of Cologne, Amsterdamer Straße. The cytostatic agents were freshly dissolved as stock solutions in DMSO prior to the experiments. They were diluted with the respective cell culture media or buffer during the assay procedures. The aluminium complex **MBR-8** (prepared according to reference 2) was obtained from the University of Cologne, Department for Chemistry, Prof. Dr. A. Berkessel, and dissolved in a 40 mM stock solution of DMSO. Besides the regular control cells in the experiments, some cells were incubated with an equal amount of DMSO only, as DMSO control. The results were comparable to those obtained with an untreated control.

Cell lines and cell cultures

The cell line Nalm6 (human b cell precursor leukemia cells) was provided by AG Henze, Charité, Berlin. The daunorubicin-resistant Nalm6-cell line (NDau) was generated in our lab by exposing the cells to increasing concentrations of the cytostatic drug until they tolerated high concentrations without loss of cell vitality. Furthermore, BJAB mock cells (Burkitt like lymphoma) were kindly donated by AG Daniel, Charité Berlin. The MCF-7-cells are human breast adenocarcinoma cells. Usually the cells do not have caspase-3 included (MCF-7/mock). The caspase-3 is incorporated into the MCF-7-cells (MCF-7/casp-3). Cells were kindly provided by Prof. Dr. R. Jänicke, University of Düsseldorf.

The cell lines were incubated in 250 ml cell culture bottles at 37 °C. For the suspension cells RPMI 1640 medium (GIBCO, Invitrogen, Karlsruhe, Germany) was used, supplemented with heat inactivated fetal calf serum (FCS, 10%, v/v), L-glutamine (0.56 g/l), penicillin (100,000 i.u.) and streptomycin (0.1 g/l). Adherent cells were grown in DMEM supplemented with FCS (10%, v/v) and geniticine (0.4 mg/ml). Cells were passaged 2–3 times per week by dilution to a concentration of 1×10^5 cells/ml. To secure standard conditions in growing, the cells were adjusted to 3×10^5 cells/ml 24 h before the assay setup. For proliferation and apoptosis assays cells were diluted to $1x10^5$ cells/ml immediately before treatment with the substances.

Determination of Cell Concentration and Cell Viability of Cells

Cell count and viability were determined using a CASY cell counter and analyzer system from Roche. Settings were specifically defined for the requirements of the cells used. With this system, in one measurement the cell concentration is simultaneously analyzed in three different size ranges: the cell debris, dead cells and viable cells (Voisard et al. 1991). The cells were seeded at a density of 1×10^5 cells/ml in 6-well-plates and they were treated with different concentrations of the substances. As a control, some cells were incubated untreated or with DMSO. After 24 h of incubation at 37 °C, the cells were resuspended and 100 µl of each well was diluted in 10 ml of CASYton (ready-to-use isotonic saline solution) for an immediate automated count of the cells. The control group of the cells was defined as 100% growth. A cell concentration that was not higher than at the beginning of the experiment showed the maximal inhibition of proliferation.

Measurement of cell death by LDH release assay

To measure the cytotoxicity of a given substance, release of lactate dehydrogenase (LDH) was analyzed. After 1 h incubation with different concentrations of **MBR-8**, LDH released by BJAB cells was measured in the cell culture supernatants using the Cytotoxicity Detection Kit from Roche (Mannheim, Germany). After centrifugation at 350×*g* for 5 min, 20 µl of cell-free supernatants were diluted with 80 µl phosphate-buffered saline (PBS), and 100 µl reaction mixture containing 2-(4-iodophenyl)-3-(4-nitrophenyl)-5-phenyltet-razolium chloride (INT), sodium lactate, NAD+ and diaphorase. Time-dependent formation of the reaction product was quantified photometrically at 490 nm. The maximum amount of LDH release was determined after lysis of the cells using 0.1% Triton X-100 in culture medium and set to represent 100% cell death.

Measurement of DNA fragmentation

The DNA fragmentation was measured by a modified cell cycle analysis which detects DNA fragmentation on the single cell level as described (Essmann et al. 2000). The cells were seeded at a density of 1×10^5 cells/ml and they were treated with different concentrations of the substances. They were incubated at 37 °C for 96 h. After incubation, cells were collected by centrifugation at 1500 rpm for 5 min. Adherent cells were washed with 180 µl phosphate-buffered saline (PBS) and treated with trypsin for 5 min at 37 °C before centrifugation. The cells were fixed in 200 µl PBS/2% (v/v) formaldehyde on ice for 30 min. After fixation, the cells were centrifuged again at 1500 rpm for 5 min at 4 °C, then incubated with 180 µl ethanol/PBS (2:1, v/v) for 15 min, pelleted, and resuspended in 50µl PBS containing 40 µg/ml RNase A. RNA was digested for 30 min at 37 °C and the cells were centrifuged again, then finally resuspended in 200 µl PBS containing 50 µg/ml propidium iodide. Nuclear DNA fragmentation was quantified by flow cytometric determination of hypodiploid DNA (fluorescence-activated cell sorting, FACS). By using a FACScan (Becton Dickinson, Heidelberg, Germany), equipped with the CELLQuest software, data were collected and analyzed. The number of apoptotic cells was reflected by the percentage of hypoploidy (subG1). Apoptosis, specifically induced by the compounds was calculated by subtracting background apoptosis, observed in control cells, from total apoptosis detected in the treated cells.

Immunoblotting

After 48 h of incubation with different concentrations of **MBR-8**, BJAB cells were washed twice with PBS and lysed in buffer containing 10 mM Tris–HCl, pH 7.5, 300 mM NaCl, 1% Triton X-100, 2 mM $MgCl_2$, 5 µM ethylenediaminotetraacetic acid (EDTA), 1 µM pepstatin, 1 µM leupeptin, and 0.1 mM phenylmethyl-sulfonyl fluoride (PMSF). By using the bicinchoninic acid assay from Pierce (Rockford, IL, USA),(Smith et al. 1985) the protein concentration was determined and equal amounts of protein were separated by SDS–PAGE (Laemmli 1970). The immunoblotting was performed as described (Wieder et al. 1994). The blocking of the membrane was done for 1 h in PBST (PBS, 0.05% Tween-20) containing BSA and incubated with different primary antibodies for 1 h. The anti-caspase-3 and anti-β-actin from Sigma, Saint Louis, USA were used. After the membrane was washed in PBST, the secondary antibody (anti-mouse IgG HRP from Bioscience, San Diego, USA and anti-rabbit IgG HRP from Promega, Minneapolis, USA) in PBST was applied for 1 h. After washing, the protein bands were detected using the ECL enhanced chemiluminescence system (Amersham Buchler, Braunschweig, Germany).

Measurement of the mitochondrial permeability transition

After 48 hours of incubation with the substance, Nalm6 cells were collected by centrifugation at 300×*g*, 4 °C for 5 min. Mitochondrial permeability transition was then determined by staining the cells with 5,5‘,6,6‘-tetrachloro-1,1‘,3,3‘-tetraethyl-benzimidazolylcarbocyanin iodide (JC-1; Molecular Probes, Leiden, The Netherlands) as described (Lambert et al. 1989; Reers et al. 1995). 1×10^5 cells were resuspended in 500 µl phenol red free RPMI 1640 without supplements, and JC-1 was added to give a final concentration of 2.5 µg/µl. The cells were incubated for 30 min at 37°C and moderately shaken. Control cells were incubated in the absence of JC-1 dye. The cells were harvested by centrifugation at 300×*g*, 4 °C for 5 min, washed with ice-cold PBS, and

resuspended in 200 µl PBS at 4 °C. Mitochondrial permeability transition was then quantified by flow cytometric determination of cells with decreased fluorescence—that is, with mitochondria displaying a lower membrane potential. Data were collected and analyzed using a FACScan (Becton Dickinson) equipped with the CELLQuest software. Data are given in percentage cells with low $\Delta\Psi_m$, which reflects the number of cells undergoing mitochondrial apoptosis.

Isolation of healthy human leucocytes

50 ml blood of a healthy test person was taken, 10 ml RPMI 1640 medium was added. Next 4 ml of Ficoll (Saccharose-Epichlorhydrin-Copolymer) was pipetted in a 15 ml tube, then 5 ml blood was carefully added on the top. After 18 min of centrifugation at $657\times g$, 20 °C, leucocytes were collected by slowly transferring them with a Pasteur pipette into a 45 ml tube. 20 ml of RPMI 1640 was added, then the solution was centrifuged at 1500 rpm for 5 min. The cell count and viability were determined by CASY cell counter and analyzer system from Roche. Cells were seeded at a density of 3×10^5 cells/ml. The following treatment is equal to the steps in measurement of DNA fragmentation as described above.

Synthesis of the aluminium-salen tosylate complex MBR-8

For the synthesis of the tosylate complex **MBR-8**, the corresponding chloride was first prepared from (*S*,*S*)-1,2-diaminocyclohexane as reported (Sammis and Jacobsen 2003). This chloride complex (100 mg, 180 µmol, 1.00 eq.) was dissolved in 70.0 ml abs. acetonitrile. This solution was added, with continuous stirring and in a dropwise manner, to a solution of 49.0 mg (170 mmol, 1.09 eq.) silver tosylate in 7.00 ml abs. acetonitrile. The resulting suspension was stirred at ca. 20 °C for 12 h. The precipitate was removed by filtration through Celite, and the solvent was removed in vacuo. Drying in vacuo afforded a yellowish solid (121 mg, 163 µmol, 99 %) of m.p. > 250 °C.

M.W.: 742.99 g/mol

See the Supporting Information of ref. 2 for the characterization of **MBR-8** by ^{1}H, ^{13}C NMR, IR, ESI-MS and HR-EI-MS.

Acknowledgements We thank the Dr. Kleist Foundation Berlin for its financial support and Prof. Dr. R. Jänicke, University of Düsseldorf for generating the MCF-7/casp-3 cells. Generous support by the Fonds der Chemischen Industrie (Doctoral Fellowship to M.B.) is gratefully acknowledged.

Compliance with ethical standards

Conflict of interest All authors declare that they have no conflict of interest.

References

Berkessel A, Brandenburg M (2006) Catalytic asymmetric addition of carbon dioxide to propylene oxide with unprecedented enantioselectivity. Org Lett 8:4401–4404. https://doi.org/10.1021/ol061501d

Doulain PE et al (2015) Towards the elaboration of new gold-based optical theranostics. Dalton Trans 44:4874–4883. https://doi.org/10.1039/c4dt02977a

Dragoun M, Gunther T, Frias C, Berkessel A, Prokop A (2018) Metal-free salan-type compound induces apoptosis and overcomes multidrug resistance in leukemic and lymphoma cells in vitro. J Cancer Res Clin Oncol 144:685–695. https://doi.org/10.1007/s00432-018-2592-x

Duraj J, Bodo J, Sulikova M, Rauko P, Sedlak J (2006) Diverse resveratrol sensitization to apoptosis induced by anticancer drugs in sensitive and resistant leukemia cells. Neoplasma 53:384–392

Engels IH, Totzke G, Fischer U, Schulze-Osthoff K, Janicke RU (2005) Caspase-10 sensitizes breast carcinoma cells to TRAIL-induced but not tumor necrosis factor-induced apoptosis in a caspase-3-dependent manner. Mol Cell Biol 25:2808–2818. https://doi.org/10.1128/MCB.25.7.2808-2818.2005

Essmann F, Wieder T, Otto A, Muller EC, Dorken B, Daniel PT (2000) GDP dissociation inhibitor D4-GDI (Rho-GDI 2), but not the homologous rho-GDI 1, is cleaved by caspase-3 during drug-induced apoptosis. Biochem J 346 Pt 3:777-783

Fischer-Fodor E et al (2014) Gallium phosphinoarylbisthiolato complexes counteract drug resistance of cancer cells. Metallomics 6:833–844. https://doi.org/10.1039/c3mt00278k

Ghelli Luserna Di Rora A et al (2018) Targeting WEE1 to enhance conventional therapies for acute lymphoblastic leukemia. J Hematol Oncol 11:99. https://doi.org/10.1186/s13045-018-0641-1

Gupta G et al (2016) Novel BODIPY-based Ru(II) and Ir(III) metalla-rectangles: cellular localization of compounds and their antiproliferative activities. Chem Commun (Camb) 52:4274–4277. https://doi.org/10.1039/c6cc00046k

Jung Y, Lippard SJ (2007) Direct cellular responses to platinum-induced DNA damage. Chem Rev 107:1387–1407. https://doi.org/10.1021/cr068207j

Kater L et al (2012) The role of the intrinsic FAS pathway in Titanocene Y apoptosis: the mechanism of overcoming multiple drug resistance in malignant leukemia cells.

Toxicol In Vitro 26:119–124. https://doi.org/10.1016/j.tiv.2011.09.010

Klumper E et al (1995) vitro cellular drug resistance in children with relapsed/refractory acute lymphoblastic leukemia. Blood 86:3861–3868

Laemmli UK (1970) Cleavage of structural proteins during the assembly of the head of bacteriophage T4. Nature 227:680–685

Lambert IH, Hoffmann EK, Jorgensen F (1989) Membrane potential, anion and cation conductances in Ehrlich ascites tumor cells. J Membr Biol 111:113–131

Ledwitch KV, Gibbs ME, Barnes RW, Roberts AG (2016) Cooperativity between verapamil and ATP bound to the efflux transporter P-glycoprotein. Biochem Pharmacol 118:96–108. https://doi.org/10.1016/j.bcp.2016.08.013

Lv M et al (2018) CMyc inhibitor 10058F4 increases the efficacy of dexamethasone on acute lymphoblastic leukaemia cells. Mol Med Rep 18:421–428. https://doi.org/10.3892/mmr.2018.8935

Majno G, Joris I (1995) Apoptosis, oncosis, and necrosis. An overview of cell death. Am J Pathol 146:3–15

Ndhundhuma IM, Abrahamse H (2017) Susceptibility of in vitro melanoma skin cancer to photoactivated hypericin versus aluminium(iii) phthalocyanine chloride tetrasulphonate. Biomed Res Int 2017:5407012. https://doi.org/10.1155/2017/5407012

Poulard C, Baulu E, Lee BH, Pufall MA, Stallcup MR (2018) Increasing G9a automethylation sensitizes B acute lymphoblastic leukemia cells to glucocorticoid-induced death. Cell Death Dis 9:1038. https://doi.org/10.1038/s41419-018-1110-z

Reers M, Smiley ST, Mottola-Hartshorn C, Chen A, Lin M, Chen LB (1995) Mitochondrial membrane potential monitored by JC-1 dye. Methods Enzymol 260:406–417

Sammis GM, Jacobsen EN (2003) Highly enantioselective, catalytic conjugate addition of cyanide to alpha, beta-unsaturated imides. J Am Chem Soc 125:4442–4443. https://doi.org/10.1021/ja034635k

Smith PK et al (1985) Measurement of protein using bicinchoninic acid. Anal Biochem 150:76–85

Tang J, Yin HY, Zhang JL (2018) A luminescent aluminium salen complex allows for monitoring dynamic vesicle trafficking from the Golgi apparatus to lysosomes in living cells. Chem Sci 9:1931–1939. https://doi.org/10.1039/c7sc04498d

Tasan S et al (2013) BODIPY-phosphane as a versatile tool for easy access to new metal-based theranostics. Dalton Trans 42:6102–6109. https://doi.org/10.1039/c2dt32055j

Trommenschlager A et al (2017) Gold(i)-BODIPY-imidazole bimetallic complexes as new potential anti-inflammatory and anticancer trackable agents. Dalton Trans 46:8051–8056. https://doi.org/10.1039/c7dt01377a

Tuluce Y, Lak PTA, Koyuncu I, Kilic A, Durgun M, Ozkol H (2017) The apoptotic, cytotoxic and genotoxic effect of novel binuclear boron-fluoride complex on endometrial cancer. Biometals 30:933–944. https://doi.org/10.1007/s10534-017-0060-8

Van Cruchten S, Van Den Broeck W (2002) Morphological and biochemical aspects of apoptosis, oncosis and necrosis. Anat Histol Embryol 31:214–223

Voisard R, Dartsch PC, Seitzer U, Roth D, Kochs M, Hombach V (1991) [Cell culture as a prescreening system for drug prevention of restenosis?] Vasa Suppl 33:140-141

Wieder T, Geilen CC, Wieprecht M, Becker A, Orfanos CE (1994) Identification of a putative membrane-interacting domain of CTP:phosphocholine cytidylyltransferase from rat liver. FEBS Lett 345:207–210

Xu X et al (2017) Wogonin reversed resistant human myelogenous leukemia cells via inhibiting Nrf2 signaling by Stat3/NF-kappaB inactivation. Sci Rep 7:39950. https://doi.org/10.1038/srep39950

Zhou SF (2008) Structure, function and regulation of P-glycoprotein and its clinical relevance in drug disposition. Xenobiotica 38:802–832. https://doi.org/10.1080/00498250701867889